CHARACTERIZING THE SIGNALING AND TUMOR SUPPRESSOR ROLE OF FRK IN BREAST CANCER

Thesis Submitted to the College of Graduate and Postdoctoral Studies and in Partial Fulfillment of the Requirements for a Ph.D. Degree in the Department of Biochemistry, University of Saskatchewan Saskatoon

By Yetunde Ogunbolude

PERMISSION TO USE

In presenting this thesis in partial fulfillment of the requirements for a Postgraduate degree from the University of Saskatchewan, I agree that the Libraries of this University may make it freely available for inspection. I further agree that permission for copying of this thesis in any manner, in whole or in part, for scholarly purposes may be granted by the professor or professors who supervised my thesis work or, in their absence, by the Head of the Department or the Dean of the College in which my thesis work was completed. It is understood that any copying or publication or use of this thesis or parts thereof financial gain shall not be allowed without my written permission. It is also understood that due recognition shall be given to me and to the University of Saskatchewan in any scholarly use which may be made of any material in my thesis.

Requests for permission to copy or to make other use of the material in this thesis in whole or part should be addressed to:

Dean
College of Graduate and Postdoctoral Studies
University of Saskatchewan
116 Thorvaldson Building, 110 Science Place
Saskatoon, Saskatchewan S7N 5C9
Canada

Dean
College of Medicine
University of Saskatchewan
107 Wiggins road, Health Science Building
Saskatoon, Saskatchewan S7N 5E5
Canada

ABSTRACT

The human Fyn-related kinase (FRK) is a non-receptor tyrosine kinase known to have tumor suppressor activity in breast cancer cells. FRK expression is mostly absent in mesenchymal breast cancer cells but present in epithelial cells. Overexpression of FRK in breast cancer cells was shown to suppress cell growth by interacting, phosphorylating and stabilizing the tumor suppressor PTEN, inhibiting breast cancer cell proliferation by arresting the G1 phase of the cell cycle, by interacting with pRb (Retinoblastoma) and decreasing STAT3 phosphorylation. However, STAT3 has not been validated as a target of FRK and the mechanisms by which FRK suppresses cell proliferation, and migration has not been fully characterized. We used the FRK-negative MDA-MB 231 breast cancer cell line in which we stably overexpressed FRK, and analyzed the effect on FRK on STAT3 signaling, cell proliferation, migration, and invasiveness. We employed both immunoblotting and RT-PCR to identify/validate FRK-regulated targets (proteins and genes) in these cells. Finally, we interrogated the TCGA and GENT gene expression databases to determine the correlation between the expression of FRK and epithelial/mesenchymal markers in breast cancer cell lines and tissues. We observed that FRK overexpression inhibited JAK/STAT signaling pathway by suppressing the expression of some STAT3 target genes. Overexpression of FRK also increased transcription of the epithelial marker gene E-cadherin, and down-regulated the transcript levels of Vimentin, Fibronectin, and Slug. We also observed an inverse correlation between FRK expression and mesenchymal markers in a large cohort of breast cancer cells. FRK suppresses breast cancer cell proliferation by inducing cellular senescence through upregulation of p21 thus, resulting in pRb dephosphorylation and the consequent inhibition of E2F1. Finally, we found that FRK suppressed mammary tumorigenesis in xenograft mice. Our data indicate that the suppression of EMT and upregulation of p21 is one of the mechanisms by which FRK suppresses breast cancer tumorigenesis. We conclude therefore that FRK acts as a tumor suppressor in breast cancer by repressing cell proliferation, migration and invasiveness by suppressing epithelial-to-mesenchymal transition and inducing cellular senescence.

ACKNOWLEDGMENTS

First and foremost, I will like to thank my all-sufficient God, who is my all in all, my life, my future, my strength, the God that changes not, the "I AM that I AM." Unto Him, I lift up my praise for how far He has helped me.

My special thanks go to my wonderful supervisor, a great scientist, who has been a teacher, a father and a mentor to me, in the person of Dr. Kiven Erique Lukong. Sir, you have impacted my research life positively, you made science so simple to understand and you brought out the best in me. Thank you for all your guidance, support, and encouragements. Words cannot express how grateful I am and I look forward to the day you will win a Nobel Prize award because you are not far from it, and you deserve it. To my co-supervisor, Dr. Keith Bonham, thank you for all your support, tutelage, advice and corrections.

My appreciation also goes to the head of Biochemistry Department, University of Saskatchewan, the postgraduate coordinator, my committee chair and all my committee members, Dr. Yu Luo, Dr. Andrew Freywald and Dr. Azita Haddadi for all your tutelage, advice, corrections, and support, which really helped me in my experiments and research. I will also like to appreciate Saskatchewan Cancer Agency (SCA) through which I obtained the Lisa Rendall Breast Cancer graduate student scholarship, the Canadian Breast Cancer Foundation, Non-devolving and devolving scholarships, for the financial support to be able to carry out my research.

Also, I will like to appreciate all the past and present members of Dr. Lukong's and Dr. Keith's lab; Dr. Edward Bagu, Dr. Sayem Miah, Raghu Goel, Erika, Chenlu Dai, Joshua, Stephanie cornea, Gabriel Blank, and Aditya Mandapati. You made my research so enjoyable, thank you all for all your support and for being there.

This acknowledgment will not be complete without thanking my loving and wonderful husband, the bone of my bone and the flesh of my flesh, in the person of Olalekan Adegbenro. Thank you for always being there, for your encouragements, sacrifices, and for supporting my career. You are the best, and you are blessed. To my loving and beautiful daughter, Taraoluwa Adegbenro and handsome son, Oluwatoni Adegbenro, thank you for being the best children I could ever dream of and also for allowing mama to focus on her research.

My profound gratitude goes to my caring and understanding parents, Mr. and Mrs. Taiwo Ogunbolude, for your support and sacrifice for me to succeed, the invaluable support and love of my siblings Mr. Akinwumi Ogunbolude and sisters Mrs. Bunmi Adenigba and Yinka Ogunbolude. To all my in-laws, Surveyor and Mrs. Henry Adegbenro, Mr. Lanre Adegbenro, Mr. Gbenga Adegbenro and Mrs. Folakemi Fanimi, thank you all for your support and for being there.

Also, the love and support of my pastor, Mr. Titus Adedapo, his wife Mrs. Olakunbi Adedapo, and their children; Esther and Daniel, deserves to be mentioned.

PERMISSION TO REPRODUCE

This thesis includes a "substantial part" of a work or other proprietary material. Hence permission to reuse figures and tables has been obtained via Copyright Clearance Center or the editor of the journal. The permission to reuse material has been listed in the list of appendices.

Additionally, I have recently published some part of the thesis in Oncotarget journal, and the permission to reuse the materials and figures have been obtained through this link (https://creativecommons.org/licenses/by/3.0/)

DEDICATION

This thesis is dedicated to the Almighty God, for the strength and wisdom to carry out this research.

It is also dedicated to every woman living with or lost their battle with breast cancer. You all were the inspirations behind this research. Don’t give up; the battle over breast cancer is going to be won someday.

Finally, I will like to dedicate this thesis to every girl child in Africa and those that have been looked down on because of their gender. Don’t give up on your dreams. So far you can dream it, you can always achieve it.

TABLE OF CONTENT

LIST OF TABLES

LIST OF FIGURES

LIST OF ABBREVIATIONS

ATCC: American Type Culture Collection

ATP: Adenosine triphosphate

BCL2: *B-cell lymphoma 2*

BD: Boyden

BFK: Breast family kinase

BRCA1: Breast cancer anti-estrogen resistance protein 1

CCK-8: Cell Counting Kit-8 (Dojindo, CK04-05)

CCLE: cancer cell line encyclopedia

cDNA: complementary DNA

DMEM: Dulbecco's modified Eagle's medium

EGFR: epidermal growth factor receptor

EMT: Epithelial-Mesenchymal Transition

ERK: extracellular signal-regulated kinases

ETS: E-twenty-six transformation-specific

FBS: Fetal Bovine Serum

FRK: Fyn-related kinase

FRK K262M: disruption of ATP binding; kinase-defective or Kinase-dead

FRK V378–F379 del (VF): Deletion of amino acid on FRK kinase domain from valine 378-lysine 380 and insertion of glutamine

siRNA: short or small interfering RNA

shRNA: short or small hairpin RNA

WT: Wild-Type

FRK-Y497F: Mutation of FRK regulatory tyrosine 497 to phenylalanine

GAPDH: Glyceraldehyde 3-phosphate dehydrogenase

GPRB: Growth factor receptor-bound protein

HEK 293: Human embryonic kidney cells 293

HER2: human epidermal growth factor receptor 2

IAP: inhibitor of apoptosis family

IHC: Immunohistochemistry

IL-6: Interleukin 6

JAK: Janus kinase

JNK: c-Jun N-terminal kinases

LOH: loss of heterozygosity

LPC: lysophosphatidylcholine

MAPK: mitogen-activated protein kinase

MCL1: myeloid leukemia cell

MEK1/2: Mitogen-activated protein kinase kinase

MEM: Minimum essential medium

MMP: matrix metalloproteinase 1

mRNA: Messenger RNA

MSL: mesenchymal stem-like

MTT: -3-(4,5-dimethylthiazol-2-yl)- 2,5-diphenyl-2H-tetrazolium bromide

PBS: phosphate buffer/phosphate saline

PEI: polyethyleneimine

PI3K: phosphatidylinositide 3-kinases

PMSF: phenylmethylsulfonyl fluoride

PTEN: Phosphatase and tensin homolog

PTK5: protein tyrosine kinase 5

pY20: anti-phosphotyrosine antibody

RSEM: RNA Seq Expectation Maximization

RT-PCR: Reverse transcription polymerase chain reaction

SDS: sodium dodecyl sulfate

SDS-PAGE: sodium dodecyl sulfate-polyacrylamide gel electrophoresis

SFKs: Src-family kinases

SH2: Src homolog 2

SH3: src homolog 3

SRMS: Src-related kinase lacking C-terminal regulatory tyrosine and N-terminal myristoylation sites

STAT: Signal transducer and activator of transcription

TCGA: The Cancer Genome Atlas

TMA: Tissue microarray

TNBC: Triple-negative breast cancer

TNM: Classification of Malignant Tumors (T- size of tumor; N- lymph nodes; M- metastasis)

1.0 OVERVIEW

Fyn-related tyrosine kinase (FRK) is a non-receptor tyrosine kinase that has been described as a candidate tumor suppressor (Brauer and Tyner, 2009; Goel and Lukong, 2016). The human FRK gene is located on chromosomes 6q21-23, a region that is destabilized by loss of heterozygosity in 30% of breast tumors and 40% of melanomas. The gene encodes a 54-kDa protein composed of 505 amino acids. FRK is a member of the breast tumor kinase (BRK) family kinase (BFK) that also includes BRK and src-related kinase lacking C-terminal regulatory tyrosine and N-terminal myristylation sites (SRMS) (Goel and Lukong, 2016). These kinases share a conserved gene structure and 60% amino acid homology, as well as display a similar architecture too and have 30–50% sequence identity with SFKs (Src family kinases). Like SFKs, FRK is functionally composed of a Src homology 3 (SH3) domain, an SH2 domain, a kinase domain and a putative C-terminal regulatory tyrosine (Y497) in addition to a conserved auto-regulatory tyrosine residue (Y387) in its catalytic domain (Ogunbolude *et al.*, 2017).

Ectopically expressed FRK was shown to inhibit the growth of breast cancer cells (Meyer *et al*., 2003; Yim *et al*., 2009b). Although FRK has been characterized as a candidate tumor suppressor, the protein has been detected in some breast cancer cell lines including BT 20, MDA-MB-468, and MCF-7, but not in BT549, MDA-MB 231, and MDA-MB-435. FRK was also detected in the normal epithelium but was absent in 16 of 21 of invasive breast carcinomas studied. Mechanistically, FRK was shown to inhibit cell growth by binding, phosphorylating and stabilizing the tumor suppressor PTEN, attenuating the PI3K/Akt signaling pathway (Yim *et al*., 2009b). Additionally, FRK suppressed glioma cell migration and invasion by inhibiting of JUN N-terminal kinase (JNK)/ c-Jun activation (Zhou *et al*., 2012), Cyclin D1 nucleus accumulation and pRb phosphorylation (Hua *et al*., 2014). Also, by promoting N-cadherin/β-catenin complex formation (Shi *et al*., 2015). Furthermore, FRK has been reported to suppress cervical cancer and non-small lung cancer proliferation and migration (Sun *et al*., 2015; Zhang *et al*., 2016).

Previous and published data from our lab have indicated that constitutively active FRK-YF induces the phosphorylation of numerous targets that do not overlap with FRK-WT targets and decreases the phosphorylation of signal transducer and activator of transcription 3 (STAT3) (Ogunbolude *et al.*, 2017). Hence, the goal of this Ph.D. project was to validate STAT3 as a

target of FRK, access the effect of FRK on STAT3-regulated cellular processes and evaluate the tumor suppressor role of FRK *in vivo*.

2.0 Background

2.1 Breast cancer

Breast cancer is a heterogeneous disease that arises from the epithelial cells of the breast, it is the most frequent female malignancy in the Western world, and it displays diversity in its morphology, molecular genetics, biology, and clinical outcome (Lukong, 2017). Breast cancer is the leading cause of cancer death in females worldwide, with nearly 1.7 million new cases in 2012 and almost 522,000 deaths globally (Ferlay *et al*., 2015; Lukong *et al*., 2017; Torre *et al*., 2015). Highest incidence rates of breast cancer in women occur in Western Europe and North America, while Africa and Asia have the lowest incidence rates (Lukong *et al*., 2017). However, African American women have the highest mortality rates whereas the lowest mortality rates exist among Korean women (Lukong *et al*., 2017). According to Statistics Canada, one in nine women is expected to develop breast cancer during her lifetime, and one in 29 will die of the disease in Canada (Statistics-Canada, 2007, 2013). There are nearly 23,000 new cases and over 5,000 deaths every year in Canada (Statistics-Canada, 2007, 2013). Higher breast cancer incidence has been attributed to breast cancer screening as well as higher prevalence of breast cancer risk factors such as weight gain after age 18 years, excess body weight (for postmenopausal breast cancer), use of menopausal hormone therapy (MHT), physical inactivity, alcohol consumption, and reproductive or hormonal factors (long menstrual history, recent use of oral contraceptives, and null parity or later age at first birth) (Chlebowski *et al*., 2013; Torre *et al*., 2016). However, the high mortality rates of breast cancer likely due to changes in risk factors, as well as limited access to early detection and treatment and this occur in most low-income countries (Lukong *et al*., 2017; Torre *et al*., 2016; Youlden *et al*., 2014).

2.1.1 Molecular classification of breast cancer

Pathologists classify breast cancer based on it histological grade, as determined by the evaluation of the degree of tumor differentiation (tubule formation) and proliferation (mitotic index) (Eliyatkin *et al*., 2015). This method has been shown to provide a very strong prediction for determining patient prognosis. However, evaluation based on histology is semi-quantitative (Eliyatkin *et al*., 2015; Rakha *et al*., 2010). Furthermore, breast cancer was classified based on

tumor, node, metastasis (TNM) parameter. This is a staging system commonly used for all cancers over the world to guide treatment planning, provide a possibility to demonstrate the effectiveness of the treatment during follow-up and predict prognosis (Denoix, 1952; Eliyatkin *et al*., 2015).

However, with advances in diagnosis and treatment of breast cancer, improving technology and increased knowledge, scientists have made efforts to evaluate tumor biology of breast cancer in details (Eliyatkin *et al*., 2015). Breast cancer was classified into four major molecular subtypes based on gene expression; these include HER2 (human epidermal growth factor receptor 2) type, Basal cell type, and Luminal A and luminal B (Perou *et al*., 2000; Prat and Perou, 2011; Sorlie *et al*., 2001). The HER2 type displays an overexpression of HER2 and is more likely to be high-grade and poorly differentiated (Brenton *et al*., 2005). Whereas, the Basal cell type (also called triple-negative breast cancer or TNBC) has a high proliferation rate, is not amenable to conventional targeted therapies, has a poor prognosis and occurs in about 5-10 % of breast cancer patients (Carey *et al*., 2010). Lastly, the luminal A and B cancers are mostly estrogen receptor (ER)-positive and histologically low- and high-grade, respectively (Perou *et al*., 2000; Prat and Perou, 2011; Sorlie *et al*., 2001). Normal-like breast cancer was also described; it represents samples with low tumor cell content and more normal tissue components (Eliyatkin *et al*., 2015; Perou *et al*., 2000).

Neve and his colleagues further classified breast cancer cell lines into two major clusters: luminal and basal-like clusters (Neve *et al*., 2006). Basal-like clusters was further divided into basal A and basal B; there is no distinct HER2 cluster. However, HER2 was shown to be distributed among luminal and basal A clusters. These clusters were shown to have distinct morphological and invasive properties. Luminal appear more differentiated, form tight cell-cell junctions and have a noninvasive phenotype (Neve *et al*., 2006), while basal B cells appear less differentiated and highly invasive with more mesenchymal-like appearance. However, basal A cells have either luminal-like or basal-like morphologies (Neve *et al*., 2006). Since breast cancer is a dynamic and adaptive process, other diagnostic methods are necessary for better-personalized therapy.

	Molecular Subtype			
	Luminal A	**Luminal B**	**HER2/neu**	**Basal like**[a]
Gene Expression Pattern	Expression of luminal (low molecular weight) cytokeratins, high expression of hormone receptors moreover, related genes	Expression of luminal (low molecular weight) cytokeratins, moderate-low expression of hormone receptors and related genes	High expression of HER2/neu, low expression of ER and related genes	High expression of basal epithelial genes and basal cytokeratins, low expression of ER and related genes, low expression of HER2/neu
Clinical and biologic properties	50% of invasive bresat cancer, ER/PR positive, HER2/neu negative	20% of invasive breast cancer, ER/PR positive, HER2/neu expression variable, higher proliferation than Luminal A, higher histologic grade than Luminal A	15% of invasive breast cancer, ER/PR negative, HER2/neu positive, high proliferation, diffuse TP53 mutation, high histologic grade and nodal positivity	~15% of invasive breast cancer, most ER/PR/HER2/neu negative (triple negative), high proliferation, diffuse TP53 mutation, BRCA1 dysfunction (germline, sporadic)
Histologic correlation	Tubular carcinoma, Cribriform carcinoma, Low grade invasive ductal carcinoma, NOS, Classic lobular carcinoma[b]	Invasive ductal carcinoma, NOS Micropapillary carcinoma	High grade invasive ductal carcinoma, NOS	High grade invasive ductal carcinoma, NOS Metaplastic carcinoma, Medullary carcinoma
Response To treatment and prognosis	Response to endocrine therapy Variable response to	Response to endocrine therapy (tamoxifen and aromatase inhibitors) not as good as Luminal A Variable response to	Response to trastuzumab (Herceptin) Response to chemotherapy	No response to endocrine therapy or trastuzumab Sensitive to platinum group

	chemotherapy	chemotherapy (better than Luminal A)	with anthracyclines	chemotherapy and PARP inhibitors
	Good prognosis	Prognosis not as good as Luminal A	Usually unfavorable prognosis	Not all, but usually worse prognosis

PARP poly-adenosinediphosphate ribose polymerase

Table 2.1: A table showing the molecular subtypes of breast cancer with their characteristics. [a]Basal like tumor group includes a low-grade group with low proliferation but expression of basal type (high molecular weight) cytokeratin and triple-negative phenotype (like adenoid cystic carcinoma, secretuar carcinoma). [b]Classical lobular carcinoma generally exhibits luminal A properties, while pleomorphic lobular carcinoma usually shows features of other molecular subtypes (Eliyatkin et al., 2015).

2.1.2 Breast cancer microcalcification

The survival rates of breast cancer have significantly increased due to a combination of improved treatment options and increased detection of early-stage tumors (Narod *et al.*, 2015; O'Grady and Morgan, 2018). X-ray based mammography are widely used for early screening and detection of breast cancers, it visualizes breast tissues clearly and screen various subtle abnormalities including pathological lesions (Tabar *et al.*, 2003; Sharma *et al.*, 2016). Mammary microcalcifications are one of the most pertinent markers of both benign and malignant lesions of the breast detected by mammography (Morgan, Cooke, and McCarthy, 2005; Sharma *et al.*, 2016). Calcification is a term referred to mineralized materials found in various parts of the body; they usually appear as bright white flecks on a mammogram (Chou et al., 1998; Morgan, Cooke, and McCarthy, 2005; Sharma *et al.*, 2016). They are broadly categorized as 'macro' and 'micro' calcification (Sharma *et al.*, 2016; Suhail *et al*., 2015). Macrocalcifications are coarse, large white dots or specks in nature (>0.5 mm in diameter) that are often randomly dispersed throughout the breast tissue, and are most often found in non-cancerous tissues (Bhargava et al., 2014; Dikshith, 2013; Sharma *et al.*, 2016). Microcalcification clusters are tiny specks (<0.5 mm in diameter) of calcium deposits appearing on the mammographic image (Sharma *et al.*, 2016; Suhail *et al*., 2015).

Microcalcification in breast cancers is classified based on morphology, size, distribution and chemical composition. Classification based on their morphological appearance include benign eggshell calcification, which consists of a thin spherical structure that are usually formed

as the result of calcium deposition on the surface of an oil cyst, and is unrelated to breast cancer (Rao *et al.,* 2016; O'Grady and Morgan, 2018). In comparison to the long, thin branching structure of fine linear (often referred to as casting) calcifications which indicates spread of calcium deposition along the lumen of a breast duct, are found in malignant breast cancers (Rao *et al.,* 2016; O'Grady and Morgan, 2018).

Classification based on distribution displays linear, clustered, diffuse or regional pattern calcification. The linear distribution represents the spread of calcified deposits along a duct. The clustered calcifications (an intermediate category) represent 5 calcifications within an area of 1 cm^2, while the diffuse (random distribution within the breast) or regional pattern calcifications spread in a larger volume > 2 cm^2 (Hernández et al., 2016; O'Grady and Morgan, 2018). The linear calcifications are considered high-risk, and more malignant when compared to the clustered calcifications (Hernández et al., 2016; O'Grady and Morgan, 2018).

In addition to morphology and spatial distribution, microcalcification can be classified based on their chemical composition. We have 2 categories of microcalcification under the chemical composition group. They include the Type I (calcium oxalate) and Type II (calcium hydroxyapatite [HA]) (Sharma *et al.,* 2018). The Type I microcalcifications are generally found solely in benign tumors while type II calcifications are found in either benign or malignant tumors (O'Grady and Morgan, 2018; Sharma *et al.,* 2018). Under the light microscope the calcium oxalate appears in amber color and are partially transparent, while the HA crystals appear grey/white and are opaque (Frappart et al., 1989; Sharma et al., 2018).

Microcalcification has been used as a strong predictor of breast cancers malignancy. For instance, HA microcalcification has been shown to induce mitogenesis in MCF-7 and Hs578T breast cancer cells (Morgan *et al.,* 2001; O'Grady and Morgan, 2018; Sharmal *et al.,* 2018). Also, treatment of breast cancer cells with HA was shown to promote matrix metalloproteinase (MMP) activity and stimulated prostaglandin production to intensify its effect (Morgan *et al.,* 2001; O'Grady and Morgan, 2018; Sharmal *et al.,* 2018). However, due to the inability of current standard clinical imaging techniques to reliably differentiate type I from type II calcifications, the chemical nature of breast calcifications is not routinely determined (O'Grady and Morgan, 2018).

2.2 Tyrosine Kinases

Protein tyrosine kinases (PTKs) are known to modulate critical pathways that drive the hallmarks of breast cancer, which include cell growth, survival, and metastasis (Manning *et al*., 2002; Parsons and Parsons, 2004). The human genome contains about 90 tyrosine kinase genes that form two classes of PTKs: receptor tyrosine kinases (RTKs) and non-receptor tyrosine kinases (NRTKs), 58 are receptors tyrosine kinases, while 32 are non-receptor tyrosine kinases (Blume-Jensen and Hunter, 2001). RTKs regulate numerous cellular processes, such as proliferation and differentiation, cell survival and metabolism, cell migration, and cell-cycle control (Blume-Jensen and Hunter, 2001; Lemmon and Schlessinger, 2010). These receptors have an extracellular region, a single transmembrane helix, and a cytoplasmic region that contains the protein tyrosine kinase (TK) domain plus additional carboxy (C-) terminal and juxtamembrane regulatory regions (Lemmon and Schlessinger, 2010). Mutation or overexpression of several receptor tyrosine kinases such as EGFR and FGFR have been implicated in most cancer-related diseases (Lemmon and Schlessinger, 2010).

NRTKs have varied sub-cellular localization and occur in the cytoplasm, nucleus or anchored to the plasma membrane (Blume-Jensen and Hunter, 2001). Some cytoplasmic or membrane-anchored NRTKs link signal transduction to specific events in the nucleus, such as cell division and gene expression (Pendergast, 2002). Deregulation of NRTKs occurs in various cancers, including breast cancer. For example, BRK also known as protein tyrosine kinase 6 (PTK6) is overexpressed in over 60% of breast carcinomas, but not in the normal mammary gland or benign lesions (Brauer and Tyner, 2010). Both the protein levels and kinase activity of c-Src, another NRTK, are frequently elevated in breast cancer (Ishizawar and Parsons, 2004).

The importance of some NRTKs in triggering oncogenic events makes them potential targets for therapeutic intervention. Oncogenic NRTKs need to overcome the negative regulatory constraints of tumor suppressors that counteract their signaling activity. Some NRTKs have also been identified as candidate tumor suppressors, but their mechanisms of action have been largely understudied. Spleen tyrosine kinase (SYK) and fyn-related tyrosine kinase (FRK, also known as protein tyrosine kinase 5 (Coopman and Mueller, 2006; Goel and Lukong, 2016; Yim *et al*., 2009b) are one of the few known NRTK candidate tumor suppressors. NRTKs are subdivided into nine main families, based on their similarities in domain structure with a high degree of homology in the catalytic Src Homology 1 (SH1), p-Tyr binding Src Homology 2 (SH2), and

protein-protein interaction Src Homology 3 (SH3) domains (Gocek *et al*., 2014). The families include Src, Fak, Csk, Tec, Abl, Syk, Jak, Fes and Aec family kinases (**Figure 2.1)**. The Src family kinases are the largest of all the NRTKs (Gocek *et al*., 2014). It is sub-divided into Lyn-related, Src-related, and BRK-related. The BRK-related subfamily is also called the BRK family kinases (BFKs) (Goel and Lukong, 2015).

2.3. SRC family kinases

The Src family kinases (SFKs) play essential roles in regulating several signal transduction pathways using a diverse set of cell surface receptors (Ingley, 2008; Parsons and Parsons, 2004). These signal transduction pathways include metabolism, viability, proliferation, differentiation, and migration within many different cell lineages (Ingley, 2008; Parsons and Parsons, 2004). The Src family kinase is divided into three main subfamilies: Lyn related, Src-related, and PTK6/Brk related. The Lyn-related family consists of four members: Lyn, Hck, Lck, and Blk (Gocek *et al*., 2014). The second subfamily consists of Src-related kinases, such as Fgr, Fyn, Yrk, Yes (Gocek *et al*., 2014). The third subfamily is the PTK6/Brk-related, also known as the BRK family kinase or BFK, consists of BRK, FRK, and SRMS (Gocek *et al*., 2014; Goel and Lukong, 2016; Ingley, 2008). All the SFKs share similar domain arrangement; they possess an N-terminal unique region (50–70 residues), Src homology 3 (SH3) domain (50 residues), Src homology 2 (SH2) domain and a Src homology 1 (SH1) (∼300 residues) domain (Ingley, 2008). The SH3 domain has high variability among the family members; it encompasses a myristoylation/palmitoylation site (Ingley, 2008; Resh, 1999). It associates with proline-rich motifs harboring the PXXP consensus (Ingley, 2008; Koch *et al*., 1991). The SH2 domain with interacts with phosphotyrosine motifs, showing highest affinity for the consensus sequence pYEEI (Ingley, 2008; Koch *et al*., 1991) and lastly the SH1 domain also known as the kinase domain is responsible for the enzymatic activity (Ingley, 2008). Some members of the SFKs have the C-terminal region which bears an auto-inhibitory phosphorylation site (**Figure 2.2**) (Gocek *et al*., 2014).

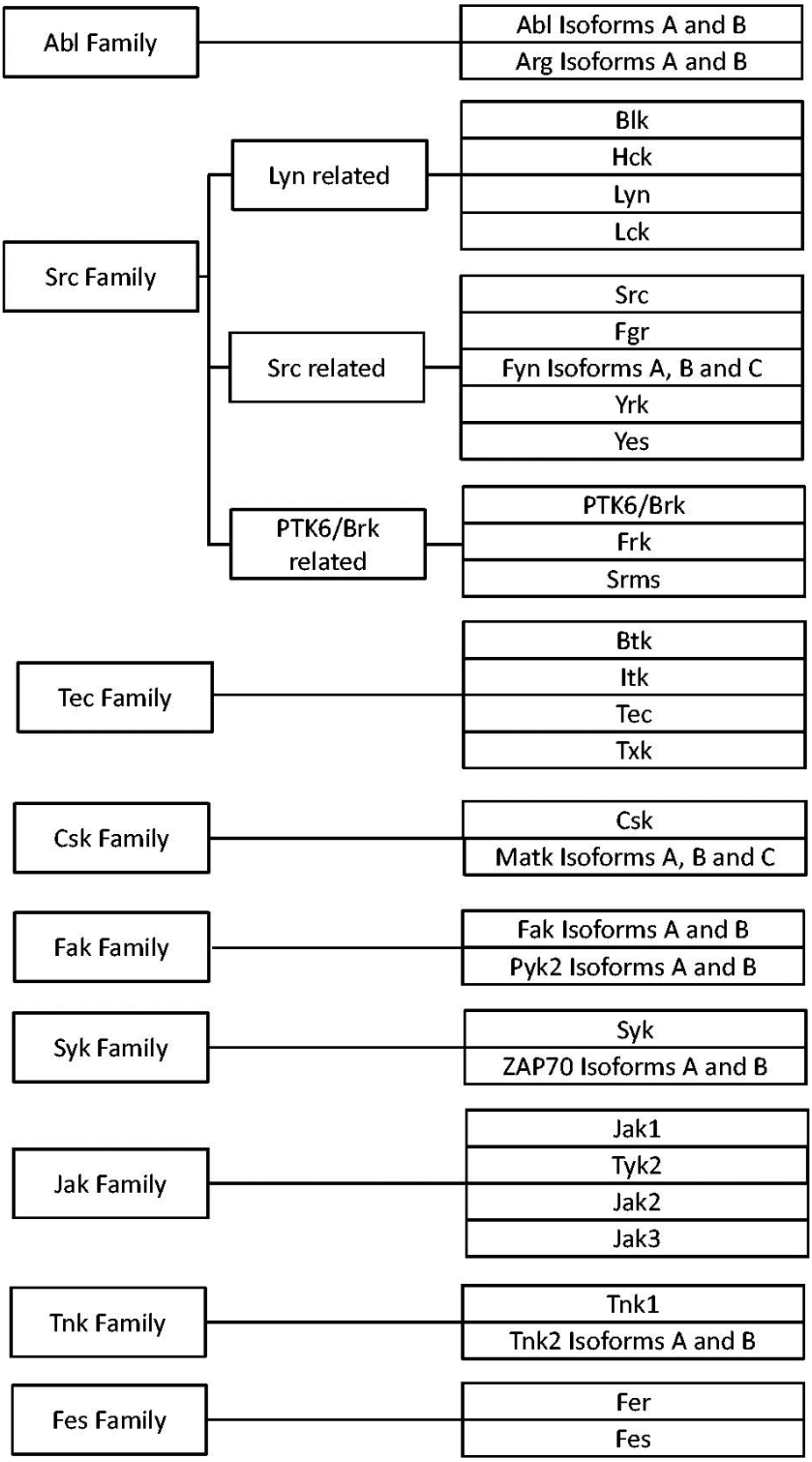
Abl Family
Abl Isoforms A and B
Arg Isoforms A and B
Src Family
Lyn related
Blk
Hck
Lyn
Lck
Src related
Src
Fgr
Fyn Isoforms A, B and C
Yrk
Yes
PTK6/Brk related
PTK6/Brk
Frk
Srms
Tec Family
Btk
Itk
Tec
Txk
Csk Family
Csk
Matk Isoforms A, B and C
Fak Family
Fak Isoforms A and B
Pyk2 Isoforms A and B
Syk Family
Syk
ZAP70 Isoforms A and B
Jak Family
Jak1
Tyk2
Jak2
Jak3
Tnk Family
Tnk1
Tnk2 Isoforms A and B
Fes Family
Fer
Fes

Figure 2.1: Families of NRTKs. NRTKs phylogram inferred from amino acid sequences of the kinase domains. Src family is subdivided into three groups: Lyn-related, Src-related, and PTK6/Brk (Gocek *et al*., 2014).

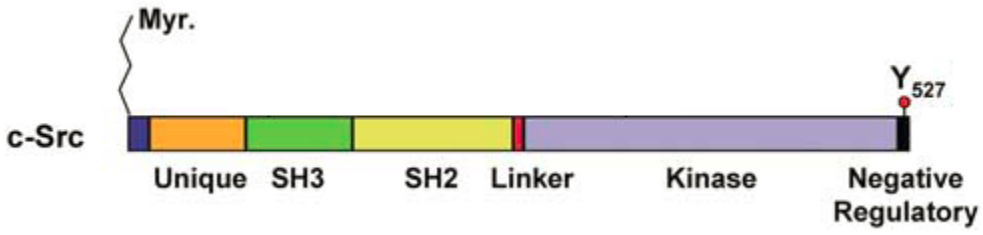

Figure 2.2: Schematics of Src family kinases showing all the domain structure. Members of the family exhibit a conserved domain organization, which includes a myristoylated N-terminal segment, followed by SH3, SH2, linker and tyrosine kinase domains, and a short C-terminal tail (Figure adapted from Parsons and Parsons, 2004)

2.3.1 Mechanism of activation and inactivation of the SRC family kinases

The SFKs are kept inactive through phosphorylation of the conserved tyrosine residues at the c-terminal (e.g., Y527 in c-Src which is usually phosphorylated by the C-terminal Src kinase (Csk) and closely related kinases), this restricts the accessibility of the kinase domain (the active site) for ATP and substrates (Summy and Gallick, 2003). The SH2 domain via intramolecular interactions binds to the phosphorylated tyrosine residue at the C-terminal, while the SH3 domain binds to the amino acids linking the SH2 and the kinase domain hence limiting the potential of these proteins to participate in cellular signaling (**Figure 2.3**) (Summy and Gallick, 2003). Activation of the SFKs occur either through displacement of the intramolecular interactions via higher affinity binding between the SH3 and SH2 domains and their cellular ligands and/or through dephosphorylating of the carboxy-terminal regulatory tyrosine (Frame, 2002; IpRby and Yeatman, 2000; Summy and Gallick, 2003). Also, the loss the carboxy-terminal sequence (as seen in v-Src and v-Yes) and mutation (Y527 in c-Src to phenylalanine) of the C-terminal tyrosine residues makes the kinase to be constitutively active (Frame, 2002; Irby and Yeatman, 2000; Summy and Gallick, 2003).

Distinct from the SFKs are the BRK-related/ BRK family kinases that comprise BRK, FRK, and SRMS (Ingley, 2008). None of these kinases are myristoylated, and only two (BRK and FRK) have potential regulatory C-terminal tyrosine but show no significant homology to the corresponding Src/Lyn like sequences (Ingley, 2008; Manning *et al*., 2002).

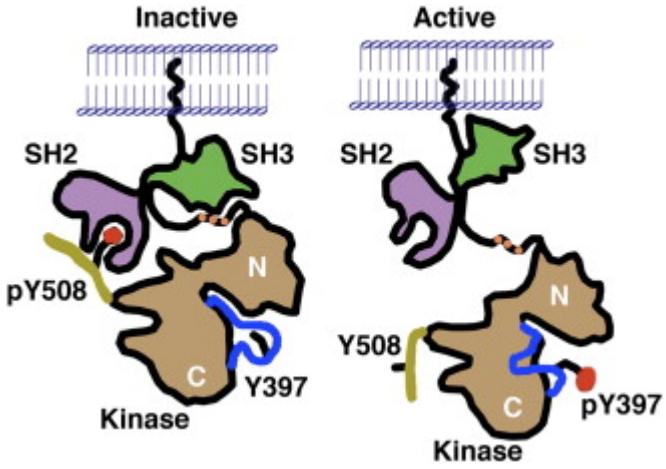

Figure 2.3: General structural schematic of the Src family kinases in their inactive and active configurations. Left, the inactive configuration showing the SH2 domain interacting with the phosphorylated C-terminal tyrosine (pY508), the SH3 domain interacting with the SH2-kinase connector which forms a left-handed polyproline type II helix, and the dephosphorylated activation loop (Y397) folded back over the substrate binding site. Right, the active configuration, showing SH2 and SH3 domains released from the intramolecular interactions and available for binding to substrates and regulatory molecules, the C-terminal tyrosine is dephosphorylated (Y508), and the activation loop is phosphorylated (pY397) and is folded away from the substrate binding site and allows the two kinase lobs (N and C) to form a kinase competent catalytic cleft (Ingley, 2008).

2.4 BRK Family kinases

The BRK family kinases were first referred to as FRK/PTK6 family of tyrosine kinases (Brauer and Tyner, 2009) and later renamed as BRK family kinases (Goel and Lukong, 2015). Members of this family include BRK or protein tyrosine kinase 6 (PTK6), FRK (PTK5) and SRMS (src-related kinase lacking C-terminal regulatory tyrosine and N-terminal myristylation sites or PTK7 (**Figure 2.4**). BFKs are distantly related to the Src-family, they are composed of the Src homology 3 (SH3), the Src homology 2 (SH2) and the kinase (SH1) domains (**Figure 2.4A**). However, they share an exon-intron structure distinct from Src-family members (**Figure**

2.4B) (Brauer and Tyner, 2009; Goel and Lukong, 2015), all three members possess 8 exons interspersed between 7 introns in a conserved/identical manner (Goel and Lukong, 2015). Additionally, the BRK family kinases are not myristoylated, and only two members of the family (BRK and FRK) have potential regulatory C-terminal tyrosine but show no significant homology to the corresponding Src/Lyn like sequences (Goel and Lukong, 2015; Ingley, 2008; Manning *et al*., 2002).

BRK is known for its ability to promote tumorigenesis by regulating several cellular processes such as cell proliferation, migration, and metastasis (Goel and Lukong, 2015). While FRK have been reported to function as a tumor suppressor as well as promote tumor growth (Brauer and Tyner, 2009; Goel and Lukong, 2016; Pilati *et al*., 2014). The actual role of SRMS in cancer is still unknown.

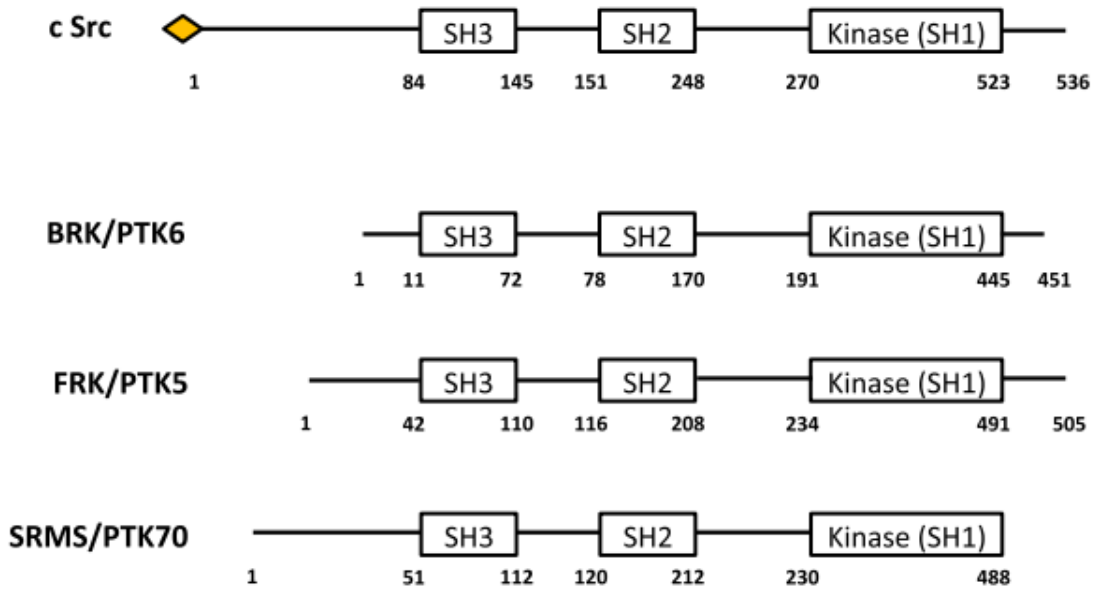

Figure 2.4A: Domain structure of c-Src and BRK family kinases. c-Src, as well as BRK family kinases (BFKs), possess 3 functional domains, namely, the Src homology 3 (SH3), the Src homology 2 (SH2) and the kinase (SH1) domains. Src family kinases also possess an N-terminal myristoylation signal absent in the BRK family kinases. The SH3 domain characteristically binds proline-containing motifs while the SH2 domain binds phosphorylated-tyrosine containing motifs (Goel and Lukong, 2015)

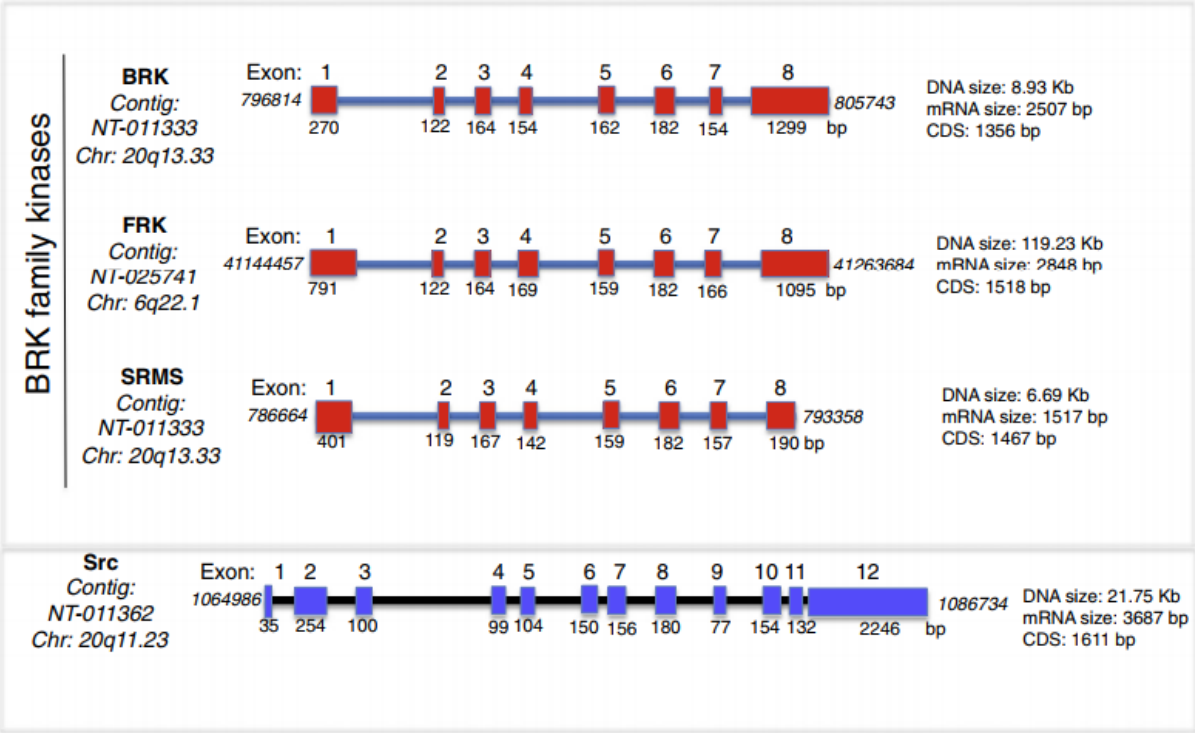

Figure 2.4B: Schematic representation of the intron-exon splicing pattern of the BRK family (BRK, FRK, and SRMS) and Src family kinases. The BRK family kinases possess 8 exons spliced between 7 introns. This differs from the Src family kinases where, as shown for the c-Src kinase, the 12 exons are separated by 11 intervening introns. Thus compared to Src family kinases (SFKs), the BRK family (BFK) displays a diverging splicing pattern conforming to differences in the number of introns/exons (Goel and Lukong, 2015).

2.5 FRK

Fyn-related tyrosine kinase (FRK) is a non-receptor tyrosine kinase that has been described as a candidate tumor suppressor (Brauer and Tyner, 2009; Goel and Lukong, 2016). The human FRK gene is located on chromosomes 6q21-23, a region that is destabilized by the loss of heterozygosity in 30% of breast tumors and 40% of melanomas. The gene encodes a 54-kDa protein composed of 505 amino acids. FRK was originally cloned from the human B-cell lymphoma cell line BL979 and human breast cancer cells (Lee *et al*., 1994). Later studies demonstrated that FRK is also expressed in the BT20, BT474 and MCF-7 breast cancer cell lines, but not in mesenchymal cells or tissues (Cance *et al*., 1994).

2.5.1 Functional features of FRK

Like SFKs, FRK is functionally composed of a Src homology 3 (SH3) domain, an SH2 domain, a kinase domain and a putative C-terminal regulatory tyrosine (Y497) in addition to a conserved auto-regulatory tyrosine residue (Y387) in its catalytic domain (Goel and Lukong 2015; Ogunbolude *et al.,* 2017) (**Figure 2.2 and 2.4**). SH2 domains in general bind to peptide sequences that contain a phosphorylated tyrosine, whereas the SH3 domain, tends to bind polyproline-containing ligands (Kaneko *et al*., 2011). The human FRK harbors a putative bipartite nuclear localization signal (NLS), $_{168}$KRLDEGGFFLTRRR$_{181}$, embedded in its SH2 domain, it lacks the myristoylated N-terminal consensus sequence (MGXXXS/T) that dictates plasma membrane anchorage of SFKs (Serfas and Tyner, 2003). However, the mouse and rat orthologs of FRK known as IYK contains N-terminal myristoylation sequences, indicating that the intracellular targets and perhaps the cellular roles may differ between the orthologs (Sunitha and Avigan, 1996; Sunitha *et al*., 1999). The C-terminal tyrosine of murine FRK (Y504, analogous to Y497 in the human sequence) is phosphorylated by the cytoplasmic tyrosine kinase (CSK), resulting in a decrease in its kinase activity (Sunitha and Avigan, 1996). Mutation of this C-terminal tyrosine of some SFKs members and as well as murine FRK has been shown to increase the catalytic activity of the enzymes (Derry *et al*., 2000; Oberg-Welsh *et al*., 1998; Roskoski, 2004). For example, the Welsh group found out that single (Y504F) and double mutation (Y504F/ Y497F) in IYK resulted in increased autophosphorylation, while Y497F alone did not exhibit an increased kinase activity when compared to the wildtype protein (Goel and Lukong, 2016; Oberg-Welsh *et al*., 1998). The human FRK contains Y387 within the kinase activation loop, autophosphorylation of this tyrosine residue is predicted to stabilize enzymatic activity and result in increased catalytic activity, this autophosphorylation site corresponds to Y394 in IYK (mouse FRK) (Cance *et al*., 1994; Goel and Lukong, 2016; Ingley, 2008). The first report of intrinsic FRK kinase activity was through an *in vitro* kinase assay, where FRK was immunoprecipitated from a BT 20 breast cancer cell line. The wild-type kinase demonstrated the capability of autophosphorylation and also immunospecificity towards an anti-phosphotyrosine antibody, thereby presenting itself as a functional tyrosine kinase (Cance *et al*., 1994; Goel and Lukong, 2016). Within the kinase domain of human FRK is a lysine residue (K262), which is conserved in BFKs and SFKs. It is critical for ATP binding, and mutation of this residue completely abrogates catalytic activity (Meyer *et al*., 2003).

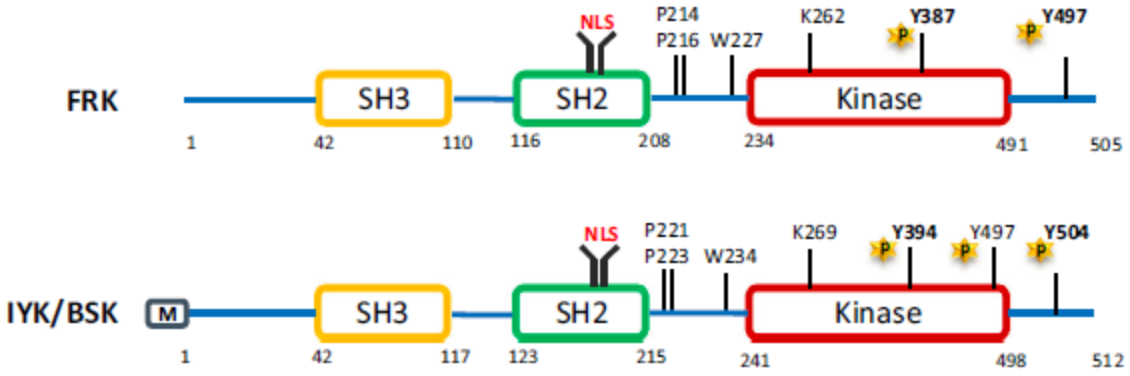

Figure 2.5: Schematic representation showing the difference between human FRK and mouse FRK was known as IYK. IYK contains N-terminal myristoylation sequences, indicating that the intracellular targets and perhaps the cellular roles may differ between the orthologs. All proteins possess three conserved functional domains, namely, the Src-homology 3 (SH3), Src-homology-2 (SH2) and the kinase domains. Additionally, the critical residues involved in the regulation of tyrosine kinase activity remain conserved. These include the ATP contacting lysine: K262 (FRK) and K269 (IYK), the autophosphorylation tyrosine within the activation loopY387 (FRK) and Y394 (IYK) and the C-terminal regulatory tyrosine: Y497 (FRK) and Y504 (IYK). Phosphorylation of the activation loop tyrosine enhances kinase activity while phosphorylation of the C-terminal tyrosine negatively regulates kinase activity (Adapted Goel and Lukong, 2016).

2.5.2 FRK localization

Human FRK has a nuclear localization signal (NLS). However, the protein variably localizes to the nucleus and cytoplasm in different cell lines and tissues. In normal human mammary tissue, FRK was detected predominantly in the cytoplasm during the proliferative follicular phase of the menstrual cycle, and when the human breast epithelium undergoes intense proliferation; nuclear localization of FRK was detected during the differentiating luteal phase (Berclaz *et al*., 2000). Another study in COS-7 monkey kidney cells showed that endogenous FRK was predominantly localized in the nucleus (Cance *et al*., 1994; Meyer *et al*., 2003b). However, ectopically expressed wild-type and kinase-inactive FRK (K262M) were shown to localize mainly in the perinuclear region in both BT474 and MCF-7 breast cancer cell lines, while deletion of NLS-hapRboring SH2 domain caused diffuse cytoplasmic localization (Cance *et al*., 1994; Meyer *et al*., 2003). Although murine FRK has a myristoylation signal, subcellular fractionation studies have shown that the constitutively active Y504F variant localizes predominantly in the cytosol, while Y497F and Y497/504F double mutant were detected in both nuclear and cytosolic fractions (Anneren *et al*., 2000; Oberg-Welsh *et al*., 1998). Interestingly, only the double mutant

decreased cell proliferation in this study, suggesting that nuclear FRK may be responsible for the tumor suppressor function of FRK. Mutation or deletions of either the SH2, SH3 domains or the ATP binding site (K262) of FRK have been shown to have a significant effect on its localization. For example, the deletion of the NLS-containing SH2 resulted to a diffused cytoplasmic localization of FRK, while deletion of the SH3 domain did not affect subcellular localization and mutation of the ATP-contacting lysine (K262) residue resulted in a punctate perinuclear distribution (Goel and Lukong, 2016).

FRK localization has also been studied in various cancers; for example, in glioma cells, endogenous FRK was found to be localized to the nuclear and perinuclear regions of the non-tumourous brain tissues and low-grade gliomas (Goel and Lukong, 2016; Zhou *et al*., 2012). However, ectopic FRK was also found to localize to the nuclear region of U87 and U251 glioma cell lines. Additionally, in A549 lung cancer cell line, FRK was shown to co-localize with EGFR in the perinuclear region (Goel and Lukong, 2016; Jin and Craven, 2014). Based on these findings Goel *et al*. suggested that FRK localization may vary in different cell types, or depend on different stages of the cell cycle, or intermolecular interactions mediated by its SH3 and/or SH2 domains and its association with other proteins following direct or indirect phosphorylation which might target FRK to specific sub-cellular sites (Goel and Lukong, 2016).

2.5.4 FRK substrates/interacting proteins

The cellular biochemical functions and the physiological roles of FRK have not been fully characterized. However, FRK-null mice are viable, and display no apparent histological abnormalities in the epithelial organs and cells, except for decreases in the levels of circulating thyroid hormone (Chandrasekharan *et al*., 2002). Furthermore, these mice are neither predisposed to spontaneous tumors nor show altered sensitivity to ionizing radiation (Chandrasekharan *et al*., 2002). The lack of an apparent defect in FRK-deficient mice is an indication that the functions of FRK might overlap with those of other members of the SFKs. Consistent with the growth inhibitory properties of FRK, FRK depletion was shown to induce transformation of the normal MCF-10A mammary epithelial cell line (Yim *et al*., 2009a). Unlike BRK, that has over a dozen characterized substrates, and binding partners, very few substrates/binding partners of FRK have been identified (Brauer and Tyner, 2009; Jin and Craven, 2014; Yim *et al*., 2009a). Reported targets of FRK include CDC2 (cell division cycle 2), CDK4 (cyclin-dependent kinase 4), pRb (retinoblastoma protein), SHB (Src homology 2

protein of beta-cells or SH2 adaptor protein B), PTEN (phosphatase and tensin homolog deleted from chromosome 10), EGFR and, BRCA 1 (Anneren *et al*., 2000; Craven *et al*., 1995b; Kim *et al*., 2014; Jin and Craven, 2014; Yim *et al*., 2009a). CDC2 and CDK4 (but not CDK5, CDK6 or CDK7) were shown to associate with FRK, but the significance of this interaction has not been determined (Pendergast, 1996). The retinoblastoma gene (pRb) is a tumor suppressor gene. The gene product pRb is a crucial regulator of the cell cycle and is frequently inactivated in some human tumors (Giacinti and Giordano, 2006; Weinberg, 1995). pRb associates with various proteins through a 400-amino acid region called the A/B pocket or the C pocket (Giacinti and Giordano, 2006; Weinberg, 1995). In breast cancer cells, FRK was shown to interact with pRb via the A/B pocket and this interaction was highest in the G1 and S phases of the cell cycle (Craven *et al*., 1995b). Also, FRK was shown to interact with ectopically expressed SHB, a ubiquitously expressed adaptor protein that positively regulates cell migration by binding to vascular endothelial growth factor receptor 2 in a Src-dependent manner (Anneren *et al*., 2000; Holmqvist *et al*., 2004).

The first known substrate of FRK reported in the literature was phosphatase and tensin homolog (PTEN). PTEN is also a tumor suppressor and was shown to enhance the stability and function of FRK (Goel and Lukong, 2016; Yim *et al*., 2009a). FRK SH3 domain was shown to interact with PTEN C2 domain thereby phosphorylating PTEN at Y336 leading to PTEN stabilization, thus preventing it from degradation by polyubiquitination (Yim *et al*., 2009a). EGFR another substrate of FRK was reported to be phosphorylated by FRK on its Y1173 hence leading to its degradation or internalization (Jin and Craven, 2014). The phosphorylation of EGFR at Y1173 negatively regulates the activation of EGFR at Y1068. The interaction between FRK and EGFR requires both the SH3 and SH2 domain of FRK (Jin and Craven, 2014). Recently BRCA1 was shown as a substrate of FRK (Kim *et al*., 2015). BRCA1 is a tumor suppressor known to play critical roles in several processes including DNA repair as well as maintenance of genomic stability (Goel and Lukong, 2016; Kim *et al*., 2015). Mutations in both BRCA1 and BRCA2 proteins have been associated with an increased risk of developing breast cancer (Goel and Lukong, 2016; Kim *et al*., 2015). As seen with PTEN, FRK enhances BRCA1 stability and function by phosphorylating BRCA1 on Y1152 thus preventing it from degradation by polyubiquitination (Kim *et al*., 2015). This interaction requires the SH3 domain of FRK and BRCA1-BRCT domain of BRCA1 (Kim *et al*., 2015).

2.5.5 Roles of FRK in cancers

Several studies on FRK in different cancer types have shown that FRK has both oncogenic and tumor suppressive roles (Goel and Lukong, 2016; Pilati *et al*., 2014; Shi *et al*., 2015; Yim *et al*., 2009a; Yim *et al*., 2009b).

The first oncogenic role of FRK was first reported by Hosoya *et al*. They found a chimeric fusion of FRK protein with oncogenic ETV6 transcription factor (Hosoya *et al*., 2005). This ETV6/FRK fused protein had higher enzymatic activity than wild-type FRK thereby promoting leukemogenesis (Hosoya *et al*., 2005). Also, FRK, as well as other SFKs, were reported to promote cell proliferation and survival of pancreatic cancers (Je *et al*., 2014). The knockdown of FRK using specific small interfering RNA transfection was reported to suppress the mRNA expression of FRK and other SFKs hence significantly reduced pancreatic cancer cell migration and invasion (Je *et al*., 2014). Additionally, FRK was found to promote hepatocellular carcinoma (Chen *et al*., 2013). Chen and his colleague's used tumor-associated gene (TAG) database identified 183 tumor-associated genes in which FRK was among them (Chen *et al*., 2013). FRK was upregulated in hepatocellular cell lines tested such as Hep3B and HepG2, and also observed a positive correlation between the levels of FRK and invasiveness of these liver cancer cells (Chen *et al*., 2013). In 2014, Pilati and his group further verified Chen findings, using exome sequencing he was able to identify recurrent somatic mutations in FRK kinase domain. These mutations were shown to induce constitutive FRK kinase activity, STAT3 activation and promote cell proliferation of hepatocellular cancers (Pilati *et al*., 2014).

There are reports of the tumor suppressive role of FRK in various cancers, including breast, glioma, cervical and non-small lung cancers (Sun *et al*., 2015; Yim *et al*., 2009a; Zhang *et al*., 2016; Zhou *et al*., 2012). FRK was first predicted to have a tumor suppressive role in a study where ectopic expression of FRK in NIH3T3 cells decreased the number of colonies. FRK was found to interact with pRb both *in vivo* and *in vitro,* and higher FRK expression was seen in the G1 phase of the cell cycle (Craven *et al*., 1995b). Also, transfection of the constitutively active form of murine FRK (double mutation of Y497/504F) in NIH 3T3 cells was shown to decrease cell growth rate, and also decreased the [3H] thymidine incorporation, this further corroborated craven findings (Oberg-Welsh *et al*., 1998).

Meyer and his group were the first to validate FRK as a tumor suppressor in breast cancer; they showed that FRK inhibits breast cancer cell growth by inducing G1 arrest of the cell cycle (Meyer *et al*., 2003). They also reported that the tumor suppressor activity of FRK was independent of pRb (Meyer *et al*., 2003). There are a few reports of the potential mechanisms by which FRK act as a tumor suppressor. For instance, Yim *et al*. found that FRK interacts and phosphorylates PTEN, thus preventing its degradation (Yim *et al*., 2009a). The group also found that exogenous expression of FRK effectively suppressed breast cancer cell proliferation and invasion, both *in vitro* and *in vivo* and the knockdown of FRK was able to transform normal mammary epithelial cells (Yim *et al*., 2009a).

FRK was shown to suppress glioma cell migration and invasion by inhibiting the c-Jun N-terminal protein kinase (JNK)/c-Jun signaling pathway. Overexpression of FRK inhibited phosphorylation of JNK, c-Jun and inhibited the excretion of the matrix metalloprotease 2 (MMP2) in glioma cells (Zhou *et al*., 2012). It was also shown to inhibit glioma cell invasion by promoting N-cadherin/beta-catenin complex formation (Shi *et al*., 2015). Furthermore, FRK was shown to suppress glioma cell proliferation by inducing G1 phase arrest of the cell cycle, promoting apoptosis, decreasing pRb hyperphosphorylation, downregulating E2F1 and inhibiting cyclin D1 accumulation in the nucleus of proliferating cells (Hua *et al*., 2014).

Another mechanism by which FRK functions as a tumor suppressor includes, internalization or degradation of EGFR (Jin and Craven, 2014) and inducing the stability and function of BRCA1 (Kim *et al*., 2015). In non-small lung cancer, antagomir-1290 was shown to significantly inhibit proliferation, clonogenicity, invasion, and migration by targeting FRK (Sun *et al*., 2015). Recently, FRK has been shown to predict favorable prognosis in patients with cervical cancer (Zhang *et al*., 2016). Here, they found that overexpression of FRK in cervical cancer cells inhibits cell migration and invasion, while the knockdown enhanced cell migration and invasion (Zhang *et al*., 2016).

2.5.6 FRK and signal transduction

In addition to protein interactions, FRK and other PTKs play essential roles in the deregulation of signaling cascades in various cancers (Blume-Jensen and Hunter, 2001). However, the precise signaling pathways regulated by FRK are unknown. Zhou *et al*. found that FRK suppressed glioma cell migration and invasion in a mechanism that involved the inhibition of JUN N-terminal kinase (JNK) and c-Jun activation (Zhou *et al*., 2012). In the context of breast cancer,

FRK was shown to negatively regulate the PI3K-Akt pathway by stabilizing PTEN (Vazquez *et al*., 2000). PTEN is a tumor suppressor frequently lost or inactivated in various human cancers including breast (Georgescu, 2010). PTEN antagonizes PI3K-Akt signaling by dephosphorylating phosphatidylinositol 3, 4, 5-trisphosphate (PIP_3), preventing the activation of PIP_3-binding effector proteins such as Akt (Georgescu, 2010). The PI3K-Akt pathway transduces signals to promote cell growth, proliferation, and survival. Phosphorylation of several serine/threonine residues in the C-tail region of PTEN is essential for PTEN stability (Vazquez *et al*., 2000). FRK was shown to bind to PTEN via its SH3 domain and phosphorylates PTEN specifically on Y336, resulting in PTEN stabilization (Yim *et al*., 2009b). Conversely, the depletion of FRK promoted PTEN polyubiquitination and subsequent degradation (Yim *et al*., 2009b). Although the mechanism of action of FRK is not fully understood, the same study suggests that phosphorylation of PTEN is one potential mechanism of FRK tumor suppressor activity.

FRK has also been shown to regulate EGFR signaling pathway (Jin and Craven, 2014). EGFR is known to promote cell proliferation and migration stimulating several mitogenic signaling pathways such as the KRAS-BRAF-MEK-ERK pathway, phosphoinositide 3-kinase (PI3K), phospholipase C gamma protein pathway, the anti-apoptotic AKT kinase pathway and the STAT signaling pathway (Seshacharyulu *et al*., 2012; Tomas *et al*., 2014). FRK has been shown to downregulates EGFR signaling by phosphorylating EGFR on Y1173 hence leading to its degradation or internalization (Jin and Craven, 2014). The phosphorylation of EGFR at Y1173 negatively regulates the activation of EGFR at Y1068 (Jin and Craven, 2014).

2.6.1 JAK-STAT signaling pathway

The Signal transducer and activator of transcription 3 (STAT3) signaling pathway is a crucial signaling pathway activated in most cancers (Yu *et al*., 2014). STAT3 which belongs to the STAT family has been extensively studied because of its many functions in animal cell growth regulation, inflammation, and early embryonic stimuli (Akira, 2000; Hirano *et al*., 2000). The STAT proteins are transcription factors that regulate the expression of a wide range of genes that promote proliferation, migration. They are constitutively activated in various cancers including breast, colon, gastric, lung, head and neck, skin, and prostate (Levy and Lee, 2002; Sansone *et al*., 2007; Siveen *et al*., 2014; Yu *et al*., 2014). STAT proteins are regulated by the entire IL-6

family of cytokines and transduce signals from receptor and non-receptor tyrosine kinases such as epidermal growth factor receptor (EGF), and JAK (Siveen *et al*., 2014; Yu *et al*., 2014).

STAT3 is thought to be activated primarily by ligand receptors such as (IL-6 and IL- 22) (Siveen *et al*., 2014; Wang *et al*., 2011). Interaction of these receptors results in dimerization of a signal transducer protein gp130 in the cytoplasm, phosphorylation of Janus-kinase (JAK) and subsequent phosphorylation of STAT3 (Siveen *et al*., 2014; Wang *et al*., 2011). The JAK family of tyrosine-kinases especially JAK1 and JAK 2 mediates the activation of STAT3 by phosphorylating it (Hirano *et al*., 2000). The phosphorylated STAT3 monomers combine to form dimers and translocate into the nucleus to induce transcription of genes involved in cell survival and proliferation (**Figure 2.6**) (Chen and Han, 2008; Weerasinghe *et al*., 2008). Several studies have identified other activators of JAK-STAT3 signaling pathway; these include Toll-like receptors (TLRs), (TLR9 and TLR4), microRNAs (miRNAs), and several G-protein-coupled receptors (GPCRs) (Guo *et al*., 2013; Tye *et al*., 2012; Xin *et al*., 2013; Yu *et al*., 2014).

STAT3 has been shown to promote tumorigenesis by regulating several cellular processes that include proliferation, survival, inflammation, invasion, metastasis, and angiogenesis (**Figure 2.7**) (Siveen *et al*., 2014). STAT3 induces cell proliferation by promoting the expression of gene/ proteins that drive the progression of the cell cycle (Carpenter and Lo, 2014). For instance, Cyclin D proteins are known to promote the G1-S phase transition of the cell cycle through it interaction and activation of cyclin-dependent kinases 4/6 (CDK4/6), which phosphorylates the retinoblastoma (pRb) protein thus initiate progression to the S-phase (Bertoli *et al*., 2013; Carpenter and Lo, 2014). STAT3 binding sites have been identified within the Cyclin D1 gene, and a direct association of STAT3 with the Cyclin D promoter have been observed as well as the induction of cell proliferation (Carpenter and Lo, 2014; Leslie *et al*., 2006). Also, STAT3 has been reported to upregulate other genes such as Cyclin B and cdc2, which are involved in cell cycle regulation and cell proliferation (Jarnicki *et al*., 2010; Siveen *et al*., 2014). In addition to cell cycle progression, STAT3 has been shown to promote cell proliferation by inhibiting apoptosis. Anti-apoptotic Bcl-2 proteins, such as Bcl-2 and Mcl-1 have been reported to have binding sites for STAT3 and overexpression of STAT3 has been shown to lead to the upregulation of Bcl-xL, another anti-apoptotic gene (Carpenter and Lo, 2014; Catlett-Falcone *et al*., 1999; Choi and Han, 2012).

STAT3 have been shown to promotes cell invasion and migration by upregulating genes that are involved in cell movement, cytoskeleton reorganization, and cell adhesion properties, these genes include; matrix metalloproteinase (MMP) and intercellular adhesion molecular-1, (ICAM-1) (Carpenter and Lo, 2014; Siveen *et al*., 2014).

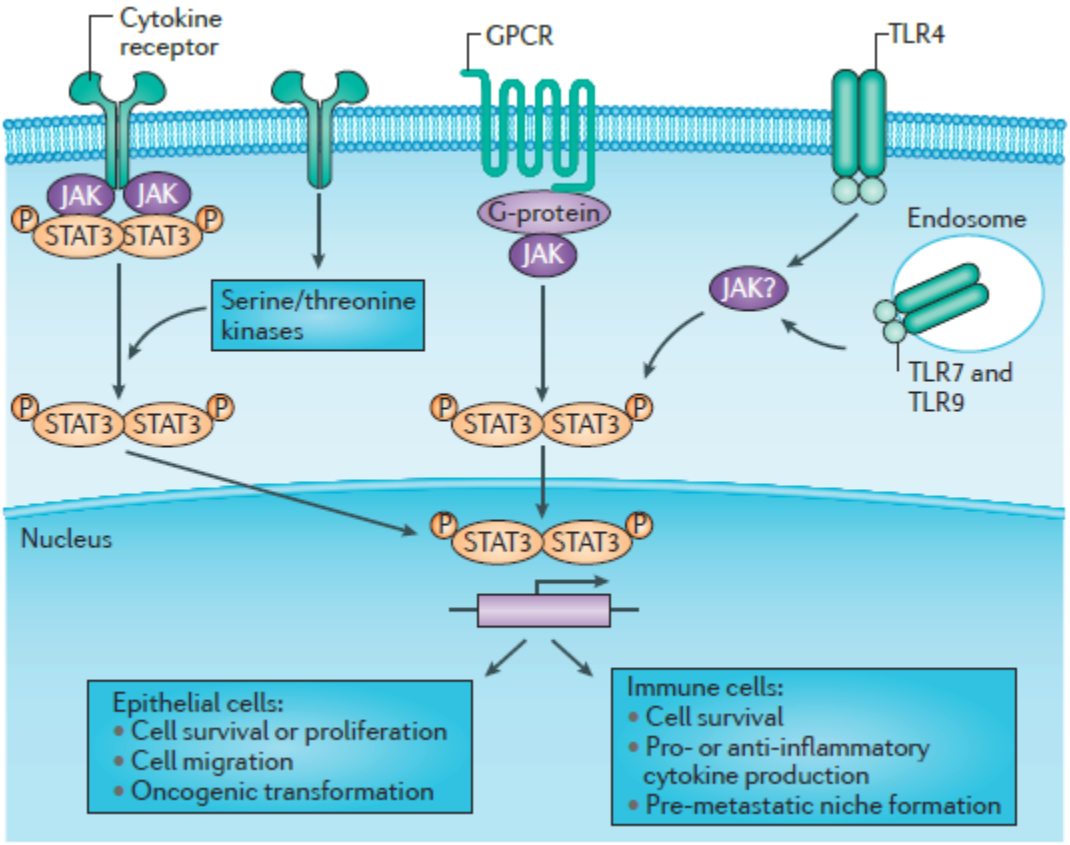

Figure 2.6: Pathways are activating JAK–STAT3 signaling in cancer. Biological processes that are crucial for cancer progression are mediated by Janus kinase (JAK)–signal transducer and activator of transcription 3 (STAT3) signaling. The JAK–STAT3 pathway is activated by diverse receptors, including those for interleukin-6 (IL-6) and IL-6 family cytokines, as well as G-protein-coupled receptors (GPCRs) and Toll-like receptors (TLRs). Unlike receptor tyrosine kinases (RTKs), these receptors lack intrinsic kinase activity. Instead, upon binding to their cognate ligands, these receptors undergo conformational changes and form interacting sites for adaptor proteins to propagate signals. For example, IL-6 receptors rely on the tyrosine kinases JAK1 or JAK2, which associate with the cytoplasmic tail of gp130 and directly phosphorylate (P) STAT3. The gp130 subunit of the IL-6 receptor is the signaling component that is shared with other cytokine receptors. While cytokine receptors and TLRs function as dimers after activation by ligands, G-protein-bound GPCRs catalyze the conversion of guanine nucleotides and activate a sequence of downstream signaling effectors and kinases, including JAK2. Also, JAK2 can act as a direct mediator of certain GPCR signals to activate STAT3. Activated JAKs, such as JAK1 and JAK2, phosphorylate STAT3 at Tyr705, resulting in translocation of activated

STAT3 dimers to the nucleus. Meanwhile, serine/threonine kinases mediate Ser727 phosphorylation of STAT3 that enhances its transcriptional activity. In the nucleus, STAT3 binds to the promoters of genes and induces a genetic program that promotes various cellular processes that are required for cancer progression (Yu *et al*., 2014).

MMP belongs to a family of proteases that are zinc-dependent, they degrade extracellular matrix proteins and also basement membrane for endothelial cell migration (Carpenter and Lo, 2014). Studies have shown that these MMP genes have binding sites for STAT3. For instance, MMP1 contains a STAT3 and an Activator protein 1 (AP-1) binding site, mutation of either the STAT3 or AP-1 site ablated STAT3-mediated gene activation (Carpenter and Lo, 2014; Zugowski *et al*., 2011). Also, STAT3 has been shown to upregulate ICAM- 1, a membrane adhesion molecule which promotes metastasis by making it easier for ICAM-1-expressing tumor cells to separate from each other and invade surrounding tissue (Carpenter and Lo, 2014; Zhu and Gong, 2013).

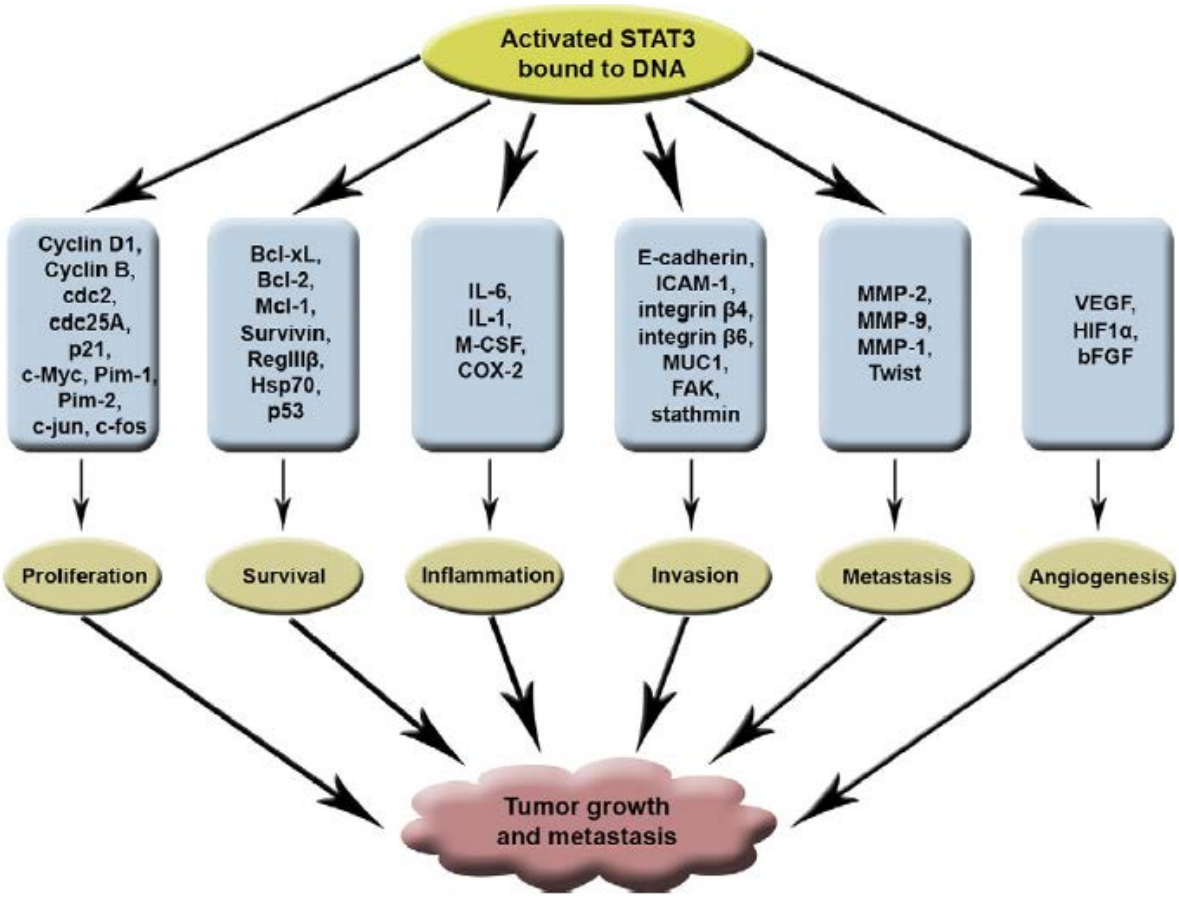

Figure 2.7: **The Multifaceted role of STAT3 in invasion and metastasis.** Activated STAT3 promotes proliferation primarily by stimulating transcription of key cancer genes linked with the

proliferation of tumor cells, such as Cyclin D1, cyclin B, and cdc2, which are involved in the regulation of cell cycle. STAT3 signaling contributes to malignancy by preventing apoptosis pathway via increased expression of Bcl-xL, a member of the anti-apoptotic Bcl-2-family. Several anti-apoptotic proteins, such as Survivin and members of the Bcl family (Bcl-xL, Bcl-2, and Mcl-1), are known to be crucial for tumor cell survival, and are direct target genes of STAT3 and are down-regulated as a consequence of STAT3 inhibition. Degradation and remodeling of the extracellular matrix (ECM) and basement membranes by proteolytic enzymes such as MMPs secreted by tumor cells play a major role in tumor invasion and metastasis. The STAT3 target genes include several members of the MMP family, which are known to contribute to tumor invasion, angiogenesis and metastasis. Excessive activation of STAT3 correlates with tumor invasion and metastasis in a variety of cancers, and high level of phosphorylated STAT3 is a prominent feature in the colon and gastric cancers associated with adverse outcomes. STAT3 interacts with Fra-1/c-Jun and binds to the specific promoter region of MMP-9 gene, leading to transcriptional activation of MMP-9 in breast cancer cell lines (Siveen *et al*., 2014).

2.6.2 Epithelial to Mesenchymal transition in breast cancers

STAT3 has been reported to promote cell invasion and migration by regulating Epithelial to Mesenchymal Transitions (EMT) (Wendt *et al*., 2014). EMT is a biological process that allows a polarized epithelial cell to undergo multiple biochemical changes that enable it to assume a mesenchymal cell phenotype, which includes enhanced migratory capacity, invasiveness, elevated resistance to apoptosis, and significantly increased production of ECM component (Kalluri and Weinberg, 2009). This process leads to a loss of cellular adhesion, changes in the polarization of the cell and cytoskeleton, migration, intravasation, survival in the vascular system, extravasation, and metastasis (**Figure 2.8**) (Fedele *et al*., 2017; Kalluri and Weinberg, 2009). There are three types of EMT programs; they include type 1, Type 2 and type 3 (Felipe Lima *et al*., 2016; Kalluri, 2009; Kalluri and Weinberg, 2009). Type 1 relates to embryogenesis, gastrulation, and neural crest formation, it neither causes fibrosis nor induces an invasive phenotype resulting in systemic spread via the circulation (Felipe Lima *et al*., 2016; Kalluri and Weinberg, 2009). The type 2 EMT is mostly related to tissue regeneration and wound healing; it begins as part of a repair-associated event that usually generates fibroblasts and other related cells to reconstruct tissues following trauma and inflammatory injury. (Kalluri and Weinberg, 2009). Unlike type 1 EMT, type 2 EMTs are associated with inflammation, and it ceases once inflammation is attenuated (Felipe Lima *et al*., 2016; Kalluri and Weinberg, 2009). Lastly, Type 3 EMT is associated with malignancy, invasion, and metastasis; it occurs in neoplastic cells that have previously undergone either genetic and epigenetic change (Kalluri and Weinberg, 2009). Cancer cells undergoing a type 3 EMT may invade and metastasize and thereby lead to life-

threatening manifestations of cancer progression (Felipe Lima *et al*., 2016; Kalluri and Weinberg, 2009).

Type 3 EMT is regulated by some signaling pathways, the major pathways that regulate EMT are the TGF-β, Notch, and Wnt signaling pathways (**Figure 2.9**) (Fedele *et al*., 2017; Felipe Lima *et al*., 2016). Additionally, several molecular processes also regulate EMT; they include transcription factors, expression of specific cell-surface proteins, reorganization and expression of cytoskeletal proteins, production of ECM-degrading enzymes, and expression of specific microRNAs (Fedele *et al*., 2017; Felipe Lima *et al*., 2016; Kalluri and Weinberg, 2009).

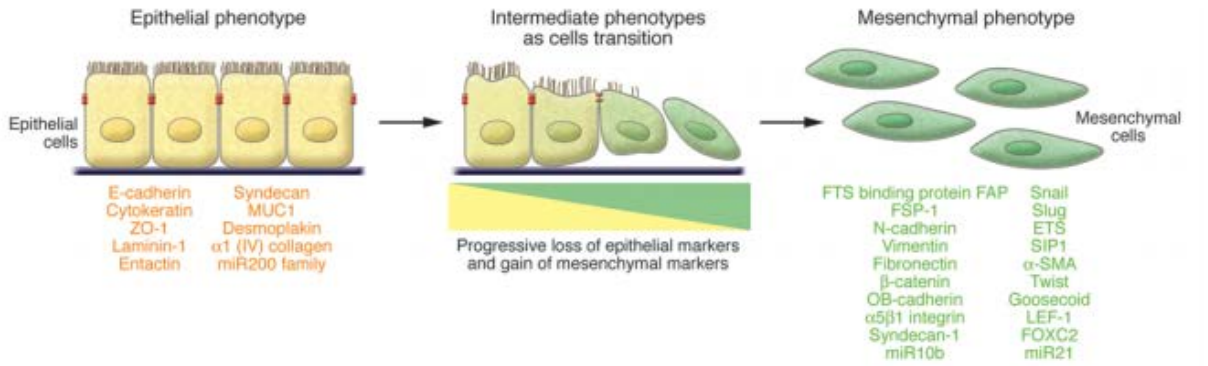

Figure 2.8: EMT. An EMT involves a functional transition of polarized epithelial cells into mobile and ECM component–secreting mesenchymal cells. The epithelial and mesenchymal cell markers commonly used by EMT researchers are listed. (Kalluri and Weinberg, 2009)

There are three main families of transcription factors that regulate EMT. These include SNAI (SNAI1/Snail and SNAI2/Slug), ZEB (ZEB1 and ZEB2), and TWIST (TWIST1 and TWIST2) family. They are all nuclear proteins and have been shown to interact with a variety of proteins involved in transcriptional regulation (Skrypek *et al*., 2017). The expression or post-transcriptional and post-translational of these transcription factors are regulated by the TGF-β, Notch and Wnt signaling pathways (Skrypek *et al*., 2017). TGF-β signaling (both canonical and non-canonical) leads to expression of Snail, Zeb, and Twist. Likewise, Notch signaling pathway induces acts the transcription of SNAI1, SNAI2 (Slug), Twist and Zeb1/Zeb2 by acting on NF-κB. The Wnt pathway leads to induction of SNAI1 expression with subsequent downregulation of E-cadherin via β-catenin (Felipe Lima *et al*., 2016; Skrypek *et al*., 2017).

These transcription factors directly bind to the E-box motifs within the E-cadherin promoter and recruit multiple co-repressors to this region to promote the gene silencing of E-cadherin (Lee and Kong, 2016; Skrypek *et al*., 2017). SNAI1 not only represses E-cadherin expression, but also down-regulates the expression of claudins, occludins, and mucin-1, inducing invasive behavior (Felipe Lima *et al*., 2016). It also leads to increased expression of mesenchymal proteins, such as the intermediate filament protein Vimentin, contributes to the enhanced migratory properties of EMT cells (Lamouille *et al*., 2014; (Karlsson *et al*., 2017). Distinct cellular and extracellular markers characterize the EMT status. Epithelial cells express a series of cell adhesion molecules, including E-cadherin, desmoplakin, ZO-1, cytokeratin, laminin, MUC-1, while mesenchymal-like cells lose these epithelial markers and gain the expression of mesenchymal markers, including Vimentin, N-cadherin, and Fibronectin (Lee and Kong, 2016).

Additionally, miRNA have been reported to play an essential role in regulating EMT (Fedele *et al*., 2017; Felipe Lima *et al*., 2016; Prieto-Garcia *et al*., 2017). For instance, the miR-200 family (miR-200a, miR200b, miR200c, miR141, and miR-429) regulate EMT by repressing the expression of transcription factors such as of ZEB1/2 transcription factors and an increase in epithelial markers expression (Prieto-Garcia *et al*., 2017).

Over 90% of all breast cancer deaths are the result of metastasis, primarily to the bone, lung, liver, and brain (Fedele *et al*., 2017; Gao *et al*., 2016). Some studies have shown a strong correlation between the EMT and high invasive and metastatic behavior of breast cancers (Fedele *et al*., 2017; Gao *et al*., 2016). For example, the basal-like breast cancer phenotype have been recently reported to be associated with mesenchymal features, hence reasons for being the most deadly subtype (Fedele *et al*., 2017; Gao *et al*., 2016). These basal-like breast cancers have been shown to have low expression of GATA3-regulated genes, genes involved in cell-cell adhesion, high expression of stem cells and EMT markers (Fedele *et al*., 2017; Gao *et al*., 2016).

2.6.3 Cell cycle regulation

In addition to EMT, STAT3 has also been shown to regulate cell proliferation by upregulating genes that inhibit apoptosis, for instance, anti-apoptotic genes such as Bcl-2 and Mcl-1 (Carpenter and Lo, 2014; Catlett-Falcone *et al*., 1999; Choi and Han, 2012). It is worth mentioning that EMT has also been reported to promote cell proliferation by regulating the cell cycle (Jiang *et al*., 2011; Karlsson *et al*., 2017). Jang and his group found that Twist, (a

transcription factor) inhibits p16 and p21 (CDK inhibitors) known to regulate the cell cycle negatively, thus promoting cell proliferation (Jiang *et al*., 2011; Karlsson *et al*., 2017). The uncontrollable growth characteristics of cancer cells are as a result of defects in the cell cycle. The cell cycle can be defined as a cell-autonomous mechanism operated by a small number of enzymes, mainly the cyclin-dependent kinases (CDKs), whose primary function is to ensure a timely control of its 2 fundamental steps: DNA replication and chromosome segregation (Bendris *et al*., 2015). These CDKs functions are regulated by specific cofactors such as cyclin and CDK inhibitors (CKI) (Bendris *et al*., 2015).

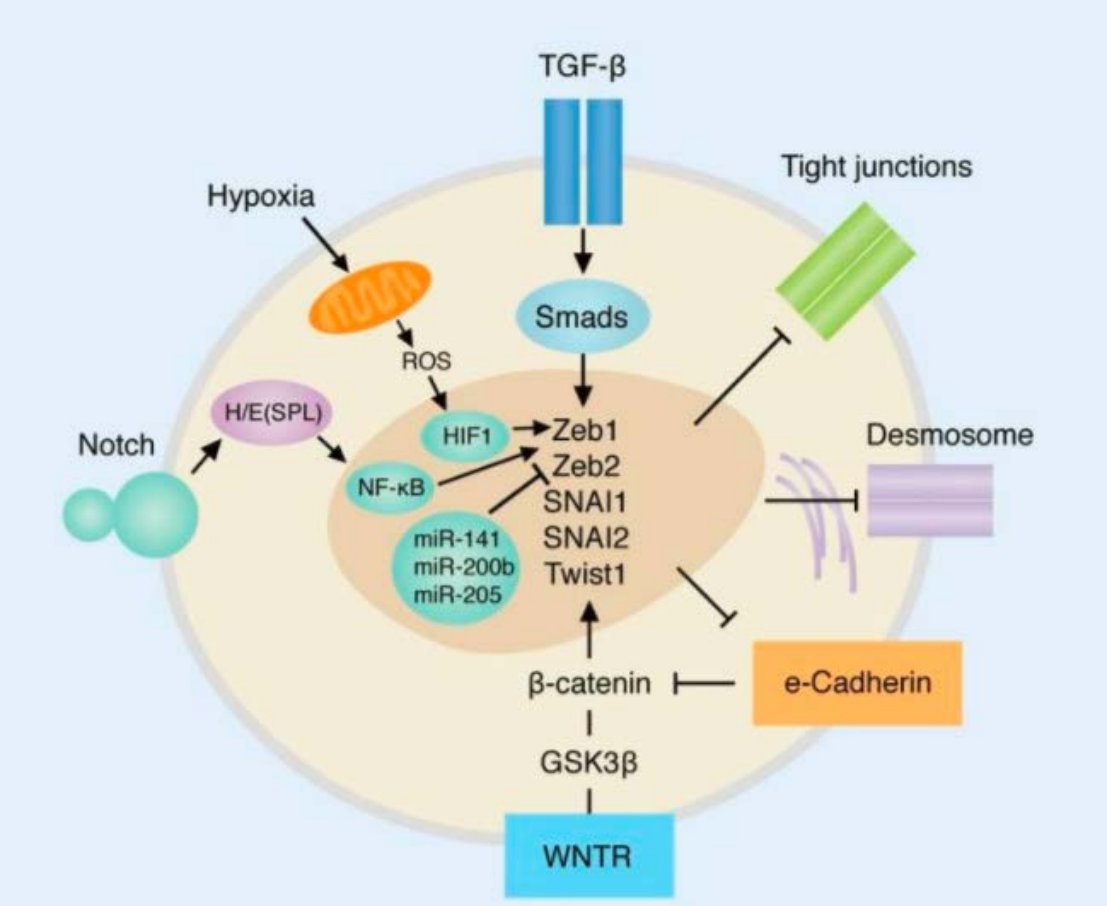

Figure 2.9: Epithelial to mesenchymal transition overview. Selected signaling pathways are depicted. Transforming growth factor-β, Notch, WNT can induce EMT through multiple pathways. EMT and MET (mesenchymal to epithelial transition) are associated with changes in the cytoskeleton and disruption of tight junctions and desmosomes. They are also influenced by the effects of the tumor microenvironment such as hypoxia as well as the differential expression of microRNAs (miRNAs). External stimulus, as in the case of hypoxia, leads to changes in mitochondrial function, leading to HIF1 stimulation, with subsequent Zeb1 expression. (Felipe Lima *et al*., 2016)

Cyclins bind to CDKs to form a cyclin-CDK complex (Bendris *et al*., 2015; Hydbring *et al*., 2016). These complexes phosphorylate a number of cellular proteins that promote entry into the cell cycle, regulate DNA synthesis and trigger segregation of the newly duplicated chromosomes to the daughter cells during mitosis (Bendris *et al*., 2015; Hydbring *et al*., 2016), whereas CKIs act both as architectural and inhibitory components (Bendris *et al*., 2015; Hydbring *et al*., 2016).

Cell proliferation depends on progression through four distinct phases of the cell cycle (G0/G1, S, G2, and M), and these phases are regulated by cyclin-dependent kinases (CDKs), their cyclin partners and CKI (Otto and Sicinski, 2017). In the G1 phase, Cyclin D interacts with CDK4 or CDK6 and phosphorylates the retinoblastoma protein (pRb), p107 and p130 proteins, which bind and regulate E2F transcription factors. Later during G1, Cyclin E1 and E2 become upregulated and activate CDK2, resulting in phosphorylation of a broader range of cell cycle-related proteins. In the S phase, Cyclin A are upregulated, this leads to the activation of CDK2 and CDK1. CDK1 are also activated by Cyclin B, this occurs at the onset of mitosis and drives the progression of cells through the remainder of the cell cycle, through phosphorylation of a large number of proteins involved in DNA replication, as well as centrosome and chromosome function (Hydbring *et al*., 2016).

The CKI belongs to two families: the INK4 (composed of P15, p16, p18 and p19) and Cip/ Kip family (composed of p21, p27, and p57) (Malumbres and BapRbacid, 2009; Otto and Sicinski, 2017). The INK4 families bind to CDK4/CDK6 and block their association with D-type cyclins, thereby extinguishing the kinase activity of CDK4 and CDK6, whereas the CIP/KIP families bind to all CDK complexes and inhibit the kinase activity of CDK2 and CDK1 (Otto and Sicinski, 2017). These inhibitors have been shown to block proliferation of adult stem cells in multiple tissue types. For instance, p21 and p27 may control self-renewal of neural, intestinal and hematopoietic progenitors (Malumbres and Barbacid, 2009).

2.6.3.1 Regulation of cell cycle in breast cancer

The cell cycle is deregulated through various mechanisms that include amplification, mutation and overexpression of the genes encoding the core components of the cell cycle such as the cyclins, CDKs, CKIs and the retinoblastoma protein pRB and E2F1 (Johnson *et al.*, 2016). For instance, Cyclin D1 gene is the second most frequently amplified locus gene in most types of human cancers (Hydbring *et al*., 2016).

E2Fs are transcription factors and comprise a family of ten proteins encoded by eight distinct genes, and they are most well known for their function in cell cycle regulation. E2Fs 1, 2, and 3a are transcriptional activators, whereas E2F3b, 4, and 5 the passive repressors, and E2F6, 7a, 7b, and 8 are active repressors. E2F 1, 2 and 3 stimulate proliferation by inducing the expression of genes that stimulate the progression of the cell cycle. In most cancers, E2Fs have been identified as a factor that promotes tumor progression. For instance, in HRAS-dependent breast cancer, E2Fs1-3 was found to induce the expression of the β4 integrin subunit, hence enhances invasion mediated by the α6β4 integrin (Johnson *et al*., 2016; Yoon *et al*., 2006).

pRb is a known tumor suppressor that associate with E2F family proteins and thereby inhibit E2F-dependent activation of genes that stimulate DNA synthesis and cell cycle progression (Dick and Rubin, 2013). pRb is regulated through phosphorylation when pRb is hyperphosphorylated by cyclin-CDK complexes, it leads to its disassociation from E2F, thus promoting the advancement of the cell cycle. However, when pRb is hypophosphorylated, it binds to E2F leading to its inhibition (Dick and Rubin, 2013). Loss of pRb has been shown to promote breast tumorigenesis. A study on a panel of breast cancer cell lines showed that the breast cancer cell lines with inactive pRb had increased expression of mesenchymal phenotype and high expression of genes involved in EMT (Arima *et al*., 2012; Johnson *et al*., 2016). Also, the loss of pRb in ERBB2 overexpressed breast cancer cell was found to altered essential molecules needed for proper cellular organization and cell-to-cell adhesion (Johnson *et al*., 2016; Witkiewicz *et al*., 2014).

CKIs have been reported to prevent pRb phosphorylation by inhibiting CDK activity thereby inducing growth arrest. For instance, p21, a regulator of cell cycle progression during the G1 and S phases have also been reported to inhibit CDK activity by indirectly interfering with phosphorylation of CDK1 and CDK2 in the activation segment by an unidentified mechanism (Abbas and Dutta, 2009; Johnson *et al*., 2016). The inhibition of these CDKs prevents the phosphorylation of pRb and the release and activation of E2F-dependent gene expression leading to growth arrest of the cell cycle (Abbas and Dutta, 2009). Loss-of-function expression of p21 and p27 have been implicated in breast carcinogenesis and progression; it has also shown to mediate drug-resistance phenotype (Abukhdeir and Park, 2008; Zagouri *et al*., 2017).

2.6.4 Cell senescence

In addition to growth arrest, p21 can mediate cellular senescence in a variety of mammalian cells and tissues (Georgakilas *et al*., 2017). An extensive microarray-based study showed that p21 expression positively correlates with both the suppression of gene activities directly involved in cell cycle progression and the activation of genes associated with senescence (Georgakilas *et al*., 2017).

Cellular senescence can be defined can be defined as irreversible growth arrest or lack of proliferative potential characterized by distinct metabolic activity and dramatic changes in cell morphology (Gire and Dulic, 2015; Terzi *et al*., 2016). There are two types of Senescence; they are replicative and oncogene-induced senescence. Replicative senescence is one of the common types of cellular senescence. It occurs due to devoid of telomere shortening repair system or impaired telomerase activity or due to sustained DNA damage response (DDR) in normal cells (Masutomi *et al*., 2003; Terzi *et al*., 2016). While oncogene-induced senescence otherwise known as ‘‘permanent quiescent’’ occur due to overstimulation of growth-promoting pathways leading to senescence-like phenotype such as hyperactivity and hypertrophy (Blagosklonny, 2013; Terzi *et al*., 2016). Oncogene-induced senescence mediates its effect by using CDK inhibitors (Blagosklonny, 2013; Terzi *et al*., 2016).

Cells with damaged DNA as a result of telomere erosion or activated oncogenes have been reported to activate the ATM/ p53/p21 pathway hence inducing senescence-associated G1 arrest (**Figure 2.10).** This pathway activates p53, a tumor suppressor which induces the expression p21 (Gire and Dulic, 2015).The mouse double minute 2 (MDM2) proto-oncogene is a regulatory protein regulates p53 expression, when p53 intracellular levels increase, it binds to MDM2 to induce its transcription, and then MDM2 initiates the ubiquitination and proteolytic degradation of p53 under normal conditions (Terzi *et al*., 2016). A recent study shows that p53 downstream pathway players (e.g., p16, p21) also drive the transition of cancer cells into senescence in the absence of p53 by inactivation of cyclin D1-Cdk4/6 and cyclin E1-Cdk2 complexes (Kovatcheva *et al*., 2015; Terzi *et al*., 2016). p21 blocks the inactivating phosphorylation of pRb by Cdk2 and Cdk4/6, which is a critical mechanism in the senescence program. p16, another pRb regulator that inhibits explicitly the cyclin D1-associated kinases Cdk4 and Cdk6, was also implicated in senescence (Gire and Dulic, 2015).

Cellular senescence is identified by senescence biomarkers such as senescence-associated β-galactosidase (SA-β-gal), It is characterized by the senescence-associated secretory phenotype (SASP), referring to increased expression and secretion of inflammatory cytokines, chemokines, growth factors, proteases and other proteins in senescent cells (Freund *et al*., 2010; Xu *et al*., 2014). The SASP factors are critical for the initiation and maintenance of senescence in a cell-autonomous fashion. Accumulation of senescence-associated heterochromatic foci (SAHFs) have been identified in cells that undergo cellular senescence, SAHFs recruit pRb, and heterochromatin proteins to stably silence the expression of E2F target genes that are necessary for cell proliferation, these changes in chromatin brought about by SAHF formation are believed to mediate the irreversibility of senescence (Xu *et al*., 2014).

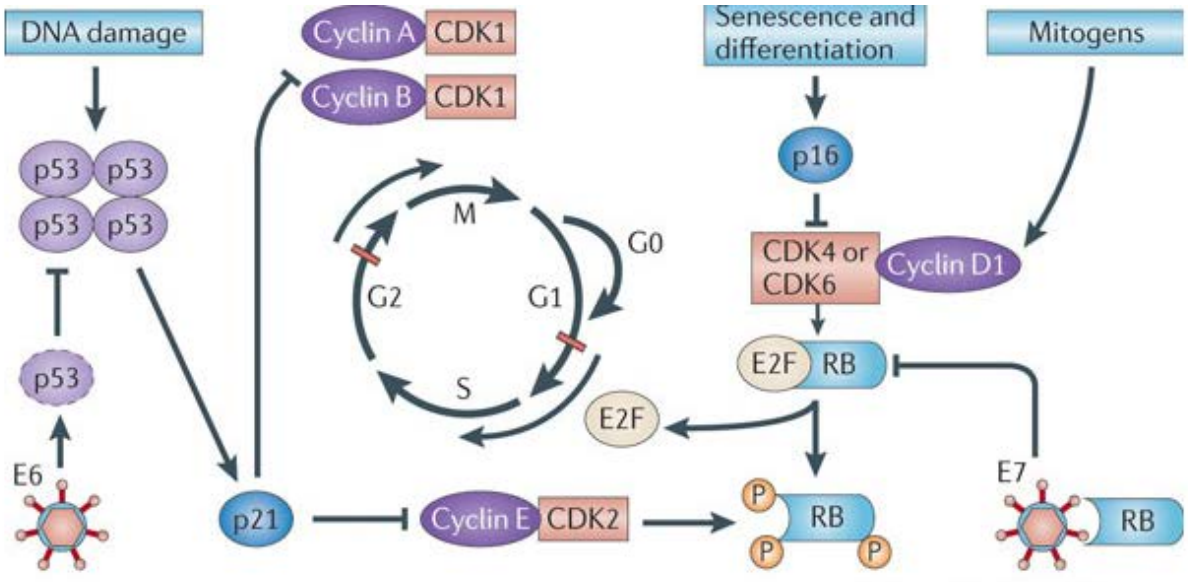

Figure 2.10: Cell cycle deregulation. The cell cycle is regulated by complexes of cyclins and cyclin-dependent kinases (CDKs). In addition, there are various important inhibitors of these cyclin–CDK complexes. These are p16 and p21. The expression of p16INK4A mediates senescence and differentiation. p53 tetramers act as a stress-induced transcription factor and induce the expression of p21CIP (also known as CDKN1A), which inhibits several cyclins–CDK complexes and halts the cell cycle. Besides its crucial role in cell cycle control, p53 is also a master regulator of apoptosis and many other stress-associated cellular functions and is, therefore, one of the primary targets for inactivation in many cancers. E6 and E7 are viral oncoproteins. The E6 protein binds p53 and targets the protein for degradation, whereas the E7 protein binds and inactivates the PRb pocket proteins (Leemans *et al*., 2011).

2.7 Objectives and rationale

2.7.1 Rationale

FRK is a candidate tumor suppressor in breast cancer. FRK was shown to suppress breast cancer tumorigenesis by negatively regulating several signaling pathways, including the AKT pathway by stabilizing PTEN and preventing it from degradation, and DNA damage pathway by stabilizing BRCA1, as well as potentially by binding to pRb.

Additionally, previous study from our lab has shown that FRK downregulates STAT3 phosphorylation. The suppression of STAT3 activation by FRK was seen with both the wild-type FRK and the constitutively active form of FRK (FRK-YF or FRK-YF). We also found that FRK-YF induces the phosphorylation of numerous targets that do not overlap with FRK-WT targets. Also, FRK inhibition of breast cancer proliferation was reported to be independent of its binding to pRb.

Based on this, we intend to identify novel FRK regulated signaling pathways in breast cancers, validate STAT3 as a target of FRK and investigate other mechanisms by which FRK suppresses breast cancer proliferation. Additionally, we intend to evaluate the effect of FRK overexpression on tumor formation *in vivo*.

2.7.2 Hypothesis and Objectives

2.7.2.1 Hypothesis

We hypothesize that FRK suppresses tumor growth by inhibiting JAK/STAT signaling and related cellular processes.

2.7.2.2 Objectives

1. To validate the effect of FRK on STAT3 signaling.
2. To determine the mechanism of action of FRK on STAT3 inactivation.
3. To determine the effect of FRK on the expression of STAT3 target genes.
4. To determine the effect of FRK on EMT and cell cycle.
5. To validate the tumor suppression role of FRK *in vivo* using xenograft mice

3.0 MATERIALS AND METHODS

3.1 Reagents

The list of reagents and antibodies used for these experiments are listed in **Table 3.1** and **Table 3.2**

Table 3.1: List of reagent and suppliers

S/N	Types of Reagent	Reagents	List of Suppliers and location
	Organic and Inorganic reagents	**<u>Western blot reagent</u>** Acrylamide, 0341	AMRESCO (North York, Ontario, Canada)
		Aprotinin, A6279	SigmaAldrich (Oakville, Ontario, Canada)
		Ammonium persulfate (APS),A3678	SigmaAldrich (Oakville, Ontario, Canada)
		Laemmli sample buffer, S3401	SigmaAldrich (Oakville, Ontario, Canada)
		SDS, 151-21-3	SigmaAldrich (Oakville, Ontario, Canada)
		Methanol, MX0485	EMD (Madison, Wisconsin, USA)
			AMRESCO (North York, Ontario, Canada)

		Glycine, 0167	
		Sodium chloride (NaCl), 0241	SigmaAldrich (Oakville, Ontario, Canada)
		Tris, 0826	SigmaAldrich (Oakville, Ontario, Canada)
		TWEEN® 20, 0777	AMRESCO (North York, Ontario, Canada)
		Difco™ skim milk, 232100	BD (Mississauga, Ontario, Canada)
		Bisacrylamide,0172	AMRESCO (North York, Ontario, Canada)
		Gelatin, G1890	SigmaAldrich (Oakville, Ontario, Canada)
		Sodium azide, S8032	AMRESCO (North York, Ontario, Canada)
		Triton™ X-100, X-100	SigmaAldrich (Oakville, Ontario, Canada)
		Paraformaldehyde, PX0055-3	AMRESCO (North York, Ontario, Canada)
		Polyethylenimine, 25987-06-8	SigmaAldrich (Oakville, Ontario, Canada)
		RT-PCR reagents	Qiagen, (Mississauga ON, Canada)
		RNeasy Plus Mini Kit	

		Iscript cDNA Synthesis Kit	Bio-Rad, (United States).
	Cell culture	Dulbecco's Modified Eagle Medium (DMEM), SH30022.01	Thermo Fisher Scientific (Whatham, Massachusetts, USA)
		Mcoy	Thermo Fisher Scientific (Whatham, Massachusetts, USA)
		Fetal Bovine Serum (FBS), SH30397.03	Thermo Fisher Scientific (Whatham, Massachusetts, USA)
		Trypsin-EDTA, T4049	SigmaAldrich (Oakville, Ontario, Canada)
		MEM Vitamin Solution, 11120-052	Gibco (Burlington, Ontario, Canada)
	Bacteria culture	Ampicillin, 0339	AMRESCO (North York, Ontario, Canada)
		Tryptone, 1.07213.1000	EMD (Madison, Wisconsin, USA)
		Fermtech® Yeast Extract, 1.11926.1000	EMD (Madison, Wisconsin, USA)

		Kanamycin sulfate, 0408 Lysogeny Broth (LB) agar, L2897	AMRESCO (North York, Ontario, Canada) SigmaAldrich (Oakville, Ontario, Canada)
	Cell cycle analysis	Senescence kit 7AAD Annexin/FTTC kit	Bio-vision Bio-vision Bio-vision

3.2 Antibodies and inhibitors

The following primary antibodies were purchased from Santa Cruz Biotechnology (California, USA): FRK (N19, sc-916), JNK 1/2 (sc-137020), pJNK (sc-81502), p38 (sc-535), p-p38-Thr180/Tyr182 (sc-17852) and β-tubulin (sc-9104), SLUG (sc-166476), Fibronectin (sc-8422) anti-GFP (sc-8334), β-actin (sc-130300), pTyr 20 (sc-508), pSTAT3- S7272 (sc-8001),. STAT3, pSTAT3 705 (9145S), AKT (9272S), pAKT-S473 (4058S), MEK1/2 (9126) and pMEK1/2-S217/21 (9154S), were purchased from Cell Signaling (Massachusetts, USA).

Table 3.2: List of antibodies used with suppliers

S/N	**Antibodies and working dilutions**	**Supplier**
	FRK (N19, sc-916), (1:1000) STAT3 (9145S), (1:2000) pSTAT3 TYR705(9145S), (1:2000)	Santa-cruz Cell Signaling (Massachusetts, USA). Cell Signaling (Massachusetts, USA). Santa Cruz

	pSTAT3 S7272 sc-8001 (1:1000)	Biotechnology (California, USA)
	E-cadherin (1:2000)	Cell Signaling (Massachusetts, USA).
	N-cadherin (1:1000)	Santa Cruz Biotechnology (California, USA)
	Fibronectin (sc-8422) (1:1000)	Santa Cruz Biotechnology (California, USA)
	pRb (1:1000)	Santa Cruz Biotechnology (California, USA)
	E2F1 (1:1000)	Santa Cruz Biotechnology (California, USA)
	Cyclin E (1:1000)	Santa Cruz Biotechnology (California, USA)
	p21 (1:1000)	Santa Cruz Biotechnology (California, USA)
	Beclin (1:1000)	Santa Cruz Biotechnology (California, USA)
	Slug (sc-166476) (1:1000)	Santa Cruz Biotechnology (California, USA)
	β -actin -sc-130300 (1:1000)	Santa Cruz Biotechnology (California, USA)

	β -tubulin -sc-9104 (1:1000)	Santa Cruz Biotechnology (California, USA) Santa Cruz Biotechnology (California, USA) Santa Cruz Biotechnology (California, USA) Santa Cruz Biotechnology (California, USA) Santa Cruz Biotechnology (California, USA)

3.3 Primers

The list of primers used in the quantitative PCR analysis of transcript expression of the target genes relative to the housekeeping gene (GAPDH) in breast cancer cells are listed in **Table 3.3**. Directions of the primers are as listed (forward or reverse).

Table 3.3: List of primers used for RT-PCR

Target Gene	**Direction**	**Sequence**
GAPDH	Forward	5′GTCAGTGGTGGACCTGACCT 3′
	Reverse	5′TGCTGTAGCCAAATTCGTTG 3′
SURVIVIN	Forward	5′GGACCACCGCATCTCTACAT 3′

	Reverse	5′GACAGAAAGGAAAGCGCAAC 3′
MMP1	Forward	5′GGACCACCGCATCTCTACAT 3′
	Reverse	5′GACAGAAAGGAAAGCGCAAC 3′
FIBRONECTIN	Forward	5′CCCAACTGGCATTGACTTTT 3′
	Reverse	5′ CTCGAGGTCTCCCACTGAAG 3′
VIMENTIN	Forward	5′ GAGAACTTTGCCGTTGAAGC 3′
	Reverse	5′ TCCAGCAGCTTCCTGTAGGT 3′
CYCLIN D1 (CCND1)	Forward	5′ GATCAAGTGTGACCCGGACT 3′
	Reverse	5′ TCCTCCTCTTCCTCCTCCTC 3′

3.4. Cell lines and Cell culture

Breast cancer cell lines (AU565, BT20, MDA-MB 231, MDA-MB-468, HCC 70, BT 549, SKBR3, T47D, MCF 10A, MCF-7) and human embryonic kidney 293 (HEK293) cells were purchased from the American Type Culture Collection (ATCC, Manassas, VA, USA). The cell lines were cultured in high glucose (4.5 g/l), Dulbecco's modified Eagle's medium (DMEM) supplemented with 10% fetal bovine serum (FBS) (Thermo Scientific, Logan, USA) and contained 4mM L-glutamine, 100 units/ml penicillin, 100 mg/ml streptomycin (Sigma-Aldrich, St Louis, MO, USA). SKBR3 cell line was cultured in McCoy culture media with 10% fetal bovine serum (FBS) (Thermo Scientific, Logan, USA). All the cell lines were incubated in a humidified CO_2 incubator (Thermo Fisher Scientific) with 5% CO_2 at 37^0C. Upon cells confluency, Trypsin-EDTA (0.25 % (w/v) was used to detached and split into new culture plates.

3.5 Transformation of plasmids into Ecoli

Green fluorescent protein (GFP)-tagged as well as retroviral lysophosphatidylcholine (LPC) of FRK-WT (wild-type), and FRK mutants plasmids (FRK-YF and FRK-K262M) were obtained from Dr.Lukong's lab. Maxi-prep was made for these plasmids. To make the maxi-prep, first, the DNA was transformed into E.coli DH5α cells which served as the host. 5 µL of the DNA was

added into 50 µL competent cells once the cells were thawed, and left on ice for 30 minutes, after which it was exposed to heat shock at 42^0C for 45 seconds and 2 minutes cold shock. 500 µL antibiotic-free LB Broth medium, containing Tryptone, Fermtech® Yeast Extract, NaCl, and ddH_2O, was added into the mixture, and the mixture was incubated in a shaker at 37^0C for 1 hour. The mixture was centrifuged at 20,000 × g for 30 seconds, and 450 µL of the cell supernatant was removed. The remaining cells were resuspended and plated on LB agar plates containing the 10% appropriate antibiotic(s) (kanamycin for pLPC; ampicillin for pEGFP-C1). The antibiotic resistance markers on plasmids facilitated the screening of the recombinants. The successful recombinants transformed plasmid DNA was selected by picking up single colonies after 16-18 hours culture 37^0C. The plasmid DNA was prepared and sent for sequencing to verify the mutations. Sequencing was performed by National Research Council Canada DNA sequencing facility (Saskatoon, SK). The DNA mutants with the right mutations were prepared in large scale using maxi-prep kit obtained from Qiagen. The procedure used was according to the manufacture protocol.

3.6 Transfection (transient and generation of stable cell lines)

Transient transfection was done according to standard operating procedure of Dr. Lukong lab. HEK 293 cells were used for the transiet transfection. The cells were cultured in 6-well plates and transiently transfected with 2.5 µg of DNA using 1% polyethyleneimine 'Max' (PEI) (Polysciences Inc., Warrington, PA, USA). For each well, 2.5 µg of DNA was added to 107.5 µL of sterile 0.15M NaCl in a microcentrifuge tube and vortexed gently for 10s. 15 µl 0.1% PEI was added to the DNA mixture and vortexed gently for 10 seconds. The DNA–PEI complex was incubated for 10 min at room temperature, and the mixture was added dropwise to wells containing 2 mL of complete media and incubated at 37 ^{0}C. The cells were incubated for 24 h post transfection and harvested the next day. Transient knockdown of FRK in SKBR3 and MCF-7 was carried out using FRK-siRNA (Santa Cruz, CA, USA), as recommended by the manufacturers.

MDA-MB 231 stably expressing FRK-wild-type and FRK-YF was generated using the method previously described (Miah *et al*., 2012). HEK 293-derived Phoenix packaging cells were transfected with the retroviral plasmids constructs. The viral supernatant was used to infect MDA-MB 231 cells. Puromycin was used to select the pLPC-containing cells. All untransduced MDA-MB 231 cells died within 7 days of selection. However, the selected stable cell lines were

cultured in puromycin for 4 weeks. FRK expression levels were measured in the stable cells using western blot analysis.

3.7 Preparation of cell lysates

The whole procedure was done at 4^0C before adding the Laemmli sample buffer. 10 cm cultures plates containing breast cancer cells were harvested using Trypsin-EDTA (0.25 % (w/v), and transferred into pre-cooled microcentrifuge tubes. The cells were centrifuged at 750 × g for 5 minutes and washed twice with ice-cold PBS. Cells were lysed using freshly prepared lysis buffer (20 mM Tris ph 7.5, 1% Triton, 150 mm NaCl, protease inhibitors: Aprotinin 5 mg/l and PMSF 0.1 mM) for 30 minutes on ice and centrifuged at 14,000 rpm for 15 minutes at 4^0C. Cell debris was removed by full speed centrifugation for 15 minutes, and the Lowry's assay was used to measured protein concentration. 2× Laemmli sample buffer was added to the lysates, and boiled at 100^0C for 5 minutes, the lysates were stored at -20^0C.

3.8 Sodium Dodecyl Sulfate Polyacrylamide Gel Electrophores

Sodium Dodecyl Sulfate Polyacrylamide Gel Electrophoresis (SDS-PAGE) using vertical Mini-PROTEAN® Tetra cell electrophoresis system (Bio-Rad 165-8006). The gel was made according to the standard operating procedure of Dr. Lukong lab. 1.5 mm thickness gel was clamped between a short plate and a spacer plate, and the casting frame was assembled on casting stands. 10% resolving gel was used for SDS-PAGE in these experiments. The 10% resolving gel consists of dH_2O, 375 mM Tris-HCl (pH 8.8), 30% (w/v) acrylamide/bisacrylamide (29:1), 0.4% (w/v) SDS and 0.16% (w/v) ammonium persulfate, and 0.1% N,N,N',N'-Tetramethylethylenediamine was poured in the plates and left for 45 minutes to solidify. After the solidification of the resolving gel, the stacking gel which consisted of dH_2O, 0.5 M Tris-HCl (pH 6.8), 30% (w/v) acrylamide/bisacrylamide (29:1), 0.4% (w/v) SDS and 0.16% (w/v) ammonium persulfate, and 0.1% N,N,N',N'-Tetramethylethylenediamine was added and left for 30 minutes to solidify. 10-well or 15-well-forming combs were inserted in the stacking gel according to the loading volume of the samples. The samples were preheated and prestained protein ladder (ColorPlus, NEB, P7711S) was added. The mixture were loaded when the polymerization of the gel was completed. The SDS-PAGE was performed using 1× running buffer containing 0.1% SDS, 25mM Tris, 192 mM glycine, and dH2O; pH 8.3 at a constant

voltage of 125 V for 90 minutes at room temperature. Subsequently, the gel was analyzed by western blot analysis.

3.8. 1. Western blot analysis

After resolving the proteins derived from whole cell lysates via SDS-PAGE in 10% polyacrylamide gels, a western blot analysis was done. First, a transfer stack was prepared as follows: the SDS-PAGE gel was overlayed with the BioTrace™ nitrocellulose membrane (Pall Corporation, P/N 66485), and was sandwiched between 3 sheets of 3 MM filter paper (Whatman 3030-6189). The nitrocellulose membranes were pre-soaked in the transfer buffer (20% methanol, 25 mM Tris, 192 mM glycine, and dH2O; pH 8.3) at 4^0C for 15 minutes. The proteins were transferred to the nitrocellulose membrane by placing the prepared transfer stack in Mini Trans-blot® electrophoretic transfer apparatus (Bio-Rad, 170-3930) within transfer buffer, and then a constant voltage of 100 V was applied for 80 minutes at 4^0C.

The transferred nitrocellulose membrane was soaked in blocking solution (5% Difco™ Skim Milk, 0.05% sodium azide, and 1× TBST) at room temperature for 40 minutes, and rinsed with 1× TBST. The nitrocellulose membranes were immunoblotted with the appropriate antibodies via overnight incubation at 4^0C. The membranes were washed three times for 5 minutes each with PBST and incubated for 1 h with fluorescent secondary antibodies (LI-COR Biotechnology, Guelph, ON, Canada). LI-COR Odyssey imaging system (LI-COR Biotechnology) was used to obtain the protein images.

3.9. RT-PCR

Total RNA was isolated from cell lines using RNeasy Plus Mini Kit (Qiagen, Mississauga ON). The RNA quantity and quality was analyzed using a spectrophotometer (Nanodrop) and gel electrophoresis. 1.0 μg of total RNA was used as a template to generate cDNA according to the manufacturer procedure using the Iscript cDNA Synthesis Kit (Bio-Rad, United States). 1.0 μg of the RNA was added to 4 μl 5x iScript reaction mix, 1 μl iScript reverse transcriptase, and sufficient nuclease-free water to a reaction volume of 20 μl. The reaction was incubated at 25°C for 5 min, 42°C for 30 min, and 85°C for 5 min, and then stored at −20°C. The cDNA synthesized was used as a template in quantitative RT-PCR reactions. Quantification of the expression *GAPDH*, *SURVIVIN*, *MMP1*, *FN1,* and *VIMENTIN* was performed using primers listed in **Table 3.3** and sybr green SsoFast^{TM} EvaGreen Supermix$^{(R)}$ (BIO-RAD) as described previously (Miah *et al*., 2014). The expression of *FRK*, *SLUG*, and *GAPDH* was determined

using TaqMan probes Hs00176619_m1, Hs00950344-m1, and Hs02758991-g1, respectively as recommended by the manufacturer (Life Technologies, Burlington, ON, Canada. 0.5 µL of probes for the target and housekeeping genes were added to each well containing 0.6 µL cDNA and 5 µL TaqMan$^{(R)}$ Master Mix (Life Technologies, Burlington, ON, Canada), then topped up with dH_2O to a volume of 10 µL. Probes for *GAPDH* and target genes (*FRK* and *SLUG*) were labeled with VIC^{TM} and FAM^{TM} dyes, respectively. The expression of both the target and housekeeping genes were detected using an Applied Biosystems^{TM}, Step One Plus qRT-PCR machine (Life Technologies, Burlington, ON, Canada).

3.10 Cell analysis using flow cytometer.

Cell cycle analysis was done by quantifying the DNA content at each phase of the cell cycle using flow cytometer. MDA-MB 231 stably overexpressing FRK-WT and FRK depleted MCF-7, and SKBR3 breast cancer cells were used. These cells were seeded into a 6-cm culture plate. Upon confluency, the cells were harvested using trypsin and washed with PBS. The cells were then fixed with 100% ethanol for at least an hour and then stained with Propidium Iodide (PI) (Biovision); a fluorescent that directly binds to the DNA in the nucleus. The flow cytometry measures the amount of dye taken up by the cells, which indirectly amount to the DNA content.
Apoptosis was detected using Annexin V-FITC Apoptosis Detection Kit. MDA-MB 231 stably overexpressing FRK-WT and FRK-YF as well as the parental cells were seeded into 6-well plate. Upon confluency, the cells were harvested by centrifugation at 1000 rpm for 10 min and washed with PBS. The cells were resuspended in 500 µl of 1 X binding buffer, and subsequently, 5 µl of Annexin V-FITC and 5 µl of propidium were added and incubated in the dark for 5 min at room temperature. The cells were analyzed using a flow cytometer (Ex = 488 nm; Em = 530 nm) using FITC signal detector (usually FL1) and PI staining by the phycoerythrin emission signal detector (usually FL2). The procedure used was according to the manufacture protocol.

Also, the cell viability, as well as the number of cell death was determined with a flow cytometer using 7-amino-actinomycin D (7AAD) purchased from Bio-vision. Breast cancer cells were harvested cells and aliquoted up to 1 x 10^6 cells/100 µL in a FACS tube. The cells were washed twice by adding 2 mL PBS (or HBSS), centrifuged at 300 x g for 5 minutes. The supernatant was decanted, and the pelleted cells were resuspended in 100 µL of flow cytometry Staining Buffer. 5 µL of 7-AAD staining solution was added to the cells and mixed gently then incubated for 30 minutes at 4 °C in the dark. The 7-AAD fluorescence (using the FL-2 or FL-3

channel) was determined with a flow cytometer, and viable cells were counted from a dot-plot of forward scatter versus 7-AAD. The procedure used was according to the manufacture protocol

3.11. Cell Proliferation assay

Cell proliferation was carried out using a Cell Counting Kit-8 (CCK-8) (Dojindo, CK04-05) according to the manufacturer's protocol. CCK-8 contains water-soluble tetrazolium salts (WSTs) (2-(2-methoxy-4-nitrophenyl)-3-(4-nitrophenyl)-5-(2,4-disulfophenyl)-2Htetrazolium) which is reduced by dehydrogenase to form an orange water-soluble 40 formazan dye, indicating cell mitochondrial viability. Parental MDA-MB 231, as well as MDA-MB 231 cells stably expressing FRK-WT and FRK-YF, were seeded into 96-well plates (BD, 353077) containing 100 µL culture medium (1000 cells/well). 10 µL CCK-8 solution was added to each well, and then the cells were incubated for 2 hours. Following treatment with CCK-8, absorbance at 485 nm was measured using a POLARStar OPTIMA microplate reader (BMG Labtech, 413-1040). The cell proliferation assay was designed for 4 days that is after 0, 24, 48, 72 and 96 hours. The procedure used was according to the manufacture protocol

3.12 Senescence assay

Cell senescence assay was performed using senescence-associated β-galactosidase (SA-β-Gal) staining kit purchased from Bio vision, the procedure used was according to the manufacturer instructions. Culture medium was removed from the cells grown in a 6-well plate. The cells were washed once with 1 ml of 1X PBS and fixed at room temperature for 10-15 minutes using 0.5 ml of fixative solution. After fixation of the cells, the cells were washed twice with 1 ml of 1X PBS. 0.5 ml of the staining solution mix containing 470 µl of staining solution, 5 µl of staining supplement and 25 µl of 20 mg/ml X-gal in DMF was added to each well and incubated overnight at 37°C. The following morning, the cells were observed under a microscope for development of blue color (200X total magnification).

3.13 *in vivo* xenograft studies

Xenograft experiments were done as described by (Miah *et al*., 2012). Six-week-old female athymic nude mice used were purchased from the Charles River (Canada). Parental MDA-MB 231 and MDA-MB 231 cells stably expressing each of the LPC- FRK-WT as well as LPC-FRK-YF were harvested in PBS and resuspended in Matrigel (BD Biosciences, Bedford, MA, USA). For each injection, 400,000 MDA-MB 231 cells in a 100 ml volume of Matrigel were injected

subcutaneously bilaterally into the fourth mammary fat pads according to standard injection procedures, with four animals injected per cell line. Once tumors were palpable (about 2 weeks after injection of tumor cells), mammary primary tumor growth rates were monitored and analyzed by measuring tumor length (L) and width (W), for about 8 weeks. Tumor size was measured with a digital Vanier caliper. Volume was calculated as 0.50 x length x width^2. Nude mice xenograft experiments were performed under an animal protocol approved by the Animal Care Unit and Committee of the University of Saskatchewan. Mice were killed humanely when the tumor size exceeded the approved limit by animal ethical authority.

3.14 Gene expression datasets (*in-silico)*

GENT, (http://medicalgenome.kribb.re.kr/GENT/reference.php) a bioinformatic software was used to analyzed the gene expression profiles of the different breast cancer cell lines. GENT utilizes datasets created by the Affymetrix platforms (U133A and U133plus2). The normalized expression profiles of target genes in all cancer cells generated from the Affymetrix platform 133plus2 was downloaded. The expression data of target genes in breast cancer cell lines were selected, and the cell lines nomenclature were harmonized and classified based on their phenotype and molecular subtype (Basal A, (BA); Basal B, (BB); or Luminal, (LU)). Correlation analysis was run on all the breast cancer cells (n = 56) with GEO accession numbers GSE10021, GSE10843, GSE3156, GSE10890 and GSK's cell line project (https://array.nci.nih.gov/caarray/project/woost-00041/) to determine consistency across the different profiles

3.14 Tumor expression data

Breast cancers expression datasets were downloaded from the online database, The Cancer Genome Atlas (TCGA; http://tcga-data.nci.nih.gov). 1104 breast tumors and 114 normal mammary tissue samples were used for the analysis. The immunohistochemistry (IHC) data available for these samples were used and the samples were classified into three sub-types. Gene expression data normalized using RSEM (RNA Seq Expectation Maximization) algorithm was used to analyze the correlation in expression. The sub-type classification was analyzed using python scripts pylab, while the sciPy stat library was used to generate the graphs and Spearman rank correlation between FRK and EMT/MET markers.

3.15 Statistical analysis

For statistical analysis, one-way analysis of variance followed by a post hoc Newman–Keuls test was used done using GraphPad Software, San Diego, California, USA, www.graphpad.com. The results are given as the means ± S.D., nX3 unless otherwise stated. $P \leq 0.05$ was considered statistically significant. The gene expression data were analyzed by a one-way analysis of variance (ANOVA; SigmaStat Version 2.0, Jadel Corporation, San Rafael, CA, USA). Multiple range comparisons of paired means were done using a Fishers LSD test or the Newman-Keuls test. The level of significance was set at $p<0.05$ and the data were reported as mean ± SEM. Pearson's correlations were done to evaluate the consistency of the data and the relationship across gene expression profiles in the different cell lines.

4.0 RESULTS

4.1 Expression of FRK and pSTAT3 in human breast cell lines

Previous work from our lab shows that overexpression of FRK-WT and the constitutively active form of FRK (FRK-YF) in MDA-MB 231 breast cancer cell line decreased STAT3 phosphorylation. Hence, to validate STAT3 as a target of FRK, we checked if there was any correlation between FRK and pSTAT3 expression in a panel of 24 breast cancer cell lines of various molecular and cellular characteristics. The lysate from 24 breast cancer cells was obtained and subjected to immunoblot analysis for basal expression of FRK and pSTAT3 (**Figure 4.1)**. HCC 1395, Hs578T, BT 549 and MDA-MB 231 had low expression of FRK and high expression of pSTAT3. HCC 1419, HCC 1937, HCC1809, MCF-7 and SKBR3, expressed high levels of FRK and low levels of pSTAT3, while MDA-MB 435, MDA-MB 134 and MDAKB2 expressed both low levels of FRK and low levels of pSTAT3 and finally, BT 20 and HCC 1599 both expressed high levels of FRK and pSTAT3 (**Figure 4.1)**. Altogether, we found about 75% inverse correlations between FRK and pSTAT3 in the 24 breast cancer cell lines tested (**Figure 4.1)**. Our results align with our hypothesis that FRK is a potential negative regulator of STAT3 signaling.

Furthermore, to validate STAT3 as a target of FRK, we determined the effect of FRK knockdown on STAT3 phosphorylation. To do this, we needed a breast cancer cell line that expresses high FRK and low pSTAT3. From our immunoblot of the 24 breast cancer cell lines, the candidate cell lines were HCC1419, HCC1937, HCC1809, MCF-7 and SKBR3. Another

criterion for sorting the choice of breast cancer cell line to be used for this study was the tumorigenicity of the cell lines. Hence, we further classified the 5 breast cancer cell lines based on the tumorigenicity **(Table 4.1**). Only 3 of these breast cancer cells with a high protein level of FRK and low/no pSTAT3 were tumorigenic. These cell lines were SKBR3 (HER2 positive), MCF-7 and T47D (ER-positive). Hence, we chose SKBR3 and MCF-7 for our knockdown studies as well as MDA-MB 231 for overexpressing FRK mutants.

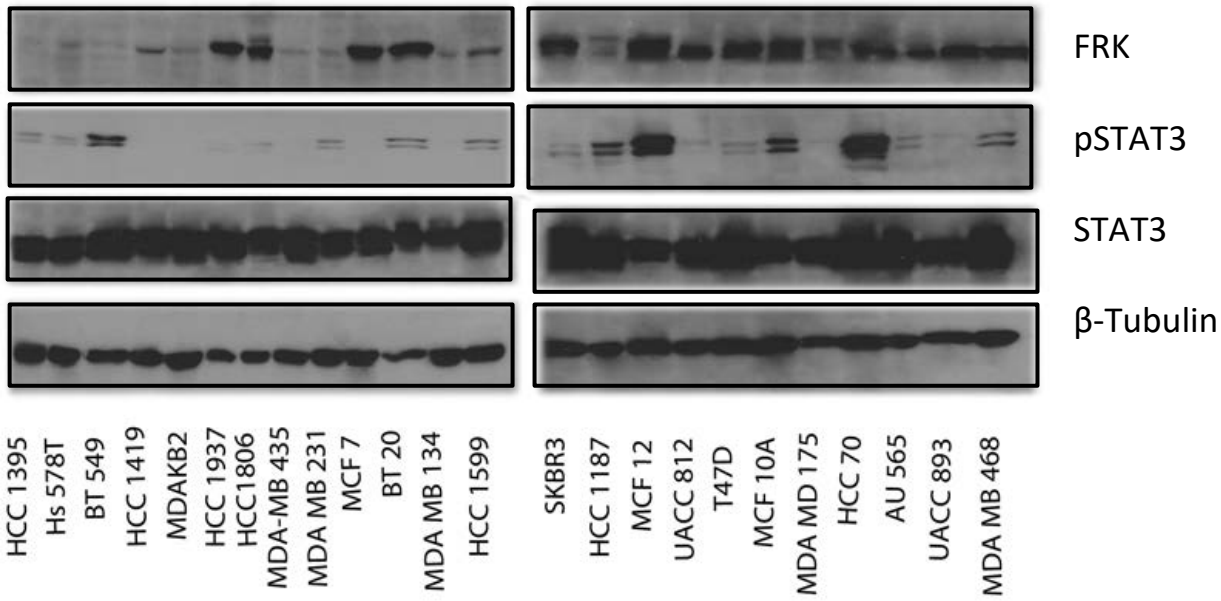

FIGURE 4.1: FRK and pSTAT3 expression in several breast cancer cell lines: 24 breast cancer cell lines were probed for FRK, pSTAT3, and STAT3 protein expression. β-tubulin was used as the loading control. The cells were lysed, and western blotting was done. Anti-FRK, pSTAT3, STAT3 and beta-tubulin antibodies were used to determine the expression of the different proteins. There was an inverse correlation between FRK and pSTAT3 expression in the breast cancer cell lines tested.

S/N	CELL LINE	SUBTYPE	FRK	pSTAT3	STAT3	TUMORIGENECITY
1	HCC 1395	Triple-negative	-	+	++++	-
2	Hs 578T	Triple-negative	-	+	++++	NO
3	BT 549	Triple-negative	-	++	++++	YES
4	HCC 1419	HER2-positive	+	-	++++	-
5	MDAKB2	Triple-negative	-	-	++++	NO
6	HCC 1937	Triple-negative	+++	-	++++	NA
7	HCC 1806	Triple-negative	+++	-	++++	-
8	MDA-MB 435	Normal	+	-	++++	YES
9	MDA-MB 231	Triple-negative	+	+	++++	YES
10	MCF 7	ER-positive	+++	-	++++	YES
11	BT 20	Triple-negative	+++	+	++++	YES
12	MDA-MB 134	ER-positive	+	-	++++	YES
13	HCC 1599	Triple-negative	++	+	++++	-
14	SKBR3	HER2-positive	+++	-	+++++	YES
15	HCC 1187	Triple-negative	+	++	+++++	-
16	MCF 12	Normal	++++	++++	++++	NO
17	UACC 812	ER-positive	+++	-	++++	NA
18	T47D	ER-positive	+++	-	+++++	YES
19	MCF 10A	Normal	+++	+++	++++	No
20	MDA-MB 175	ER-positive	+	-	++++	YES
21	HCC 70	ER-positive	++	++++	+++++	NA
22	AU 565	HER2-positive	+++	-	+++++	NA
23	UACC 893	Triple-negative	+++	-	++++	NA
24	MDA-MB 468	Triple-negative	++++	++	+++++	YES
25	184B5	Normal	+++	++	++++	NO

Table 4.1: Classification of 24 breast cancer cell lines based on their molecular subtype, tumorigenicity, and protein expression of FRK and pSTAT3. About 30% of the 24 breast cancer cell lines were tumorigenic including SKBR3 and MDA–MB 231. Also, FRK and pSTAT3 protein expression are inversely correlated. + (low expression), ++ (moderate expression), +++ (high expression), ++++ (very high expression)

4.2. Stimulation of breast cancer cell lines with IL-6

Next, we checked the response of these breast cancer cells to IL-6 stimulation. IL-6 is a cytokine known to activate the JAK\STAT pathway leading to constitutive activation of STAT3 (Hirano *et al*., 2000). SKBR3, MCF-7, and MDA-MB 231 were subjected to IL-6 (10ng/mL) stimulation at different time (10, 20, 30, 60 and 120 minutes) and different concentration of IL-6 (0, 5, 10, 20, 30 and 50ng/mL) for 30 minutes. pSTAT3, as well as FRK protein expression levels, was determined by western blot **(Figure 4.2).** MCF-7 and SKBR3 cells were all sensitive to IL-6 stimulation, STAT3 phosphorylation increased with increased concentration and time with exception to MDA-MB 231, where there was no effect on STAT3 phosphorylation upon IL-6 stimulation **(Figure 4.2),** we are not sure why stimulation of MDA-MB 231 with IL-6 did not affect STAT3 phosphorylation. On the other hand, a previous report had shown that STAT3 could be activated via the EGF signaling pathway (Wu *et al*., 2014). Thus, we stimulated MDA-MB 231 with epidermal growth factor (EGF) and tested the effect on STAT3 phosphorylation. Stimulation of MDA-MB 231 with EGF at various concentrations (1, 5, 10 and 30 ng/mL) did not affect STAT3 phosphorylation and FRK protein expression (**Figure 4.3).** It is possible that the phosphorylation of STAT3 in this cell line is already saturated hence no further response could be induced by stimulation with either IL-6 or EGF. However, increasing the concentration of EGF led to higher cellular levels of tyrosine phosphorylation with the peak of phosphorylation at 5 ng/mL when the samples were blotted with an antibody against phosphorylated tyrosine residues (4G10) (**Figure 4.3**). We further tested the effect of IL-6 stimulation on STAT3 phosphorylation in MDA-MB 231 transiently expressing FRK-WT, FRK-YF or FRK-K262M. We obtained a decrease in the phosphorylation of STAT3 with MDA-MB 231 transiently expressing FRK-WT as well as FRK-YF (**Figure 4.4)**.

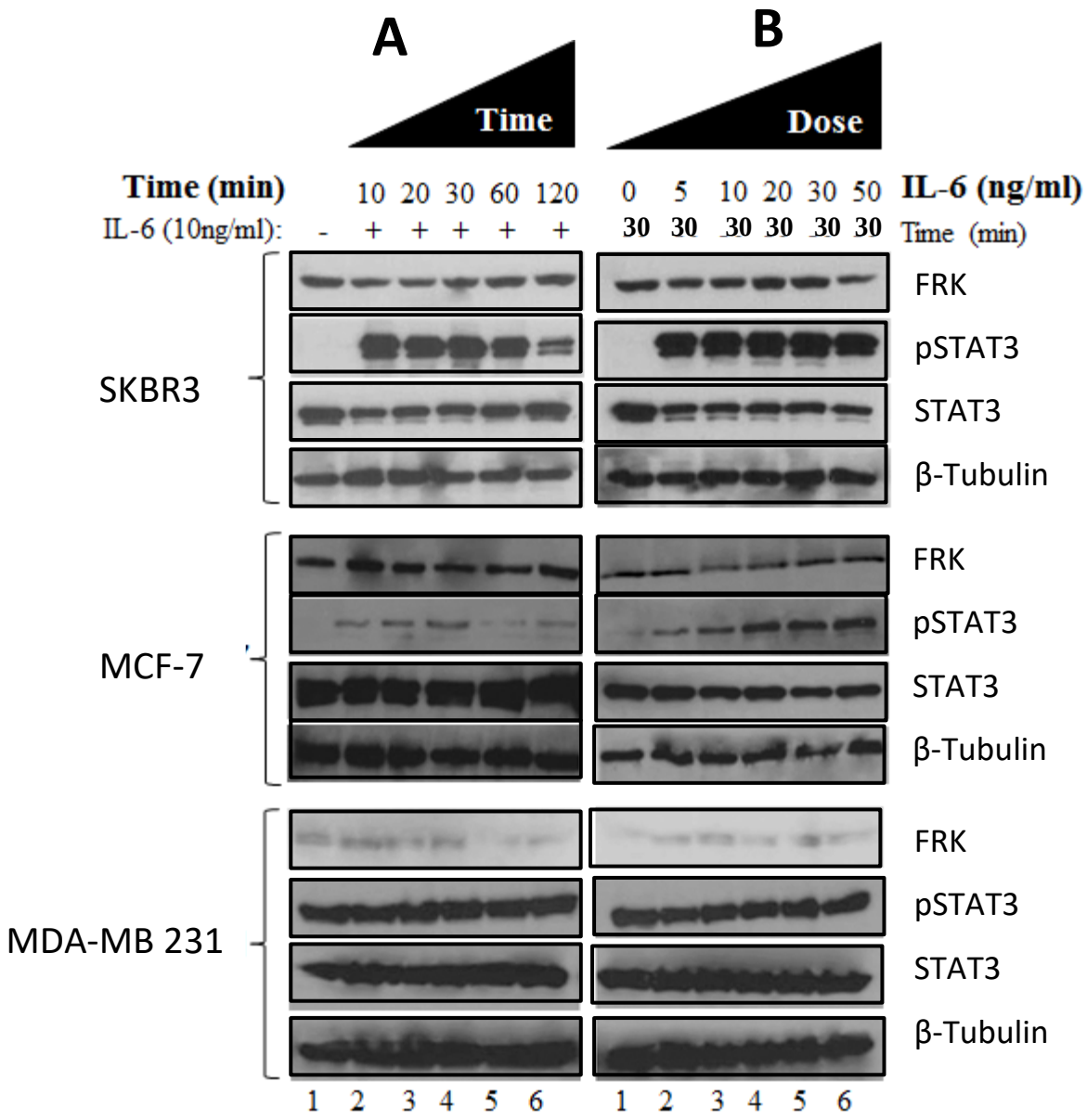

Figure 4.2: Effect of IL-6 stimulation on pSTAT3 and FRK in different breast cancer cell lines. Four breast cancer cell lines from each of the molecular subtype ER-positive -(MCF-7), HER2 positive –(SKBR3) and triple negative –(MDA-MB 231) were stimulated with **A).** A fixed concentration of IL-6 (10 ng/mL) at different time points (10, 20, 20, 60 and 120 minutes) and was repeated with **B).** different concentrations of IL-6 (5, 10, 20, 30 and 50 ng/mL) for 30 minutes. Cell lysates were subjected to SDS-PAGE analysis followed by immunoblotting with antibodies against the indicated proteins.Il-6 stimulation at different time and concentration in MDA-MB 231 did not affect both STAT3 phosphorylation and FRK protein expression.

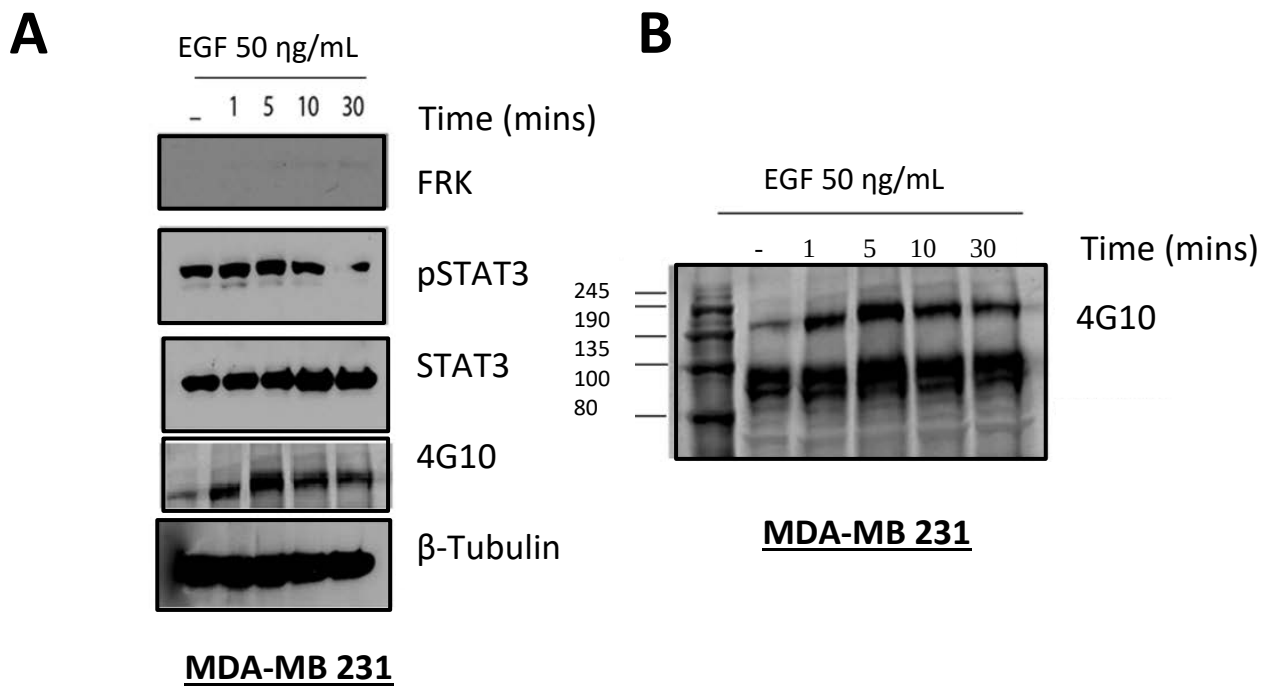

Figure 4.3: A). Effect of EGF stimulation on pSTAT3 and FRK protein expression in MDA-MB 231 breast cancer cell lines. MDA-MB 231 cells were stimulated with EGF (50ng/mL) at different time points (1, 5, 10 and 50 minutes). The cell lysates were collected at the different time points and subjected to SDS-PAGE analysis followed by immunoblotting with antibodies against the indicated proteins. EGF stimulation did not affect both STAT3 phosphorylation and FRK protein expression. **B). Effect of EGF stimulation on tyrosine phosphorylation in MDA-MB 231.** MDA-MB 231 cell were treated with EGF (50 ng/mL) at different time points (1, 5, 10 and 50 minutes). The cell lysates were subjected to SDS-PAGE analysis followed by immunoblotting with an antibody used to detect tyrosine phosphorylation (anti-4G10). There was an increase in the levels of tyrosine phosphorylation upon EGF stimulation.

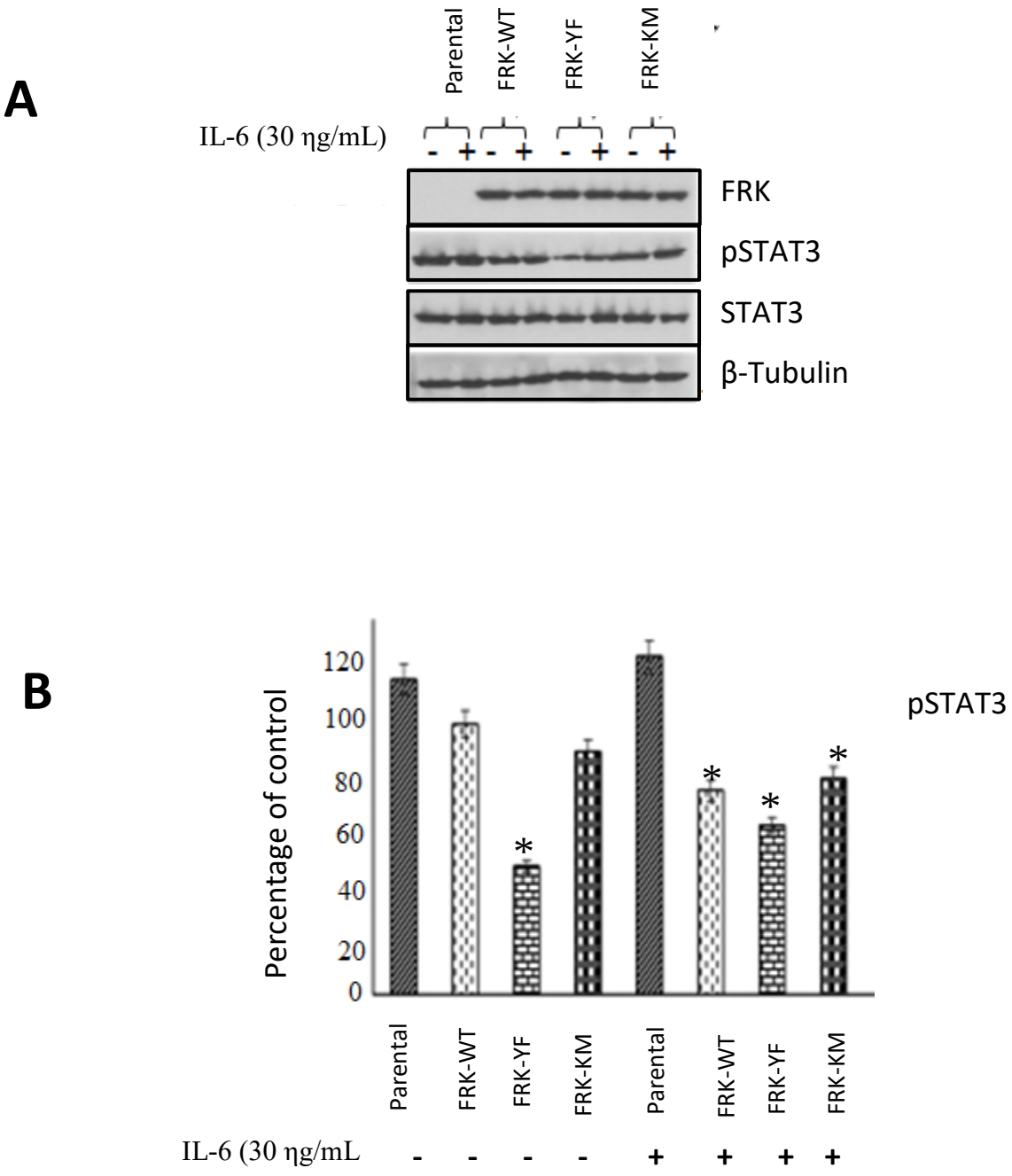

Figure 4.4: Effect of IL-6 stimulation on the FRK-mediated regulation of signaling proteins in MDA-MB 231 cells: A). The empty vector control, Wild-type FRK (FRK-WT), Mutant FRK Y497F and FRK-KM (kinase dead) cell lines were harvested, lysed and resolved via SDS-PAGE. Western blotting was performed using antibodies against the indicated signaling proteins corresponding to important signaling pathways. An antibody against FRK was used to determine the expression of FRK in MDA-MB 231 transiently transfected with FRK wild-type and FRK mutants. β-tubulin was used as the loading control. **B).** pSTAT3 protein expression levels were quantified using Image J (Ver. 1.48). The data are presented as mean ± S.D. (p-value ≤ 0.05).

4.3. Down-regulation of FRK in does not affect STAT3 activation/phosphorylation

We generated stable MDA-MB 231 breast cancer cell lines that overexpressed either FRK-WT or FRK-YF and also transiently knockdown the expression of FRK in SKBR3 and MCF-7 breast cancer cell line using siRNA. We obtained about a 60% fold increase in the expression of FRK-WT and FRK-YF mRNA expression in the respective stable MDA-MB 231 cell lines as compared to the parental cells. For the SKBR3 and MCF-7 breast cancers cells, we obtained about 70% knockdown of FRK mRNA expression. Similar trends in protein levels were seen when the stable (MDA-MB 231) and transient knockdown cells (SKBR3 and MCF-7), were compared to their respective parental cell lines (**Figure 4.5**). Western blot analysis was carried out on the cell lysates to determine the protein expression of FRK, pSTAT3, STAT3, and β-tubulin. The expression of β-tubulin was used as a loading control in both the overexpressed and knockdown cells. We noted a decrease in STAT3 phosphorylation in MDA-MB 231 cells that were stably overexpressing FRK-WT and FRK-YF as compared to the parental MDA-MB 231 parental cells. This result was similar to what we previously obtained from our lab, and this confirms that FRK downregulates STAT3 phosphorylation. However, when we knockdown FRK in SKBR3 and MCF-7 breast cancer cell lines, we expected the depletion of FRK to induce STAT3 phosphorylation; however, the knockdown of FRK neither increased nor decreased STAT3 phosphorylation in both SKBR3 and MCF-7 cell lines (**Figure 4.6**). This could have been because FRK was not completely knocked down in both SKBR3 and MCF-7. It is also possible that complete knockout of FRK may have a significant impact on STAT3 phosphorylation/activation.

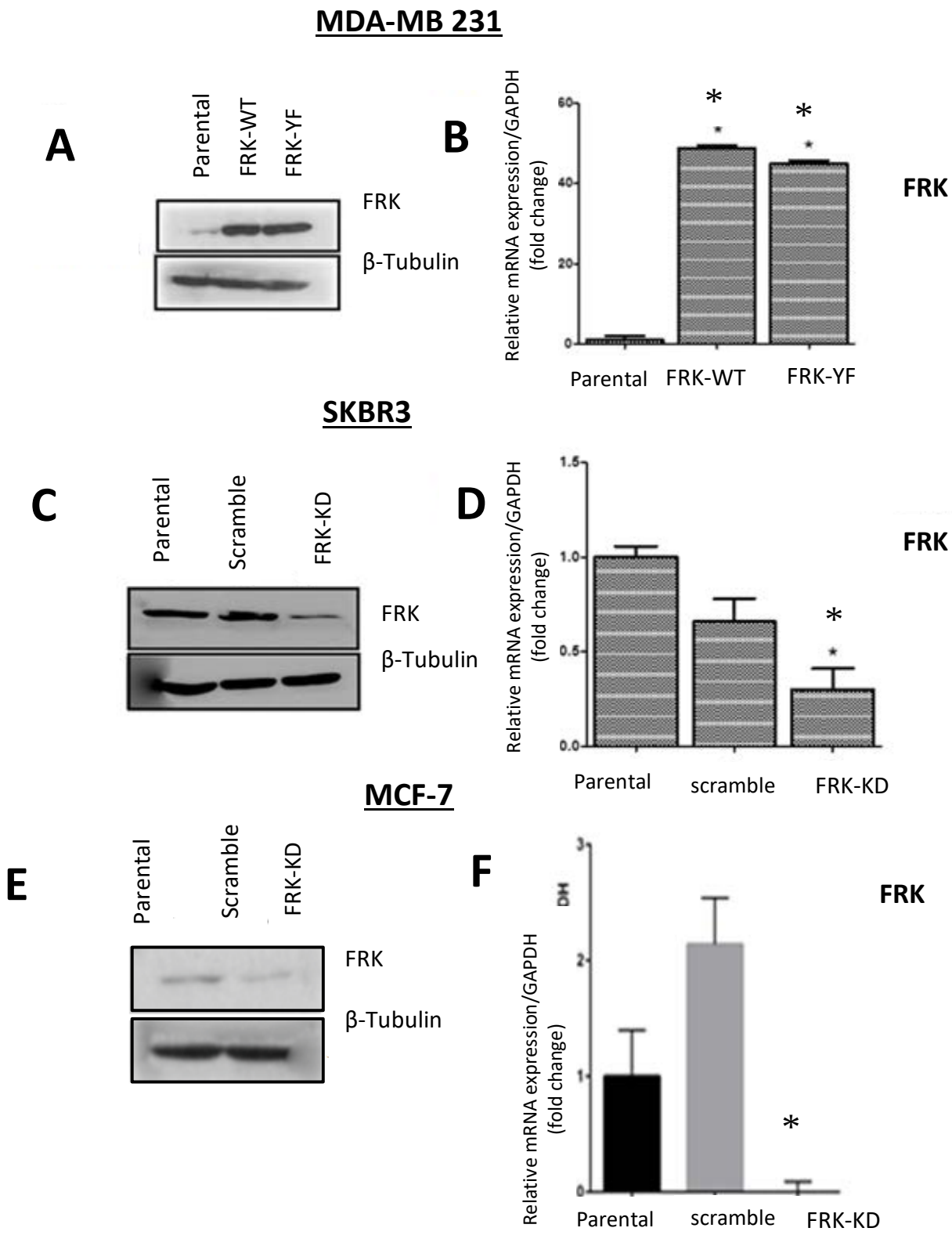
MDA-MB 231
A
Parental
FRK-WT
FRK-YF
FRK
β-Tubulin
B
Relative mRNA expression/GAPDH (fold change)
60
40
20
0
*
*
Parental
FRK-WT
FRK-YF
FRK
SKBR3
C
Parental
Scramble
FRK-KD
FRK
β-Tubulin
D
Relative mRNA expression/GAPDH (fold change)
1.5
1.0
0.5
0.0
*
Parental
scramble
FRK-KD
FRK
MCF-7
E
Parental
Scramble
FRK-KD
FRK
β-Tubulin
F
Relative mRNA expression/GAPDH (fold change)
3
2
1
0
*
Parental
scramble
FRK-KD
FRK

Figure 4.5: The expression of FRK in breast cancer cell lines following its knockdown or overexpression: The mRNA and Protein levels in; **A).** The MDA-MB 231 cell stably expressing the FRK wild-type (FRK-WT) and Mutant (FRK-YF), knockdown of FRK in breast cancer cell lines **B)** SKBR3 and **C)** MCF-7. Cell lysates were subjected to SDS-PAGE analysis followed by immunoblotting with antibodies against the indicated proteins. FRK mRNA expression was quantified using RT-PCR. The data are presented as mean ± S.D (p-value ≤ 0.05).

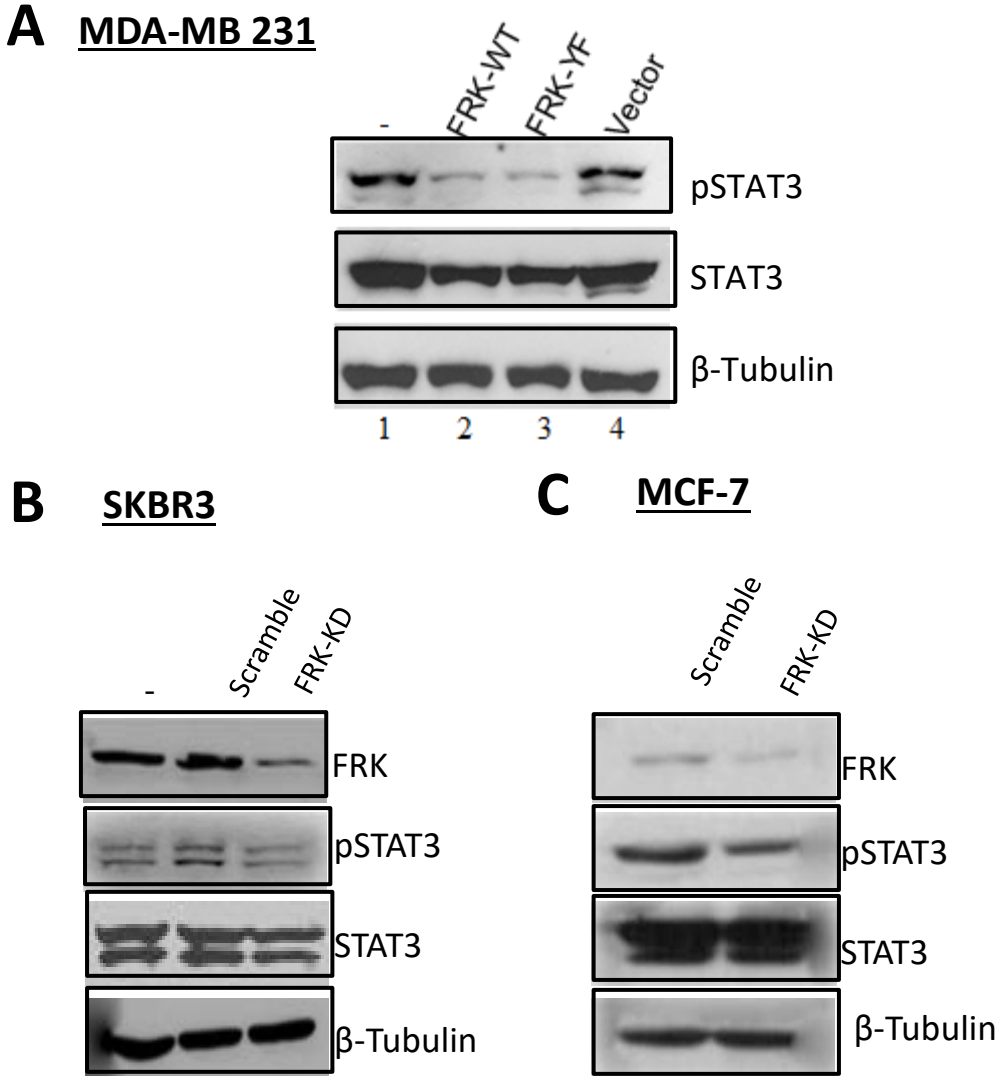

Figure 4.6: The effect of FRK overexpression on STAT3 phosphorylation. **A)** Parental MDA-MB 231 or control, FRK WT, and FRK YF stable MDA-MB 231 cells. **The effect of FRK knockdown on STAT3 phosphorylation in B) SKBR3 and C) MCF-7** Cell lysates were subjected to SDS-PAGE analysis followed by immunoblotting with antibodies against the indicated proteins. Overexpression of FRK decreased STAT3 phosphorylation, while the knockdown had no significant effect

4.4. Overexpression of FRK regulates STAT3 downstream target genes

Activated STAT3 plays a crucial role in tumorigenesis by up-regulating genes that promote cell proliferation (Cyclin D1, c-myc), survival (BCL-xL, MCL-1, and Survivin), migration and invasion (MMP-2, MMP10, and MMP-1) (Banerjee and Resat, 2016; Hsieh *et al*., 2005). Therefore, we next evaluated the effect of FRK overexpression and knockdown on STAT3 target genes. Real-Time (RT) PCR was used to investigate the effect of FRK overexpression and knockdown on the mRNA expression of some STAT3 downstream target genes; this includes Survivin, Cyclin D1, and MMP1. The overexpression of FRK-WT in MDA-MB 231 cells resulted in a significant downregulation of Survivin, Cyclin D1, and MMP-1. Although a similar observation was made for FRK-YF stable cells, on the other hand, we found that FRK-YF increased Cyclin D1 gene expression. We are not sure why this mutant increased cyclin D1 expression, we hope to investigate this in future **(Figure 4.7**). However, These results show that overexpression of FRK not only decreased STAT3 phosphorylation but also resulted in the impairment of STAT3 downstream signaling events. Although we obtained no significant effect on STAT3 phosphorylation in both SKBR3 and MCF-7 breast cancer cell lines following the knockdown of FRK expression we observed an upregulation of STAT3 target genes in both cell lines. The knockdown of FRK led to the upregulation of Survivin and cyclin D1 mRNA levels in SKBR3 **(Figure 4.7**). There was no significant effect on the mRNA levels of Survivin and cyclin D1 in MCF-7. Likewise, we observed an upregulation of MMP-1 mRNA levels in MCF-7 knockdown cells **(Figure 4.7**). MMP-1 mRNA expression was not observed in SKBR3. Taken together our data indicated that FRK overexpression decreased STAT3 phosphorylation and some of its downstream target genes. Although we obtained no significant effect of FRK knockdown on STAT3 phosphorylation, we observed an increase in expression of STAT3 target genes following FRK knockdown. Hence, our results show that FRK might regulate the genes through other mechanisms other than STAT3 signaling pathway.

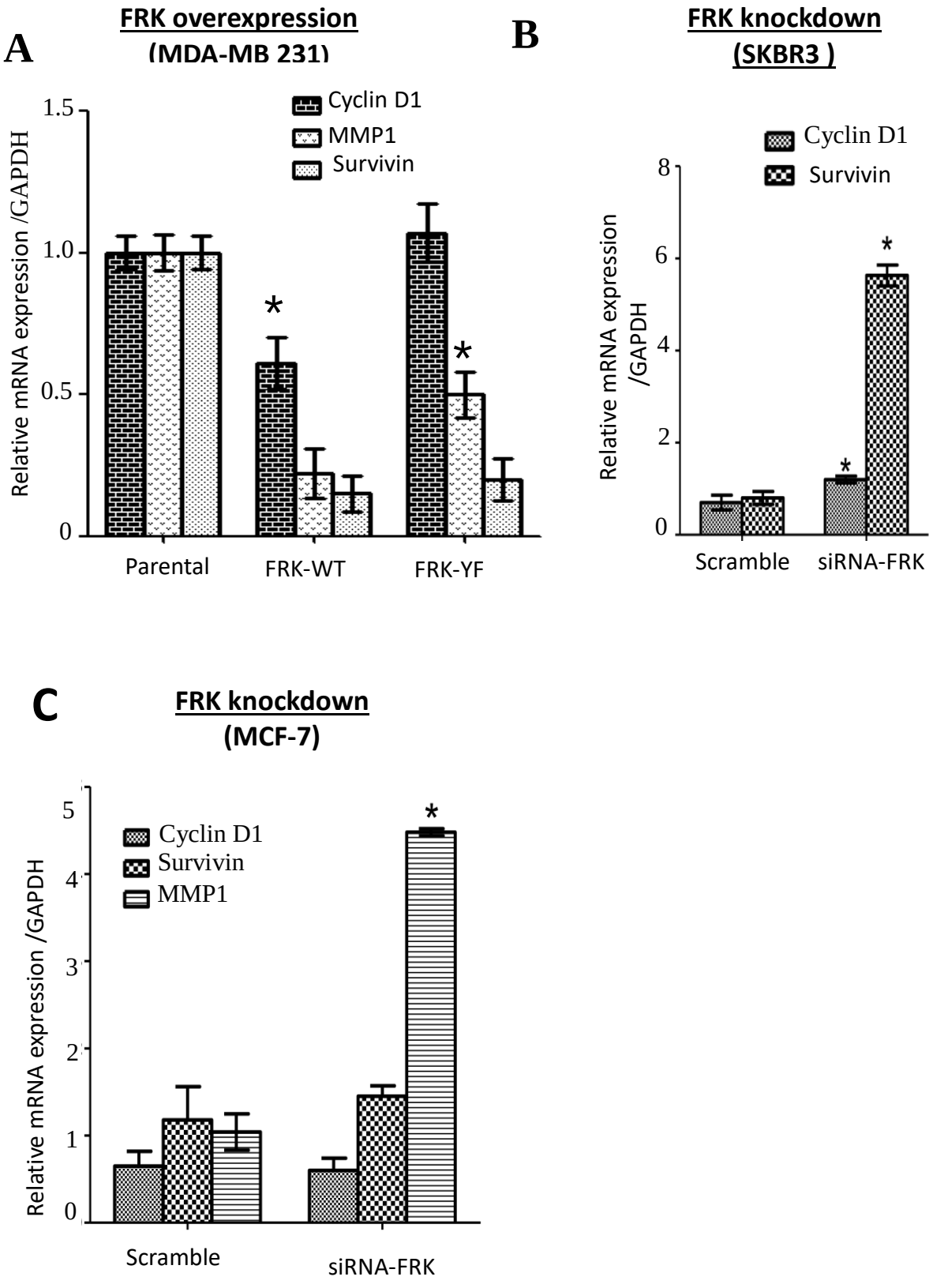
A
FRK overexpression
(MDA-MB 231)
Cyclin D1
MMP1
Survivin
Relative mRNA expression /GAPDH
1.5
1.0
0.5
0
*
*
Parental
FRK-WT
FRK-YF
B
FRK knockdown
(SKBR3)
Cyclin D1
Survivin
Relative mRNA expression /GAPDH
8
6
4
2
0
*
*
Scramble
siRNA-FRK
C
FRK knockdown
(MCF-7)
Cyclin D1
Survivin
MMP1
Relative mRNA expression /GAPDH
5
4
3
2
1
0
*
Scramble
siRNA-FRK

Figure 4.7: The effect of FRK overexpression and knockdown on STAT3-target genes in breast cancer cell lines: A). MDA-MB 231 stable cell lines were transfected with the empty vector control, FRK wild-type (FRK WT) and mutant FRK-YF plasmid constructs. **B).** SKBR3 **and C).** MCF-7. The mRNA levels of Survivin, Cyclin D1 and MMP1 in SKBR3 and MCF-7 cells were quantitatively measured relative to their respective parental cell lines using quantitative RT-PCR. The data are presented as mean ± S.D. (p-value ≤ 0.05).

4.5. FRK inhibits STAT3 activation through ERK1/2 activation

We showed that overexpression of FRK in MDA-MB 231 cells decreased STAT3 phosphorylation **(Figure 4.6 A)**. However, we do not know the exact mechanism by which FRK decreases the phosphorylation of STAT3. Therefore, we decided to investigate if FRK directly binds to STAT3. An immunoprecipitation assay was carried out by using MDA-MB 231 (FRK-negative breast cancer cell) transiently transfected with FRK-WT. Cell lysates were immunoprecipitated with an anti-STAT3 antibody or anti-IgG and anti- FRK antibody and vice versa. There was no direct interaction between FRK and STAT3 (**Figure 4.8)**. The decrease in STAT3 phosphorylation with FRK overexpression could have been as a result of indirect binding of FRK to STAT3, or FRK could have phosphorylated/ activated an intermediate, for example, a phosphatase and the latter subsequently dephosphorylating pSTAT3 (**Figure 4.6A**). It is worth mentioning that FRK is not a phosphatase, hence cannot directly dephosphorylate pSTAT3.

Previous studies showed that activated ERK1/2 (pERK1/2) negatively regulates the activation of STAT3 (pSTAT3 Tyr705) by phosphorylation of STAT3 at Ser727. Phosphorylation of STAT3 Ser727 was shown to decrease the phosphorylation of STAT3 Tyr705 (Chung *et al*., 1997; Wakahara *et al*., 2012). Based on this, we investigated the effect of FRK overexpression and knockdown on pERK1/2 and pSTAT3 Ser727. Cell lysates of MDA-MB 231 stably overexpressing FRK-WT and FRK-YF as well as SKBR3 FRK knockdown cells were immunoblotted with antibodies against pSTAT3 Ser727, ERK1/2, and pERK1/2. We expected pERK1/2 to increase the phosphorylation of STAT3 Ser727 because data from our lab had shown an increase in protein expression pERK1/2 following FRK overexpression in MDA-MB 231 **(Figure 4.8).** Interestingly, we saw an increase in pSTAT3 Ser727 in MDA-MB 231 overexpressing FRK when compared to the parental cells **(Figure 4.8).** Several reports have shown that phosphorylation of STAT3 at Ser727 negatively regulates phosphorylation of STAT3 Tyr705 (Chung *et al*., 1997; Wakahara *et al*., 2012). Hence, it is possible that FRK decreases STAT3 phosphorylation by phosphorylating ERK1/2, which activates STAT3 Ser727. However,

transient knockdown of FRK in SKBR3 cells did not affect the protein expression of pERK1/2 and pSTAT3 Ser727 when compared with the parental cells (**Figure 4.8**). This could explain why we saw no effect of FRK knockdown on STAT3 phosphorylation in SKBR3 and MCF-7 breast cancer cells **(Figure 4.6 B and C)**. Our results suggest that activation of ERK1/2 by FRK could probably be the mechanism by which FRK downregulates STAT3 Tyr705 activation.

It is worth mentioning that ERK1/2 is serine/threonine kinase, hence cannot be phosphorylated directly by FRK a tyrosine kinase. However, Jin *et al.* showed that overexpression FRK phosphorylates EGFR Tyr1173 (Jin and Craven, 2014) Phosphorylated EGFR Tyr1173 have been reported to activate ERK (Hsu *et al*., 2011). Therefore, it possible that FRK decreases STAT3 phosphorylation through EGFR signaling pathway, we intend to investigate the role of FRK in ERK1/2 activation and further identify the particular substrate/phosphatase activated by FRK which possibly dephosphorylate STAT3.

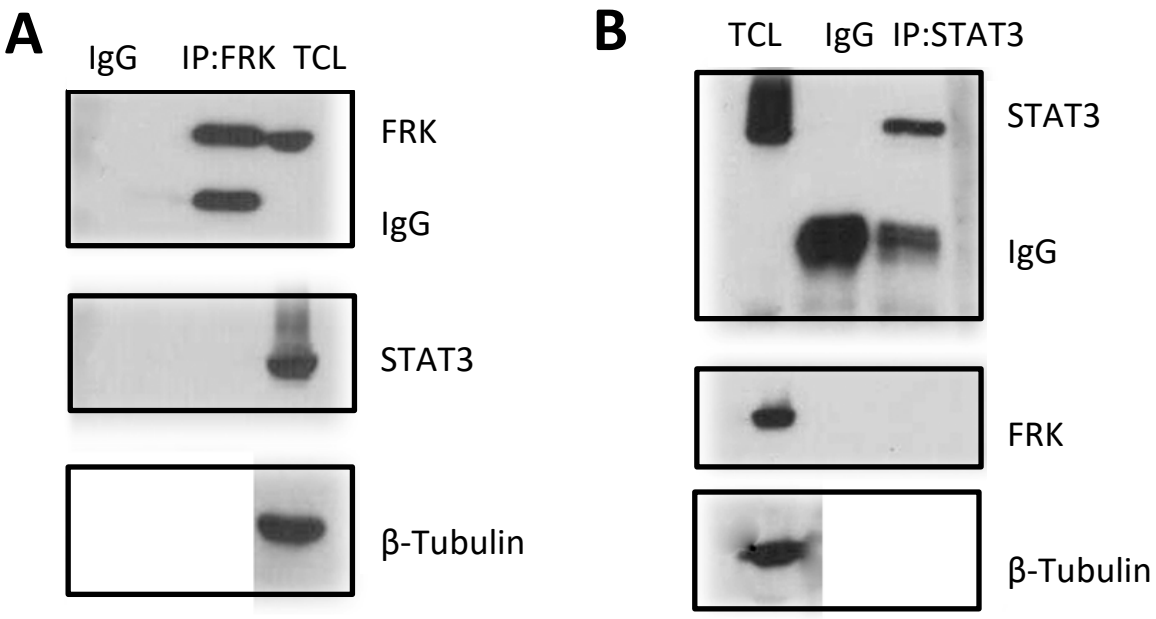

MDA-MB 231 WT

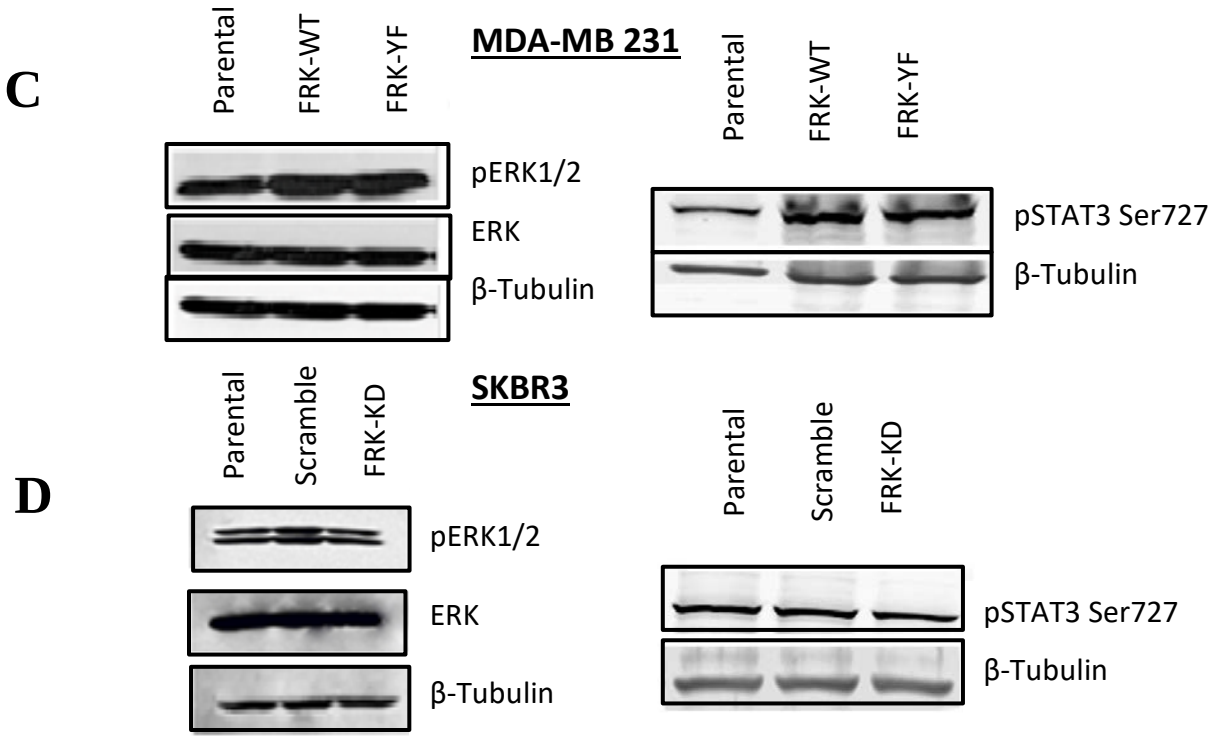

Figure 4.8: A and B) FRK does not interact with STAT3. FRK-negative MDA-MB 231 cells were transiently transfected with FRK-WT. Interaction of FRK with STAT3 was done using Immunoprecipitation assay. Cell lysates were immunoprecipitated with an anti-FRK antibody or anti-IgG to precipitate STAT3 and immunoblotted with anti- STAT3 antibody and vice versa. (TCL-Total cell lysate) β-Tubulin protein expression was not detected in the IgG and in the IP: STAT as well as IP:FRK lane of the bottom panel **C and D) FRK increases ERK1/2 and STAT3 serine phosphorylation.** Cell lysates obtained from MDA-MB 231 stably overexpressing FRK-WT, FRK-YF, as well as FRK-depleted SKBR3 cells, was immunoblotted with an antibody against pERK1/2, ERK1/2, and pSTAT3 Ser727. Overexpression of FRK-WT and FRK-YF increases ERK1/2 phosphorylation and pSTAT3 ser727, while FRK depletion in SKBR3 did not affect ERK1/2 phosphorylation and pSTAT3 ser727.

4.6 FRK expression is high in epithelial-like breast cancer cells and the normal breast epithelium

Although we did not observe any change in the phosphorylation of STAT3 following the knockdown of FRK, we, however, noted upregulation of STAT3 target genes (**Figure 4.5**). We concluded that the tumor suppressive role of FRK might be through other mechanisms other than phosphorylation of STAT3. Hence, we further investigated other mechanisms by which FRK exerts its tumor suppressive role in breast cancer.

In glioma cells, FRK has been shown to inhibit cell migration by suppressing several mesenchymal markers (Shi *et al*., 2015). Although FRK has been reported to be expressed mainly in epithelial cells but not in mesenchymal cells (Berclaz *et al*., 2000; Cance *et al*., 1994), there is no report on the mechanisms by which FRK suppresses cell migration in breast cancer cells. Hence, we hypothesized that FRK possibly regulates Epithelial to Mesenchymal Transition (EMT). EMT is a biological process by which cells undergo a transition from an epithelial to a mesenchymal phenotype (Nantajit *et al*., 2015). Breast cancer cells have been classified into three subtypes (luminal, Basal B and Basal A) based on their morphology and invasive properties (Neve *et al*., 2006). Luminal cells are more differentiated with epithelial-like phenotype while the Basal B cells are less differentiated and possess mesenchymal-like appearance; Basal A cells have either luminal-like or basal-like morphology (Neve *et al*., 2006).

To investigate the role of FRK on EMT, first, we checked the protein, and mRNA expression of FRK, epithelial marker (E-cadherin) and mesenchymal marker (Fibronectin) in 11 breast cancer cell lines classified based on their morphology and invasive potential using western blot analysis and RT-PCR. The cell lines used were MCF-7, T47D, SKBR3, and AU565 (Luminal), MDA-MB 468, HCC 70 and BT20 (Basal A), MDA-MB 231, BT 549, and Hs 578T (Basal B). From our data, we found out that all luminal and Basal A breast cancer cells expressed FRK, as well as E-cadherin, except for SKBR3 and AU565 that don't express E-cadherin (Neve *et al*., 2006). However, basal B cells had low or no FRK and E-cadherin protein expression but a high expression of Fibronectin protein, a mesenchymal marker **(Figure 4.9)**. The expression FRK in MCF10A was low/moderate. These results were generally consistent with the mRNA expression data showing high and low expression of FRK transcripts in Basal A and Basal B cell lines, respectively (**Figure 4.9**). To further validate our findings, we carried out immunohistochemical staining for FRK expression in both normal and malignant breast tissues using breast microarray (TMA) samples. The TMA used included TNM, clinical stage and pathology grade, from 6 cases of breast invasive ductal carcinoma and matched adjacent normal breast tissue, with quadruple cores per case). Immunohistochemistry (IHC) for FRK expression and scored for staining was performed on service by USBIOMAX and analyzed by their pathologist. We found that the majority of the samples (22 out of 24) displayed a score of 1 or less and only two samples (one normal and one tumor) showed a 2+ strength. This indicated that FRK protein expression was low/moderate in both normal and cancer tissues. However, when

expressed, FRK was localized predominantly in epithelial cells of intact mammary ducts in the normal breast tissue (**Figure 4.9**). These results indicate that FRK is differentially expressed in breast cancer cells and that expression of FRK is higher in epithelial-like cell lines, compared with those with mesenchymal characteristics. No apparent correlation was observed between FRK expression and the clinicopathological characteristics such as tumor grade and TNM in the small sample size used in this study. However, our expression data corresponding to cell lines and TMA together indicate that the expression of FRK is enriched in epithelial cells/tissue and downregulated in mesenchymal-like Basal B breast cancer cells

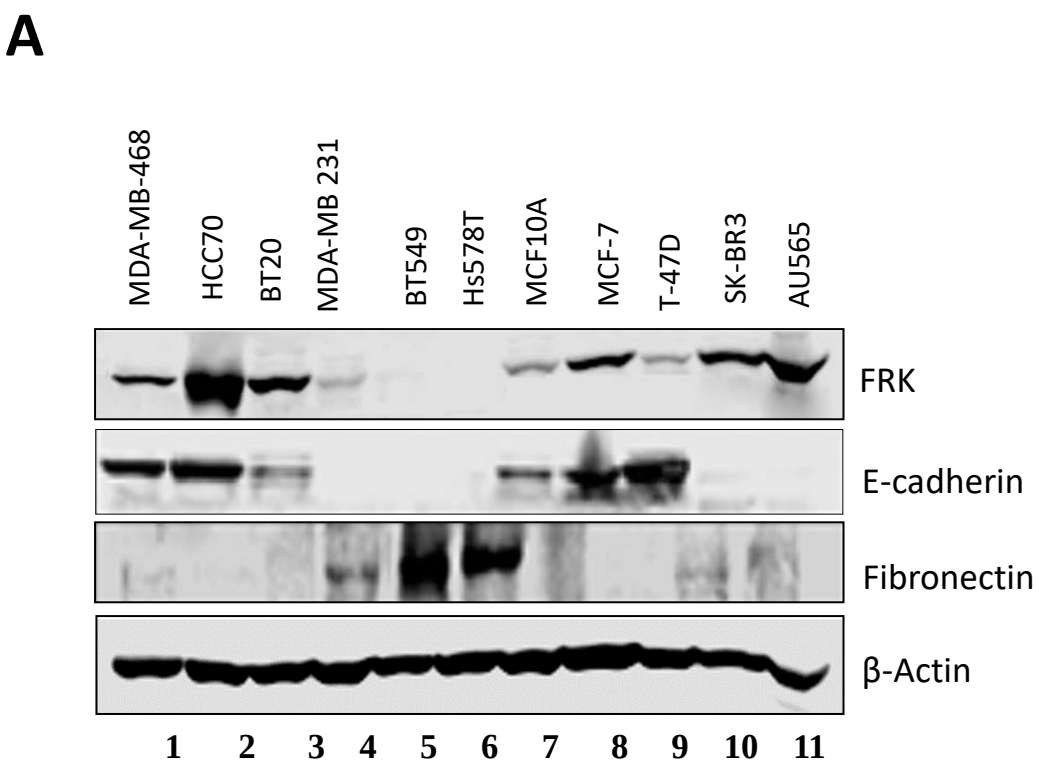

B

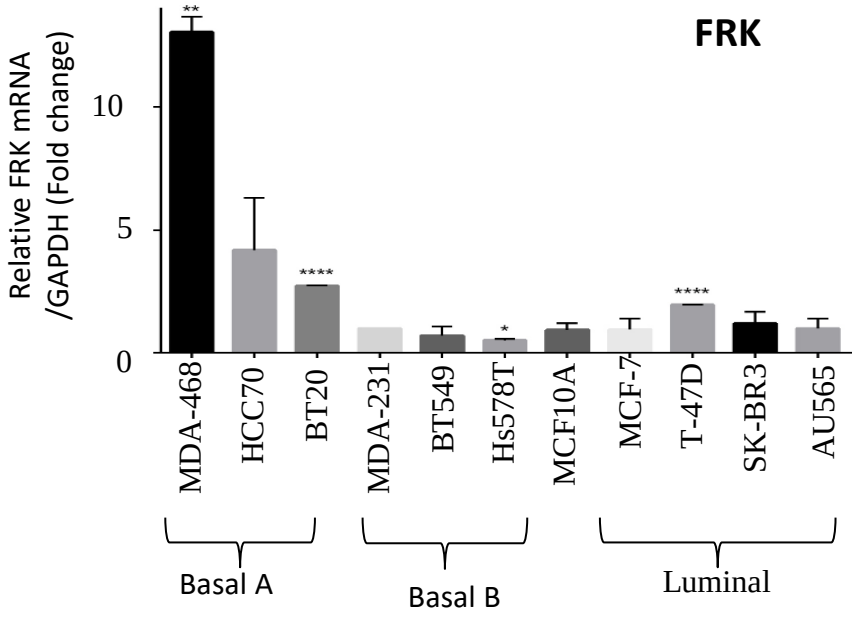
FRK
Relative FRK mRNA /GAPDH (Fold change)
10
5
0
**
****
*
****
MDA-468
HCC70
BT20
MDA-231
BT549
Hs578T
MCF10A
MCF-7
T-47D
SK-BR3
AU565
Basal A
Basal B
Luminal

C

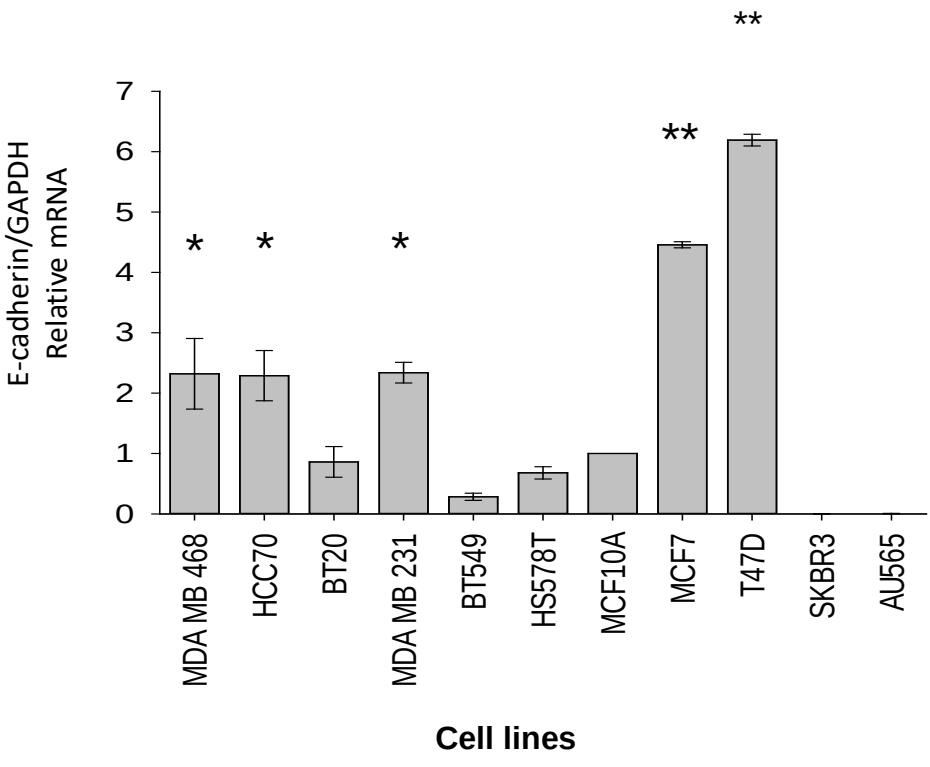
E-cadherin
E-cadherin/GAPDH Relative mRNA
7
6
5
4
3
2
1
0
*
*
*
**
**
MDA MB 468
HCC70
BT20
MDA MB 231
BT549
HS578T
MCF10A
MCF7
T47D
SKBR3
AU565
Cell lines

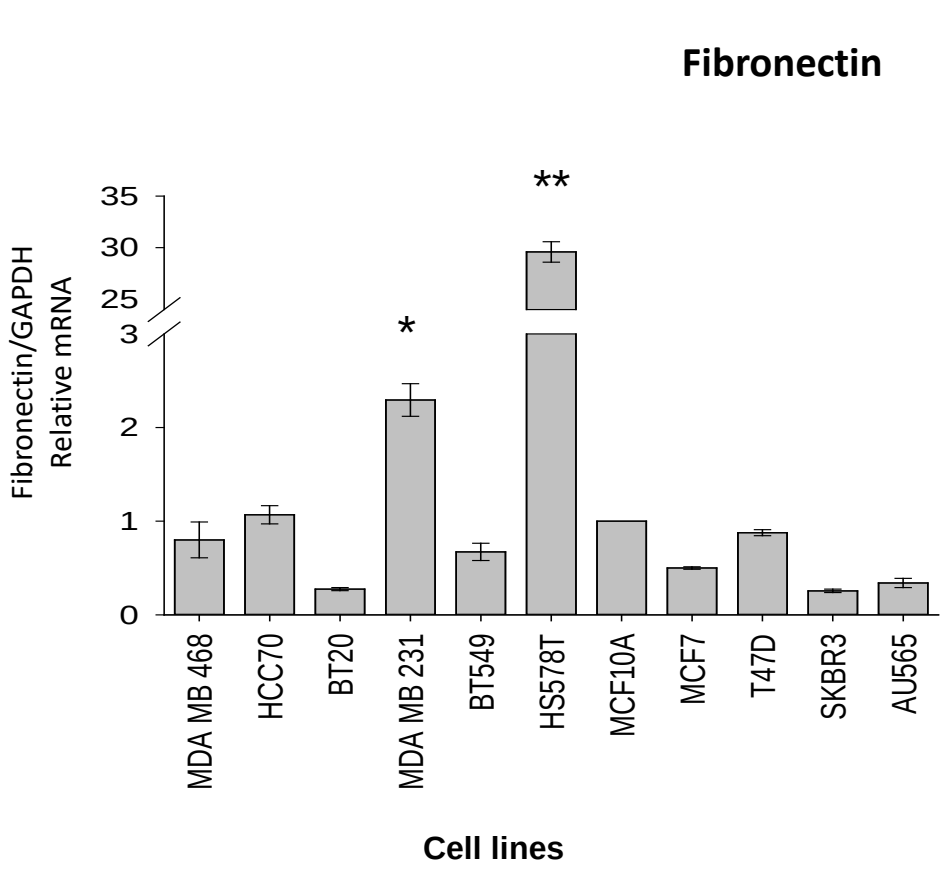

Figure 4.9: Protein and mRNA expression of FRK, E-cadherin and Fibronectin in 11 breast cancer cell lines A). Protein expression, the immortalized normal mammary epithelial cell line MCF10A as well as the indicated breast cancer cell lines, corresponding to either the Basal A, Basal B or the luminal subtypes, were probed for FRK, E-cadherin, and Fibronectin expression, β-Actin was used as the loading control**. B), C) and D).** FRK, E-cadherin and Fibronectin mRNA levels in the same cell lines were determined via quantitative RT-PCR analyses using appropriate probes. FRK protein and mRNA expression positively correlate with E-cadherin (epithelial marker) protein and mRNA expression. However, there was an inverse correlation between FRK and Fibronectin (a mesenchymal marker) protein and mRNA expression. The data are presented as mean ± SEM. (p-value ≤ 0.05).

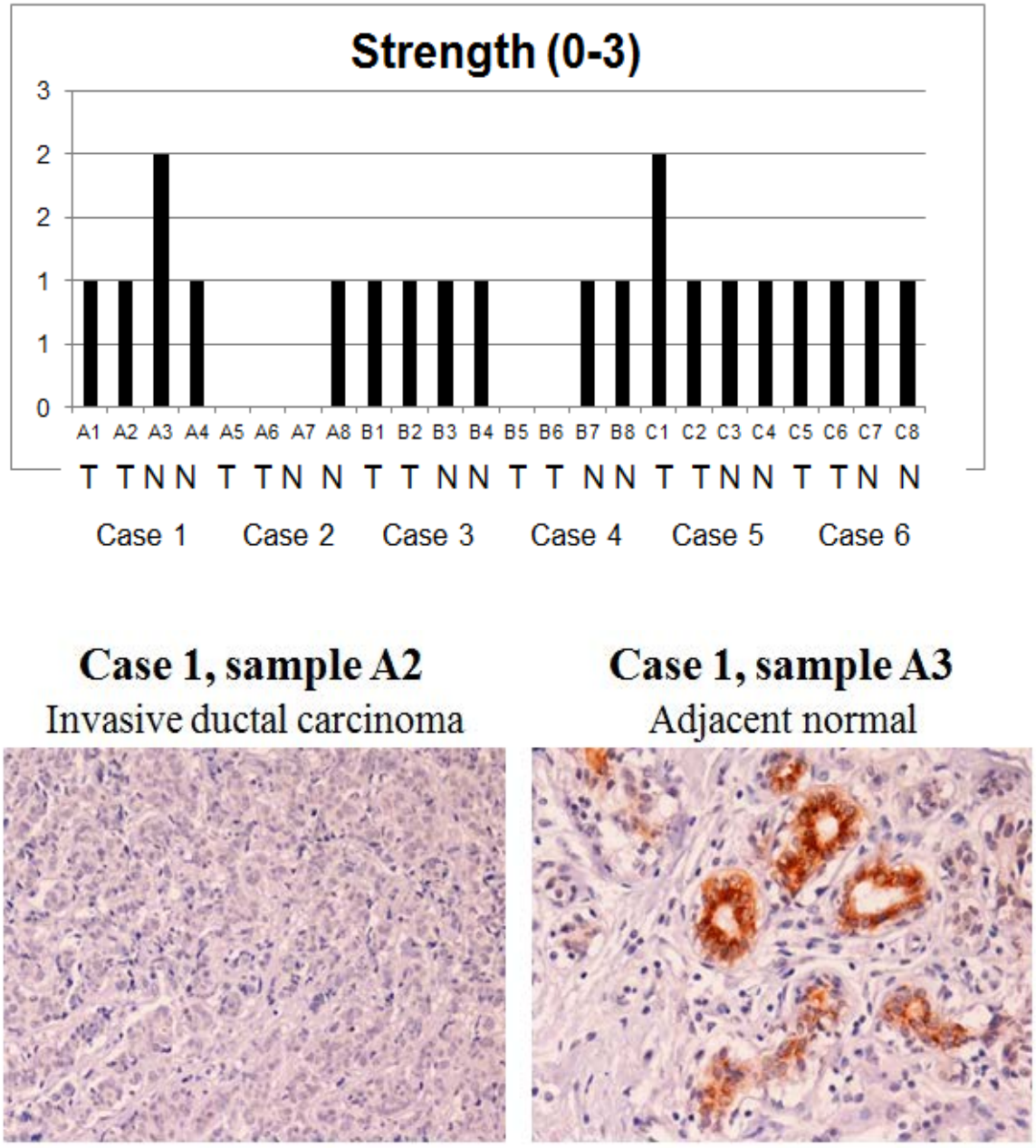

Figure 4.10: Expression of FRK in breast cancer tissues: Using FRK-specific antibodies, FRK expression was determined via immunohistochemical (IHC) analyses of a breast cancer tissue array containing 6 cases of breast invasive ductal carcinoma and matched adjacent normal breast tissue, quadruple cores per case. The array also contained clinical information that included TNM, stage and pathology grade (USBIOMAX, array BR243f) **A)** graphical representation of FRK staining strength. **B)** Shown here is a representative image of FRK expression in invasive ductal breast carcinoma tissues and matched normal control tissues.

4.7. FRK regulates Epithelilal to Mesenchymal Transition in breast cancer cells

FRK have been shown to suppress EMT markers in glioma cells (Shi *et al*., 2015). Our results shown in **Figure 4.9** show that FRK protein and mRNA expression was moderate/high in Luminal and Basal A cells that display an epithelial-like phenotype, and low or undetected in Basal B cells which are more mesenchymal**.** Further, we detected the expression of FRK predominantly in the epithelial layer lining the mammary ducts of the normal breast tissue **(Figure 4.10).** Based on these observations, we hypothesized that FRK might regulate EMT in breast cancer cells. To directly determine the effect FRK on EMT in breast cancer cells, we examined the expression of epithelial and mesenchymal markers in the MDA-MB 231 cells stably expressing either FRK-WT or FRK-YF, as well as in FRK depleted SKBR3 and MCF 7 cells via Real-time PCR and Western blotting analyses. Overexpression of FRK-WT and FRK-YF in MDA-MB 231 cells significantly upregulated the levels of E-cadherin mRNA and suppressed several mesenchymal markers such as Slug, N-cadherin, and Fibronectin **(Figure 4.11 A and B).** Also, we observed a significant reduction in the levels of Fibronectin and N-cadherin protein expression, but there was no change in Slug protein levels (**Figure 4.11C).** There was a minor increase in the protein levels of E-cadherin (**Figure 4.11C).** It is worth mentioning that there was a change in the cell morphology of MDA-MB 231 cells that stably overexpressed FRK when compared with the parental cells. We observed that the FRK-expressing cells lost the typical mesenchymal stellate morphology exhibited by the parental cells, and acquired a more rounded shape (**Figure 4.11D)**. To further verify the downregulation of mesenchymal markers with FRK overexpression, we took another basal B breast cancer cell line Hs578T and transiently overexpressed FRK in it**.** We also observed a decrease in Fibronectin, a mesenchymal marker (**Figure 4.11E**). Meanwhile, the knockdown of FRK in SKBR3 and MCF-7 breast cancer cells led to the up-regulation of Snail, Vimentin, and Fibronectin. We obtained a downregulation of E-cadherin in MCF-7 breast cancer cell lines at both mRNA and protein levels. The effect FRK knockdown on E-cadherin mRNA and protein expression could not be analyzed in SKBR3 because SKBR3 does not express E-cadherin (Neve *et al*., 2006). Together, our data consistently showed that the overexpression of FRK increased the expression of E-cadherin mRNA and down-regulated the transcript levels of Fibronectin, N-cadherin and Slug, while knockdown of FRK in both MCF-7 and SKBR3 cells led to the upregulation of Vimentin and Fibronectin mRNA levels. Our findings, therefore, suggest that

FRK inhibits EMT by stimulating the expression of the epithelial marker, E-cadherin and suppressing the expression mesenchymal proteins, especially Vimentin and Fibronectin **(Figure 4.11F-I).**

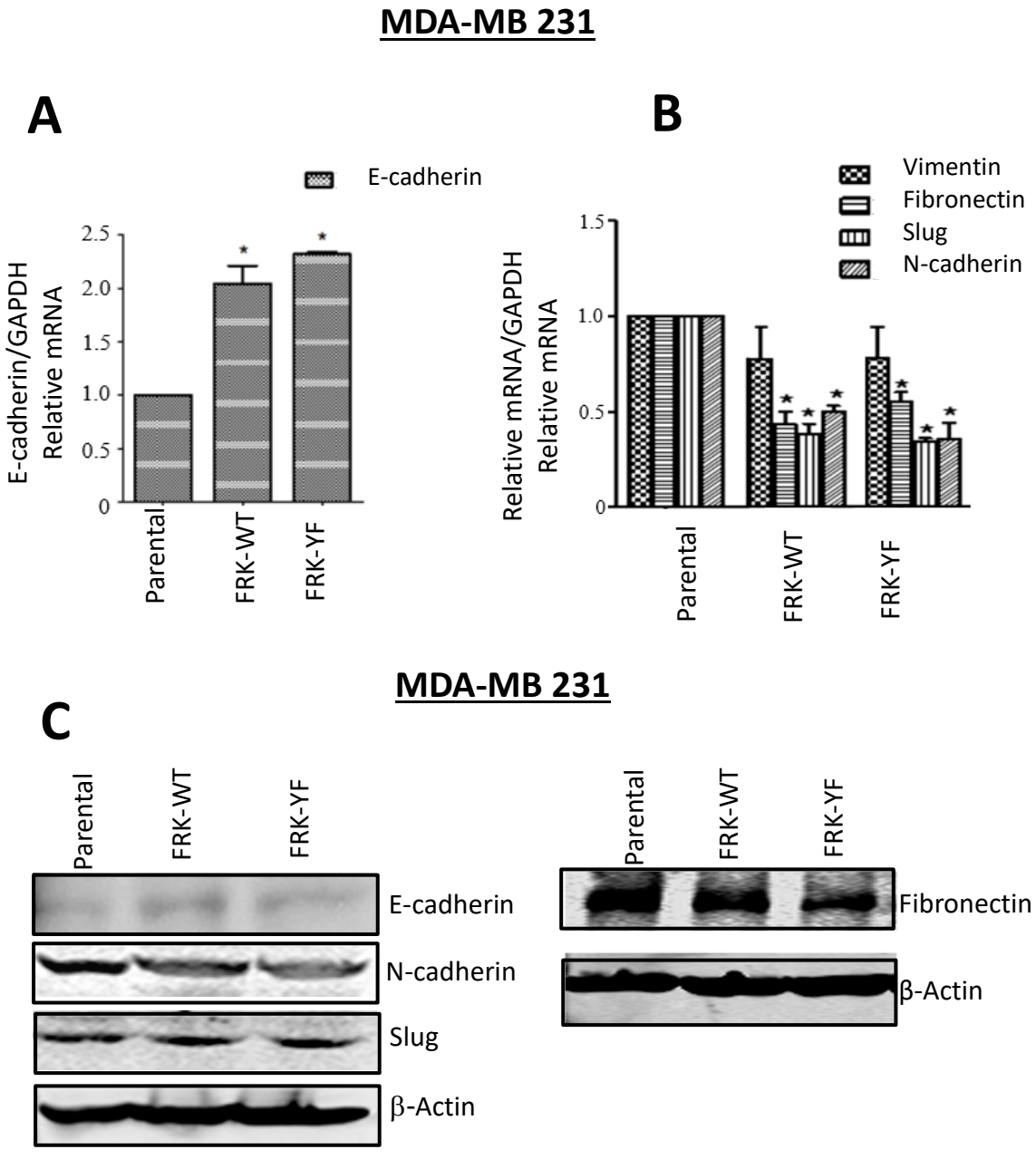

D

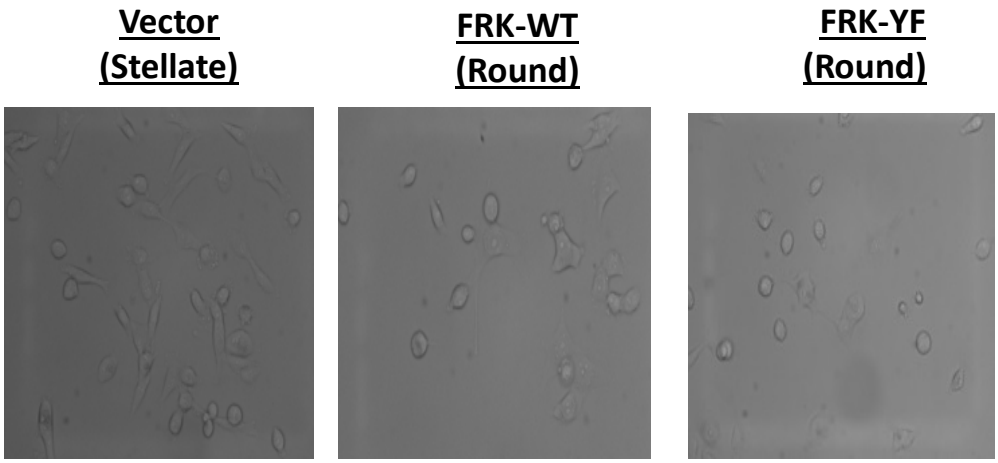
Vector
(Stellate)
FRK-WT
(Round)
FRK-YF
(Round)

E

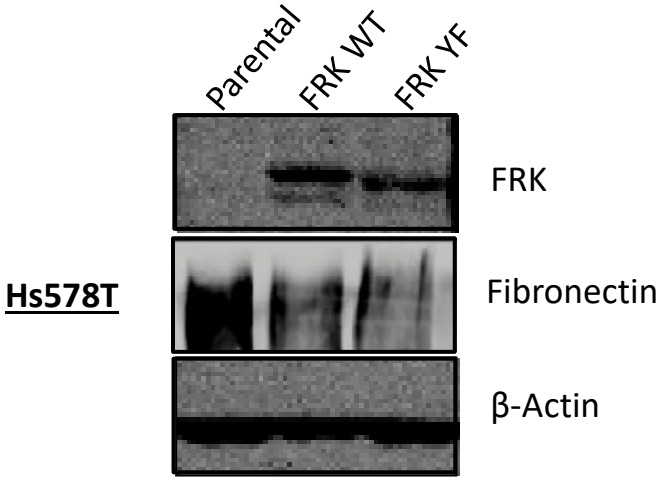
Parental
FRK WT
FRK YF
FRK
Hs578T
Fibronectin
β-Actin

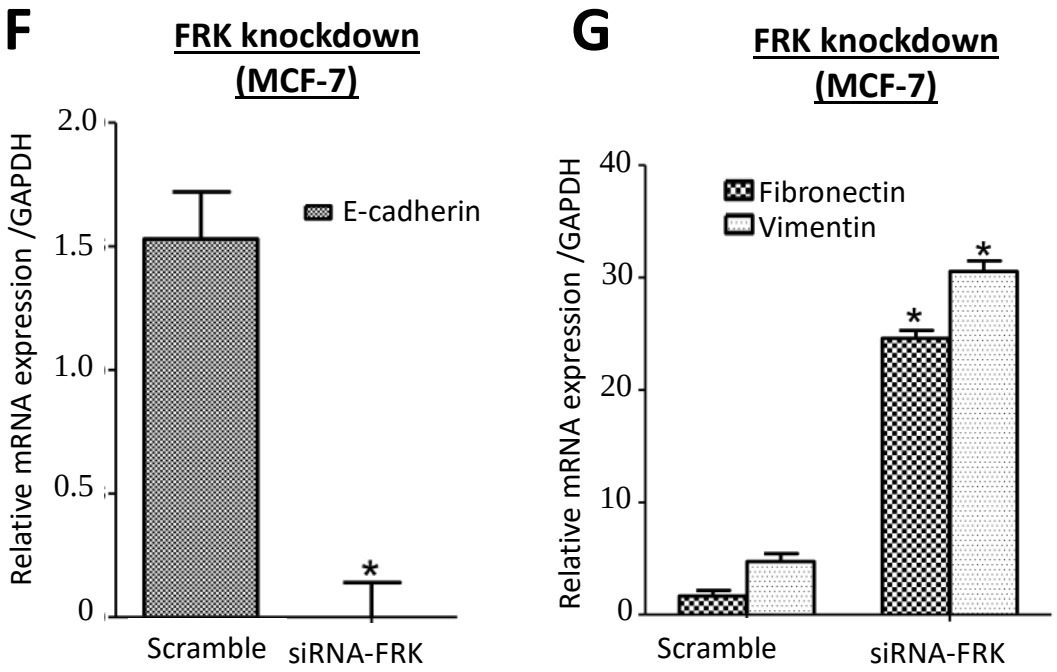
F
FRK knockdown
(MCF-7)
Relative mRNA expression /GAPDH
2.0
1.5
1.0
0.5
0
E-cadherin
*
Scramble
siRNA-FRK
G
FRK knockdown
(MCF-7)
Relative mRNA expression /GAPDH
40
30
20
10
0
Fibronectin
Vimentin
*
*
Scramble
siRNA-FRK

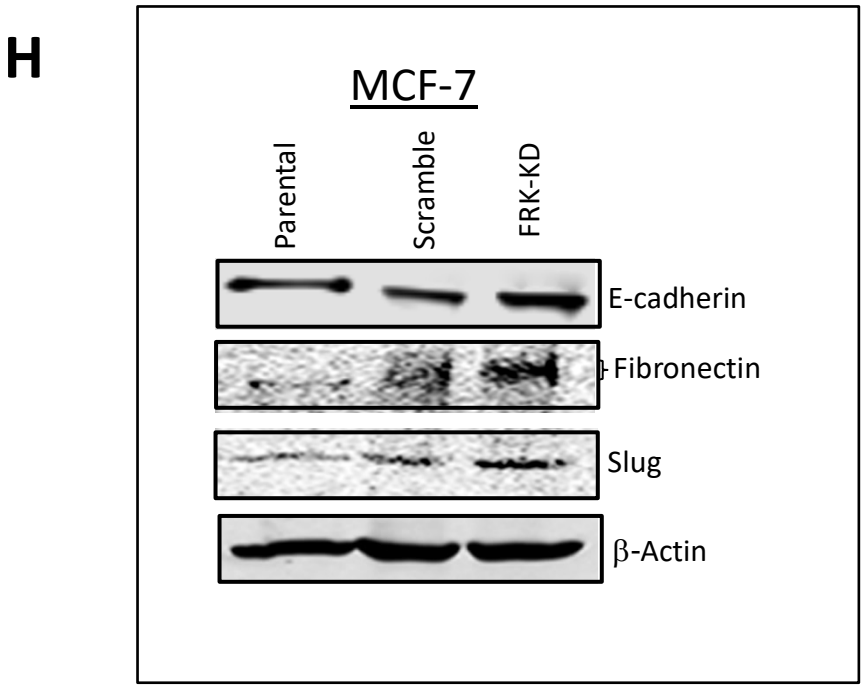
H
MCF-7
Parental
Scramble
FRK-KD
E-cadherin
Fibronectin
Slug
β-Actin

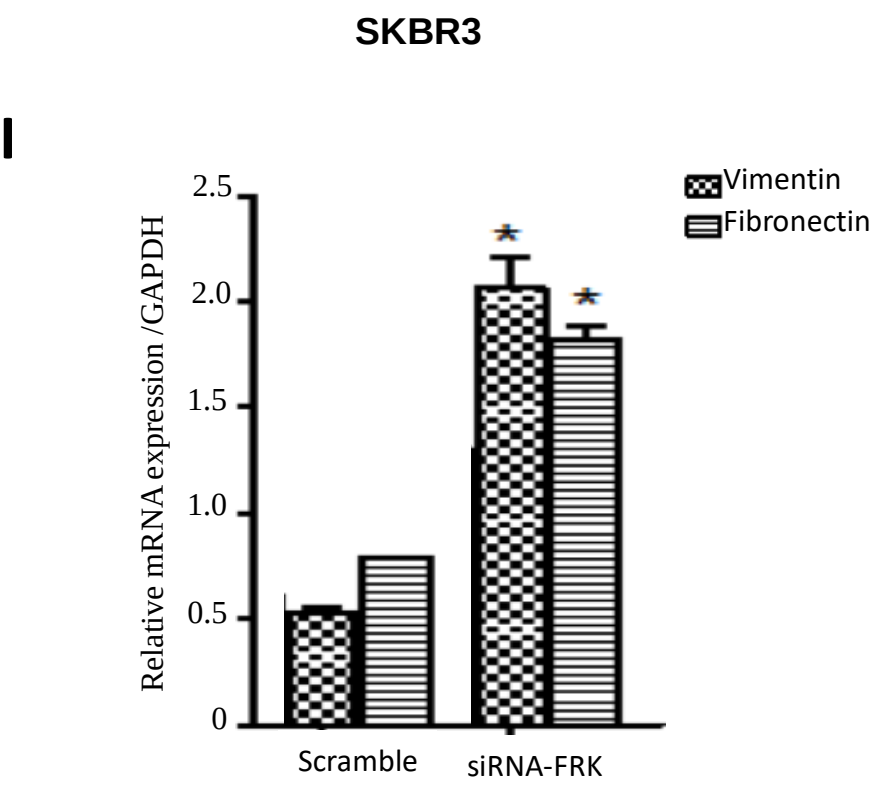

FIGURE 4.11: FRK-mediated regulation of EMT in breast cancer cell lines: A) and B). The mRNA levels of E-cadherin, Vimentin, Fibronectin, Slug, and N-cadherin, relative to GAPDH levels, were quantitatively measured in the control vector, FRK WT and FRK YF-expressing MDA-MB 231 stable cell lines. **C).** Lysates from parental MDA-MB 231 or MDA-MB 231 cells stably expressing either wild-type FRK (FRK-WT) or FRK-YF were probed for the expression of E-cadherin, N-cadherin, and Slug (left panel), or Fibronectin (right panel) using appropriate antibodies. β-Actin was used as the loading control. **D).** The microscope was used to examine the cellular morphology of the indicated stable cell lines generated. Arrows indicate the change from stellate to round shape. Phase-contrast images of the indicated stable cell lines were taken using the Olympus 1x51 microscope at 20x magnification. **E).** Parental Hs578T and Hs578T cells transiently expressing FRK- WT and FRK-YF(FRK YF) were probed for the expression of Fibronectin using appropriate antibodies. β-Actin was used as the loading control. **F) and G) Endogenous FRK was transiently knocked** down in MCF-7 cells and the mRNA levels of E-cadherin, Fibronectin and Vimentin were quantified relative to GAPDH transcript levels. Parental MCF-7 cells were used as reference **H).** Expression of E-cadherin, Fibronectin, and Slug was examined in MCF-7 cells following the transient knockdown of FRK. β-Actin was used as the loading control **I).** The mRNA levels of Vimentin and Fibronectin were quantitatively measured in SKBR3 cells following the transient knock-down of endogenous FRK. Parental SKBR3 cells were used as a reference. The data are presented as mean ± S.D. (p-value ≤ 0.05).

4.8 FRK expression negatively correlates with mesenchymal markers in a large cohort of breast cancer cells

To further substantiate our findings that FRK is a negative regulator of EMT, we mined the gene expression database, GENT (Gene Expression across Normal and Tumors; http://medicalgenome.kribb.re.kr/GENT/reference.php) to determine the correlation between FRK, epithelial and mesenchymal markers expression using 56 breast cancer cells. We checked the relationship between the expression of FRK with mesenchymal markers Vimentin (VIM), N-cadherin (CDH2), Fibronectin (FN1), Snail family transcriptional repressor 2 (SNAI2), twist family bHLH transcription factor 1(TWIST1), and epithelial markers E-cadherin (CDH1) and Keratin 18 (KRT18), in breast cancer cell lines stratified under Basal B (BB), Basal A (BA) and luminal (LU) (**Figure 4.12**). A Recent study on FRK shows that the level of FRK transcript in basal B breast cancers was low when compared to Basal A and Luminal cells (Bagu *et al*., 2017; Ogunbolude *et al.,* 2017). Data obtained from the database also showed that the mean transcript expression of VIM, CDH2, FN1, and TWIST1 were higher in the basal B breast cancer cells with low FRK transcript levels as compared to Basal A and Luminal cells that express high FRK transcript levels ($P<0.05$; **Figure 4.12**). Mean transcript levels of SNAI2 were higher in the basal B breast cancer cells with low FRK transcript levels as compared to the Luminal cells ($P<0.05$; Figure 10G). The Pearson′s correlation analysis that was run on 226 samples made up of 56 breast cancer cells showed that FRK transcript levels were negatively correlated with the transcript levels of VIM, CDH2, and TWIST1, with R-values of -0.28; -0.20; -0.25 respectively ($P<0.001$). The mean transcript expression of CDH1 and KRT18 were lower in the basal B breast cancer cells with low FRK transcript levels as compared to Basal A and Luminal cells ($P<0.05$; Figure 10C, E). FRK transcript levels correlated positively with the transcript levels of CDH1 and KRT18, with R-values of 0.39 and 0.26 ($P<1.0 \times 10^{-5}$), respectively. However, this trend was not completely reciprocated when we interrogated the cancer genome atlas (TCGA) dataset (http://cancergenome.nih.gov/) for breast cancer tissues, a positive correlation was also observed with E-cadherin and FRK in the normal tissues, and a negative correlation was observed with Fibronectin and Vimentin in normal tissues samples (**Figure 4.13**). However, no correlation was observed between FRK and Vimentin, E-cadherin and Fibronectin in the tumor samples (**Figure 4.13**). This might be because the TCGA breast carcinoma dataset, unlike the cell lines, was not classified by Basal A/Basal B mesenchymal properties, and this may explain

the discrepancy in both datasets. However, the results obtained in **Figure 4.12** suggests that FRK expression inversely correlates with mesenchymal markers in Basal B breast cancers cells and present a contextual nature for FRK in EMT-associated cellular processes. Taken together, our data demonstrate that FRK inversely correlates with mesenchymal markers in breast cancer cells and may, therefore, be a negative regulator of mesenchymal-like properties of breast cancer cells.

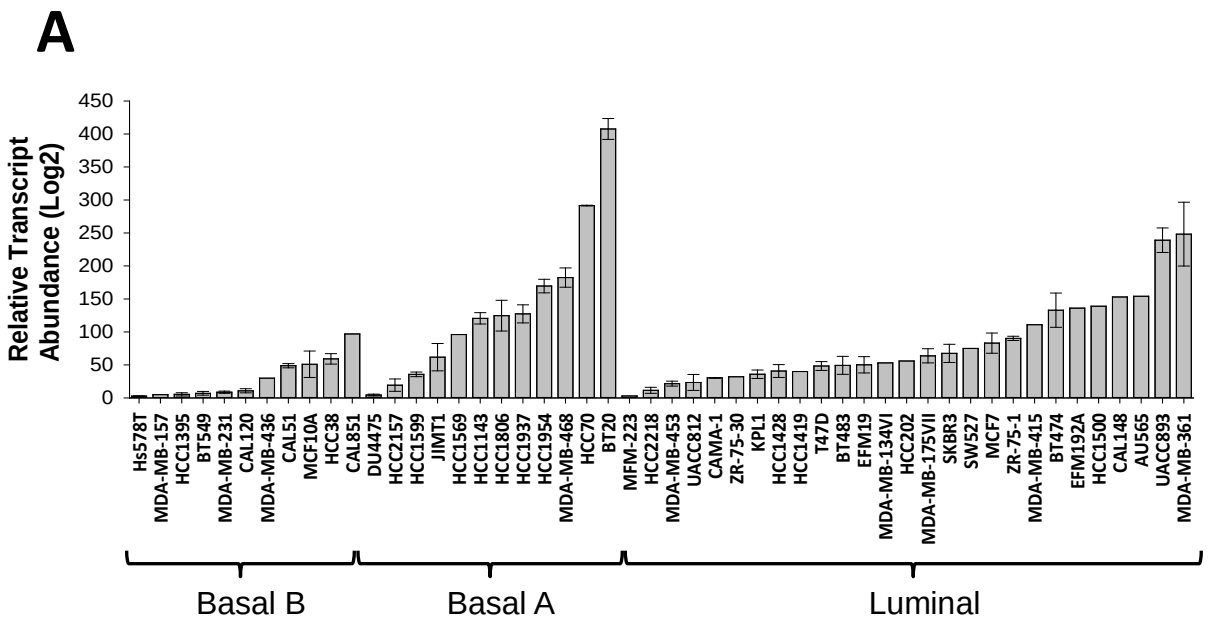

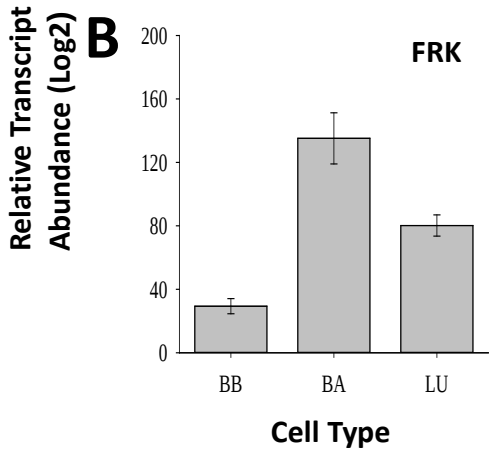
B
FRK
Relative Transcript Abundance (Log2)
200
160
120
80
40
0
BB
BA
LU
Cell Type

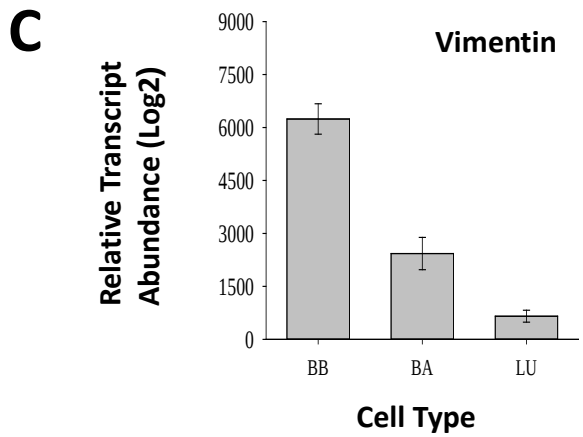
C
Vimentin
Relative Transcript Abundance (Log2)
9000
7500
6000
4500
3000
1500
0
BB
BA
LU
Cell Type

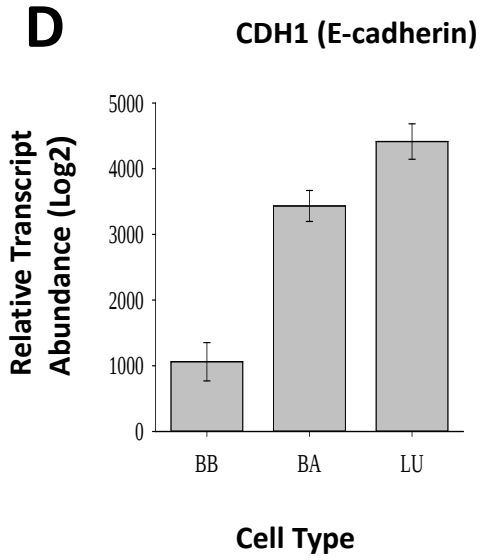
D
CDH1 (E-cadherin)
Relative Transcript Abundance (Log2)
5000
4000
3000
2000
1000
0
BB
BA
LU
Cell Type

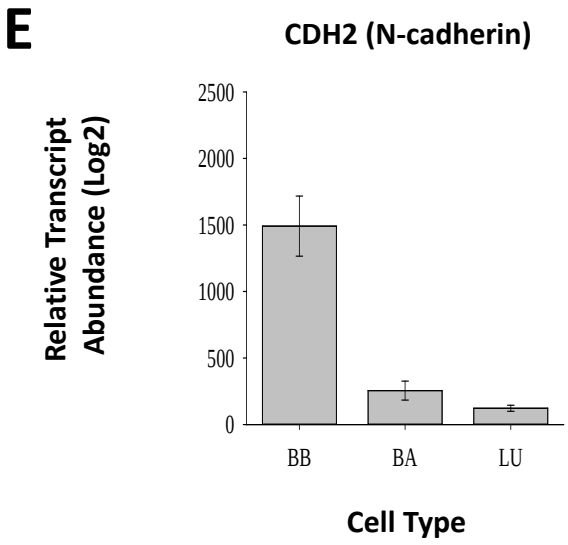
E
CDH2 (N-cadherin)
Relative Transcript Abundance (Log2)
2500
2000
1500
1000
500
0
BB
BA
LU
Cell Type

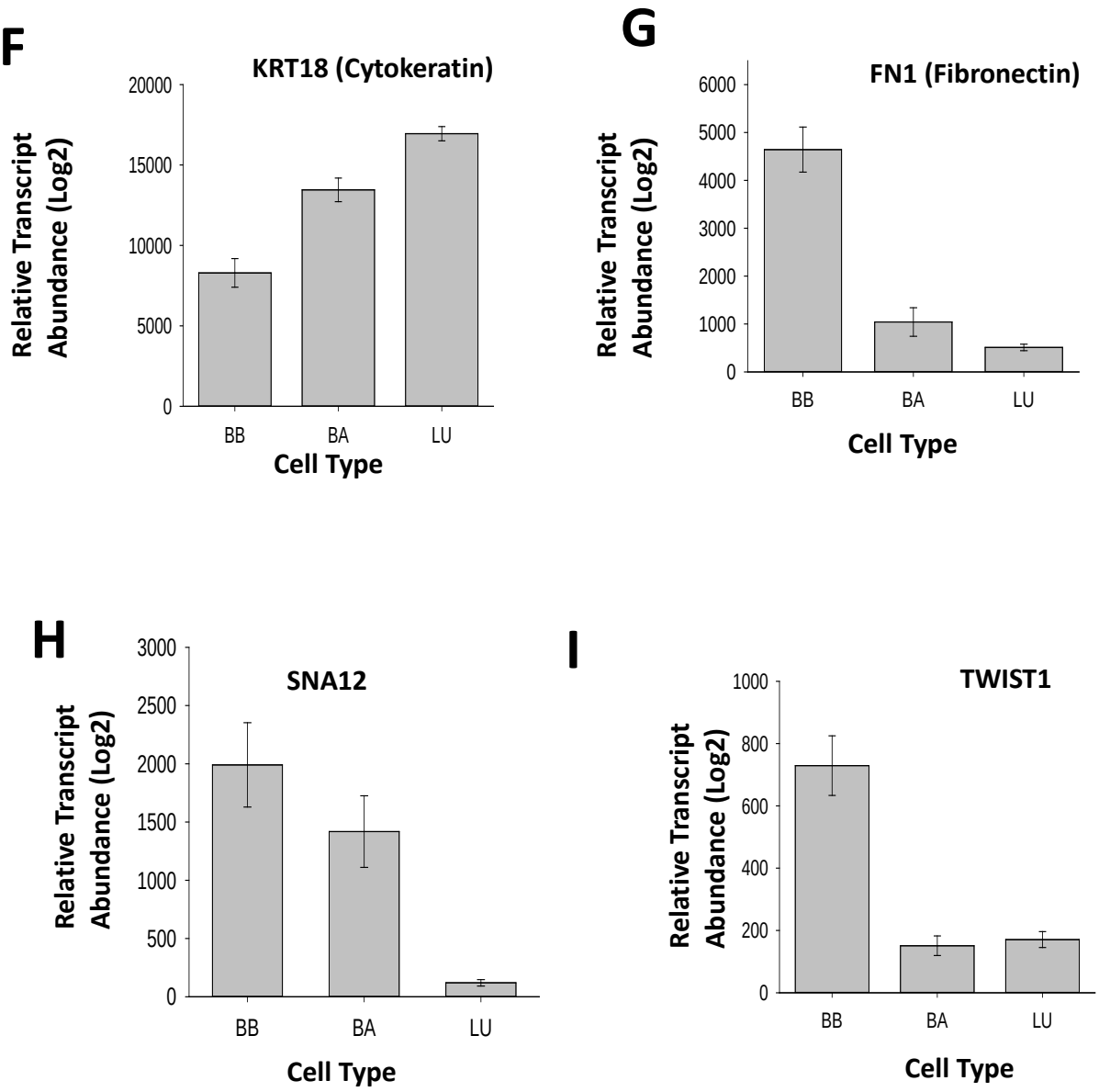

Figure 4.12: Gene expression profiles of FRK, epithelial and mesenchymal markers in Basal A, Basal B, and luminal breast cancer cell lines. Relative transcript abundances of **A).** and **B).** FRK, **C)**. Vimentin, VIM; **D)**. E-cadherin, CDH1; **E)**. N-cadherin, CDH2; **F).** Keratin 18, KRT18; **G)**. Fibronectin, FN1, **H)**. Slug, SNAI2 and **I)**. TWIST1 were assessed in Basal A (BA), Basal B (BB) and Luminal (LU) breast cancer cell lines (N=56). Mean transcript levels of the indicated genes in breast cancer cell lines were mined from the GSE10021, GSE10843, GSE3156, GSE10890 and GSK's cell line project (https://array.nci.nih.gov/caarray/project/woost-00041/) databases using the GENT software (http://medicalgenome.kribb.re.kr/GENT/reference.php). The data are presented as mean ± SEM. (p-value ≤ 0.05).

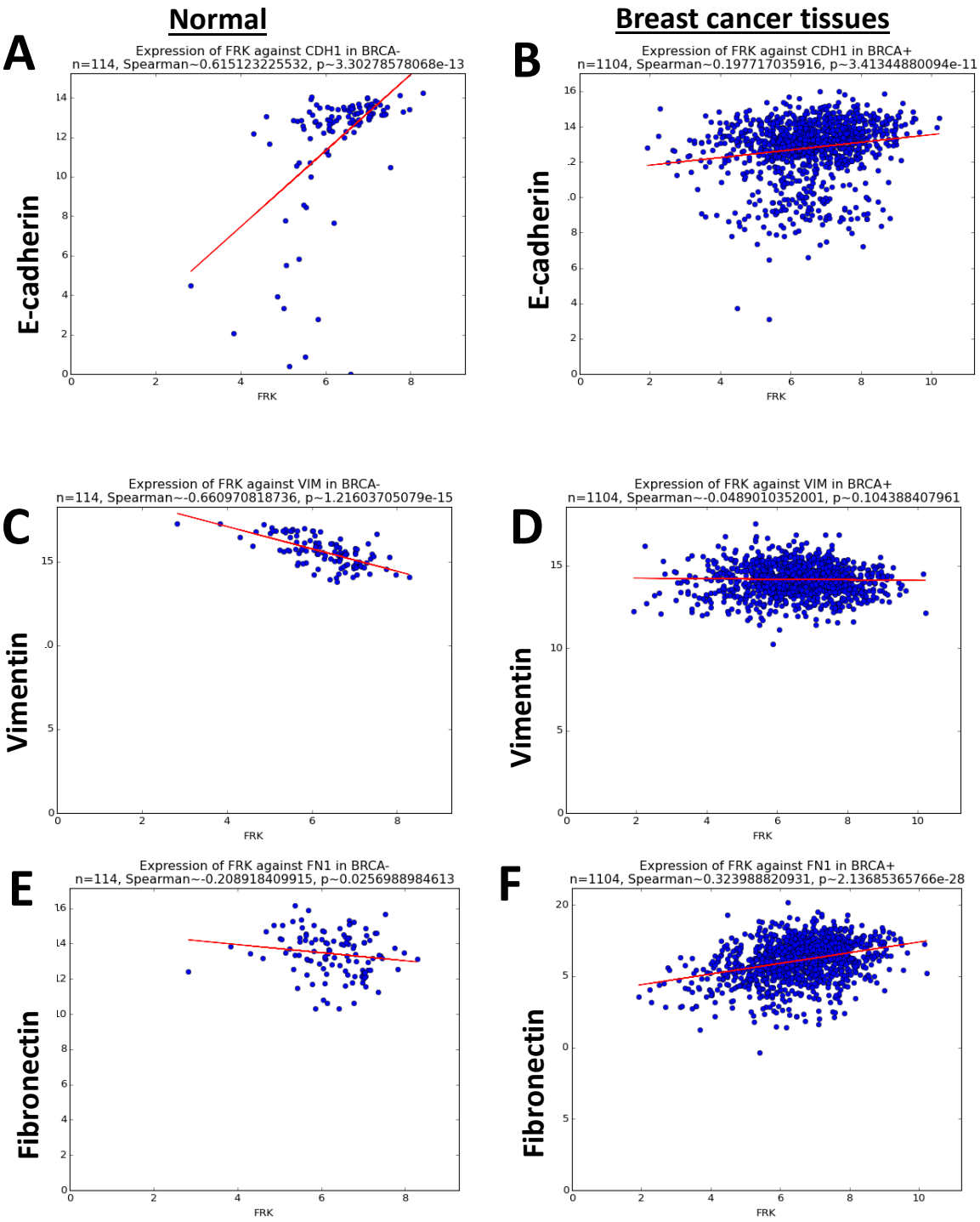

FIGURE 4.13: FRK gene expression correlation with EMT markers: Gene expression from RNA Seq V2 data from 114 normal mammary tissues (**A, B, C**) and 1104 breast cancer samples (**E, F, G**) from TCGA were downloaded and analyzed for FRK, E-cadherin, Vimentin, and Fibronectin expression. The scatterplots represent correspondence of FRK expression with E-cadherin (**A** and **D**), Vimentin (**B** and **E**) and Fibronectin (**C** and **F**) in TCGA Expression values are presented are log2 intensities. Included in the scatterplots are the Spearman rank correlation with significant P-value and lines showing the linear fit.

4.9. Effect of FRK overexpression on apoptosis

FRK is a candidate tumor suppressor in breast cancer known for its ability to inhibit breast cancer cell proliferation and migration. Previous studies have shown that FRK suppresses cell proliferation in breast cancer cells by arresting cells in the G1 phase (Meyer *et al*., 2003), negatively regulating the AKT pathway by stabilizing PTEN (Yim *et al*., 2009a), and inhibiting EGFR signaling (Jin and Craven, 2014). From our findings, we have shown that overexpression of the FRK wild-type or it's constitutively active mutant (FRK-YF) in MDA-MB 231 (an FRK-negative breast cancer cell line) downregulates the mRNA levels of Survivin.However, the knockdown of FRK in SKBR3 and MCF-7 breast cancer cell lines that normally exhibit high levels of FRK resulted in the upregulation of Survivin transcript levels. Survivin belongs to the inhibitors of apoptosis family, known to negatively regulates apoptosis (Ma *et al*., 2016). Based on this, we investigated the effect of FRK on apoptosis by using Annexin V-FITC Staining. We found that overexpression of FRK-WT and FRK-YF in MDA-MB 231 cells had no significant effect on apoptosis when compared to the parental cells. The Annexin V-PI positive cells in both MDA-MB 231 stably overexpressing FRK-WT and FRK-YF were 3.5% and 4.3% respectively when compared with the parental cells of 2.6% (**Figure 4.14)**. Although in glioma cells, transient overexpression of FRK-WT was shown to promotes apoptosis (Hua *et al*., 2014); we did not see any effect in the MDA-MB 231 cells when FRK was stably overexpressed. The reason for this cell-specific effect of FRK is unknown. Our results, therefore, suggest that FRK might not be a potent inducer of apoptosis. The inhibition of Survivin with FRK overexpression is possibly not the mechanism by which FRK inhibits cell proliferation. FRK possibly inhibits cell proliferation through other mechanisms.

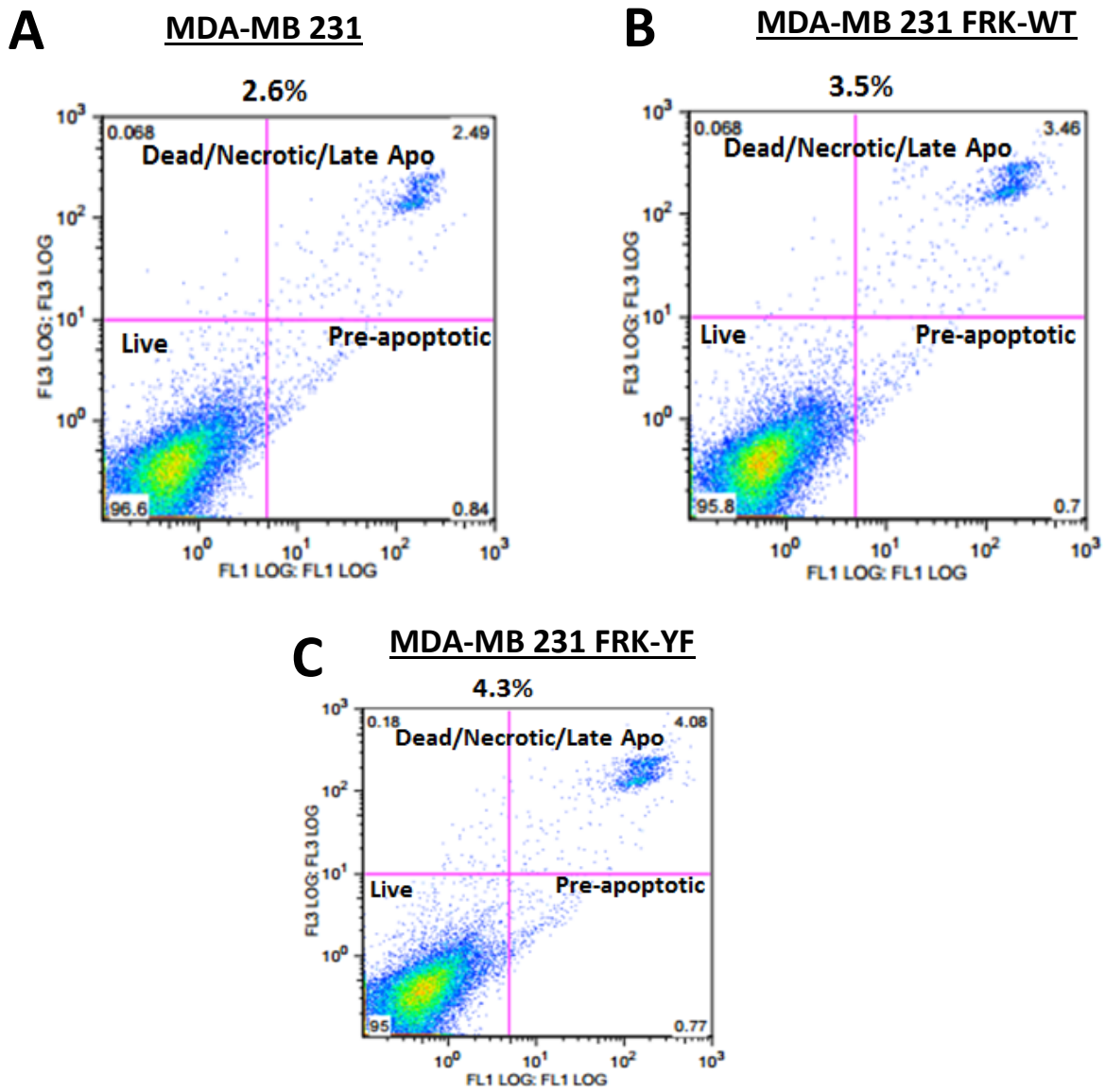

Figure 4.14: Effect of FRK on apoptosis. Representative micrographs of cell apoptosis with FRK stably overexpressed in MDA-MB 231 using Annexin V -FITC double-staining assay by flow cytometer. **A.** parental cells**, B)** FRK-WT stably expressed in MDA-MB 231 and **C)** FRK-YF stably expressed in MDA-MB 231**.** Overexpression of FRK in MDA-MB 231 breast cancer cells had no significant effect on apoptosis

4.10. Effect of FRK depletion on the cell cycle.

FRK has been shown induce the G1 arrest of the cell cycle when overexpressed in BT549 breast cancer cells (Meyer *et al*., 2003). However, how FRK depletion affects cell cycle progression was not validated in this study. To have an insight into the importance of FRK in arresting the G1 phase of the cell cycle, using a flow cytometer we investigated what the effect of knocking

down and overexpressing FRK would be on the different phases of the cell cycle. First, we stably overexpressed FRK in MDA-MB 231 and determined its effect on different stages of the cell cycle. We found that stable overexpression of FRK resulted in the G1 arrest of the cell cycle (**Figure 4.15).** This data not only confirms previous reports but also shows that the effect of FRK overexpression on the G1 phase of the cell cycle is not cell line-specific. When we transiently knockdown FRK in MCF-7 breast cancer cells, we observed a decrease in the number of cells in the G1 phase of the cell cycle, as anticipated (**Figure 4.15**). Although we expected to see an increase in the S-phase or the G2 phase, there was no significant change in the number of cells with or without FRK. Interestingly, we found a significant increase in apoptosis with FRK knockdown from 1.92% in the parental MCF-7 cells to 8.53% in the FRK-knockdown cells. Our results, therefore, suggest that FRK possibly inhibits cell proliferation by inducing the G1 arrest of the cell cycle, while the effect of FRK depletion possibly suggests that FRK might play a crucial role in maintaining the survival of some breast cancer cells.

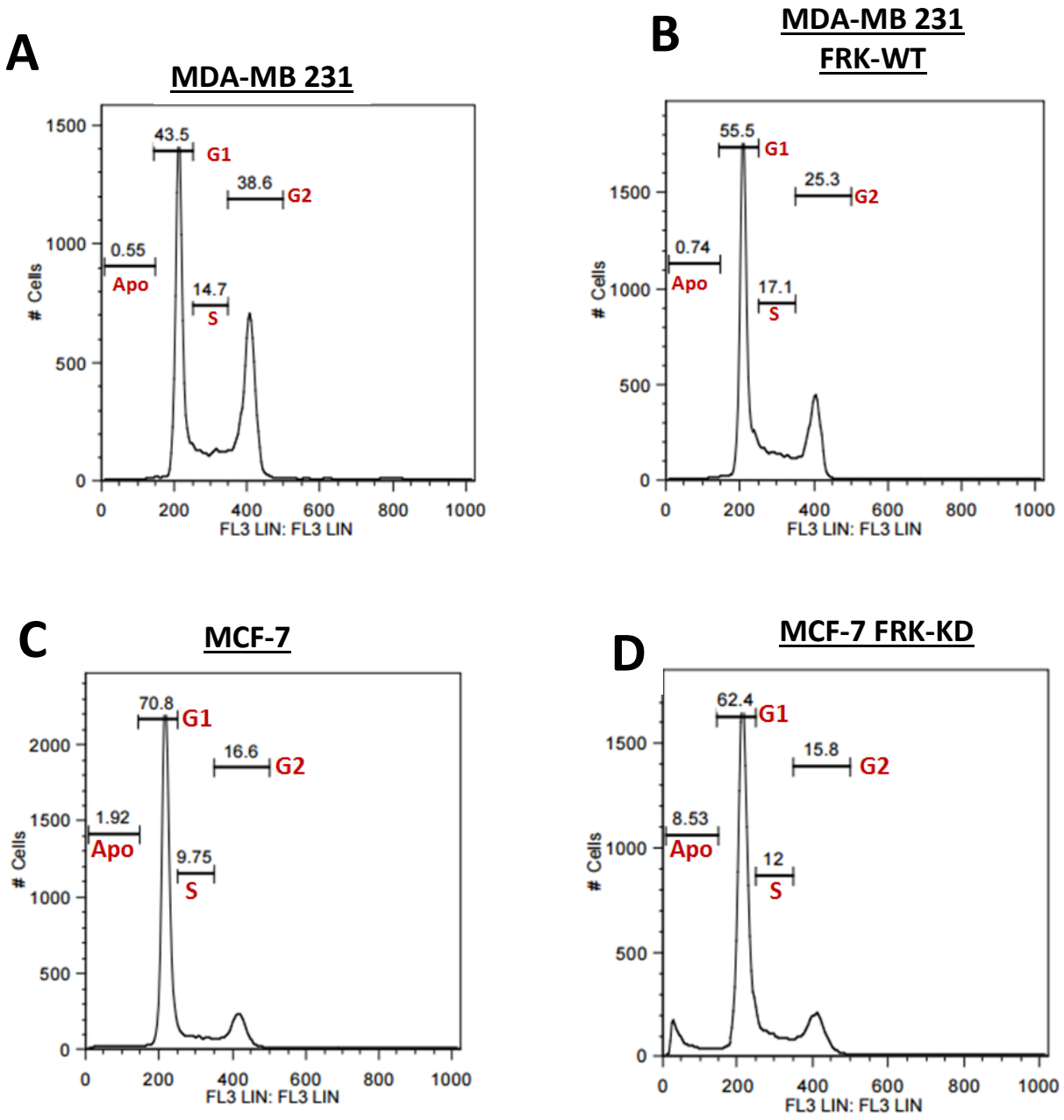

Figure 4.15: Effect of FRK on the cell cycle. **A and B)** MDA-MB 231 and MDA-MB 231 stably expressing FRK-WT **C and D) MCF-7 with transient knockdown of FRK.** Cells were harvested and stained with propidium iodide; cell cycle distribution was analyzed by flow cytometry. Left panel: Charts, the numbers indicate the proportion of cells in the different phases of the cell cycle. Right panel: the proportion of cells at G0/G1 phase. Overexpression of FRK-WT in MDA-MB 231 breast cancer cells induces the arrest of more cells in the G1 phase, however, knockdown of FRK in MCF-7 breast cancer cell lines increases apoptosis.

4.11. FRK induces G1 arrest of the cell cycle by inhibiting E2F1 and upregulating p21

The transition from the G1 to S is known to be associated with the phosphorylation of the retinoblastoma (pRb) tumor suppressor protein, leading to its inactivation and hence the consequent release of E2F from the pRb–E2F complex (Giacinti and Giordano, 2006; Hua *et al*., 2014). Although FRK has been reported to bind with pRb in breast cancer cells, there is little or no data on the effect of FRK on the pRb-E2F1 pathway in breast cancers. Therefore, we investigated the effect of FRK overexpression as well as its knockdown on the pRb-E2F1 pathway. As shown in **Figure 4.16 A and B**, stable overexpression of FRK-WT and FRK-YF in MDA-MB 231 led to upregulation of pRb mRNA and protein levels when compared with the parental cells; this corresponded with the downregulation E2F1 mRNA and protein expression (**Figure 4.16 A and B**). Furthermore, we found that the overexpression of FRK decreased the phosphorylation of pRb. Although there was a decrease the mRNA levels of cyclin E (a downstream target of E2F1) (**Figure 4.16 A and B**), FRK overexpression had no significant effect on the protein expression of Cyclin E (**Figure 4.16 B**). The knockdown of FRK in SKBR3 upregulated E2F1 mRNA expression but had no significant effect on pRb and cyclin E mRNA expression **(Figure 4.16 C and D).** However, at the protein level, we obtained an increase in pRb phosphorylation and upregulation of protein E2F1 expression in both SKBR3 as well as MCF-7 with FRK knockdown (**Figure 4.16 C, D, and E**). Our results, therefore, suggest that FRK might lead to the G1 arrest by regulating the pRb-E2F1 pathway. However, the inhibition of breast cancer cell proliferation by FRK was shown to be independent of pRb (Meyer *et al*., 2003). Hence, it is possible that FRK induces G1 arrest via other mechanisms other than regulating the pRb-E2F1 pathway.

p21 is a cyclin-dependent kinase inhibitor reported to induces G0/G1 arrest and G2/M arrest by inhibiting and blocking both CDK2 and CDK1 activity (Abbas and Dutta, 2009). The inhibition of CDK2 by p21 was shown to dephosphorylate pRb protein, which leads to cell cycle arrest via the inhibition of E2F1-dependent gene expression (Abbas and Dutta, 2009; Kang *et al*., 2016). In glioma cells, FRK was shown to upregulate p21. Therefore, we investigated the effect of FRK overexpression and knockdown on p21 protein and mRNA expression. Overexpression of FRK-WT and YF in MDA-MB 231 led to the upregulation of p21 protein levels, paradoxically associated with a decrease in p21 mRNA expression **(Figure 4.16 F and G).** However, we observed a downregulation of p21 protein and mRNA expression with the

knockdown of FRK in SKBR3 **(Figure 4.16 I, and J)**. FRK overexpression and knockdown did not affect pCDK1 (a regulator of G2/M arrest) protein expression **(Figure 4.17 H and K)**. Our result suggests that upregulation of p21 is another possible mechanism in FRK induces the G1 arrest of the cell cycle.

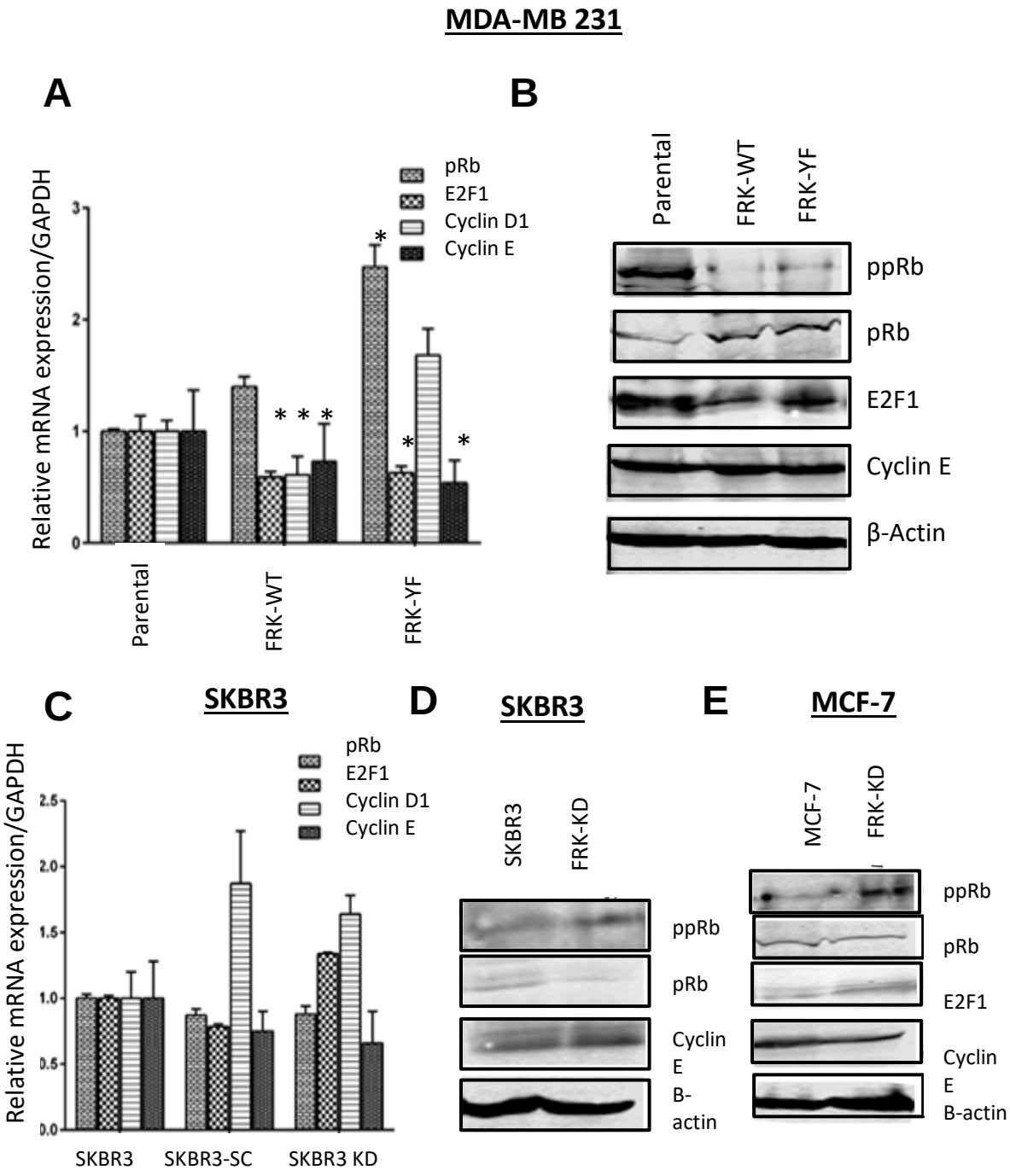

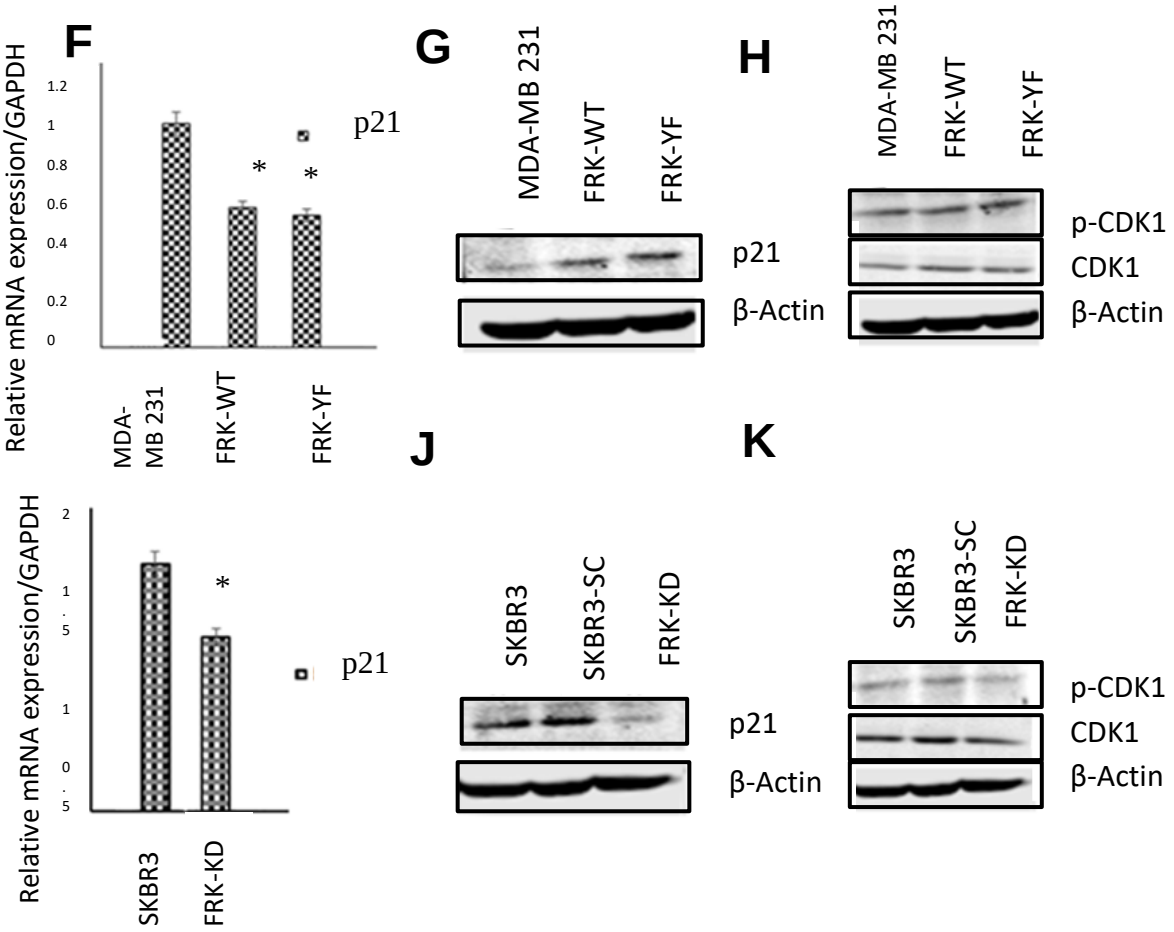

Figure 4.16: Effect of FRK on cell cycle regulators A) and B). mRNA expression of pRb, E2F1, Cyclin E and p21. Total RNA was isolated from MDA-MB 231 cells stably transfected with FRK-WT and FRK-YF and **C), D) and E)** SKBR3 transiently transfected with control or FRK siRNA. The mRNA level of pRb, E2F1, and Cyclin E level was quantified using an RT-PCR. **F), G), and H) mRNA and** protein expression of p21 and pCDK1 in MDA-MB 231 stably expressing FRK-WT and FRK-YF using western blot **I**, **J) and K)** mRNA and protein expression of p21 and pCDK1 in SKBR3 transiently transfected with control or FRK siRNA. Cell lysates were immunoblotted against CDK1, pCDK1, p21 and β-Actin as a control. The data are presented as mean ± S.D (p-value ≤ 0.05).

4. 12. FRK induces G1 arrest of the cell cycle by inducing senescence

p21 has been reported to induce the G1 arrest of the cell cycle by inducing cellular senescence (Campisi and d'Adda di Fagagna, 2007). Senescence is an irreversible form of cell cycle arrest that can be triggered by various forms of stress, such as DNA damage, or oncogene-induced senescence (Wen *et al*., 2014). Oncogene-induced senescence relies on the activation of tumor suppressors that mediate cell cycle arrest (Campisi and d'Adda di Fagagna, 2007; Wen *et al*., 2014). Since we observed an upregulation of p21 with the overexpression of FRK, we, therefore,

examined the effect of FRK on cellular senescence by using Senescence-associated β-galactosidase (SA-β-Gal) staining kit. MDA-MB 231 stably expressing FRK-WT and FRK-YF as well as the parental, were stained, fixed and examined under the microscope. Senescent cells were stained blue in the presence of SA-β-Gal. We observed more staining with FRK-WT and FRK-YF when compared with the parental cells, which hadless stains (**Figure 4.17A, B, and C**). However, transient knockdown of FRK in MCF-7 cell had no significant effect on senescence (**Figure 4.17 D and E**). Our data as a whole suggest that FRK possibly arrests the G1 phase of the cell cycle, by inducing cellular senescence through p21 upregulation.

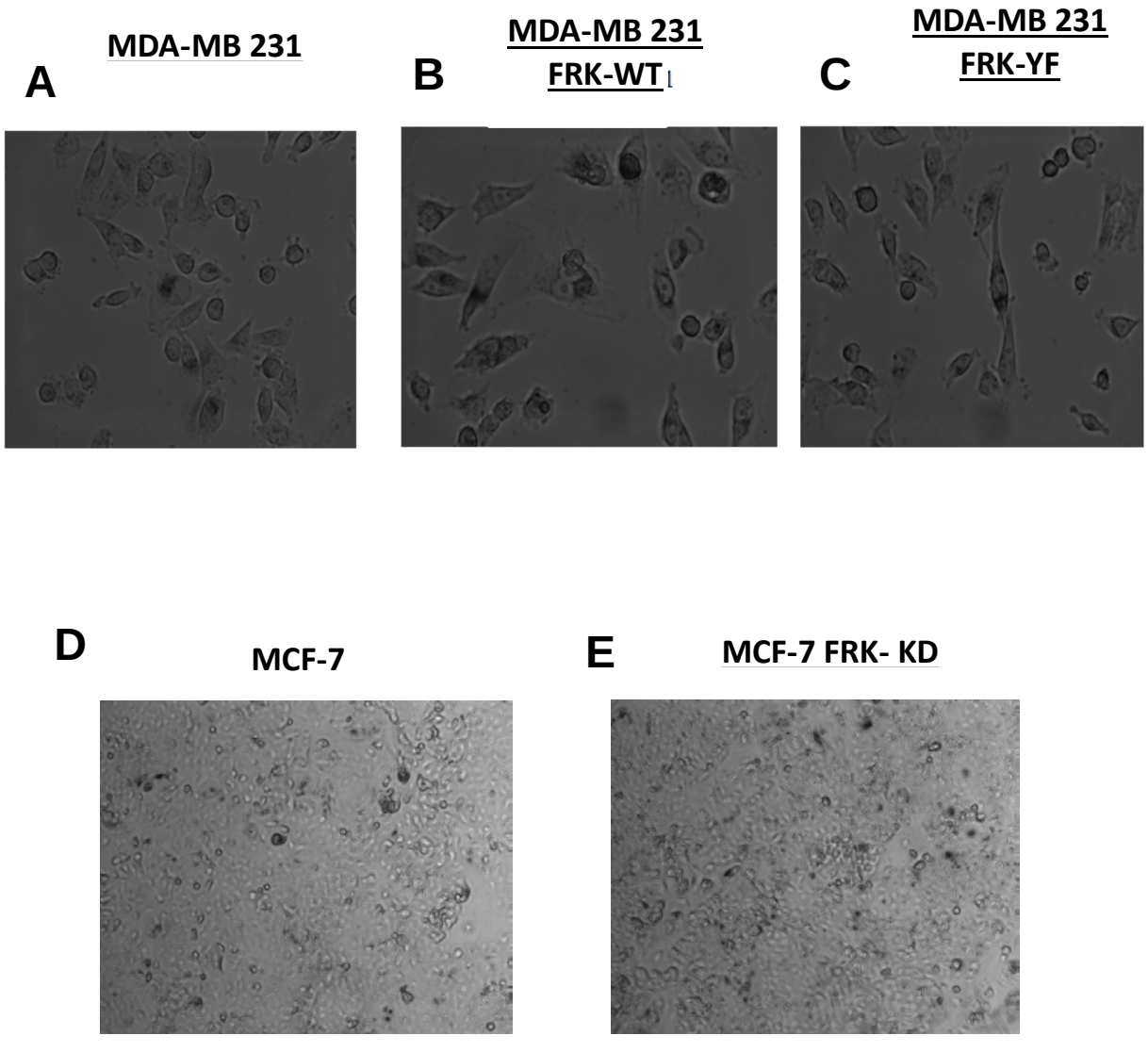

Figure 4.17: Effect of FRK on cellular senescence. A), B) and C). MDA-MB 231 or MDA-MB 231-expressing FRK-WT or FRK-YF **D and E**) MCF-7, as well as MCF-7 FRK-KD, were subjected to an SA-β-Gal assay to determine the percentage of the senescent population. SA-β-Gal staining (×20 magnification) was shown in bright-field images. Cells that have undergone senescence were stained blue under the microscope. However, the blue stains appeared black under bright-field images on the microscope.

4.13 FRK suppresses breast cancer tumorigenesis.

Finally, we investigated whether the tumor suppressive properties of FRK can be recapitulated *in vivo* using a nude mouse model. First, as proof of principle, we compared the proliferation rates of MDA-MB 231 stably expressing an empty vector (control), FRK-WT and FRK-YF using the Cell Counting Kit-8 (CCK-8). The CCK-8 assay measures dehydrogenase activity in functional mitochondria, which is a direct reflection of the cell viability. MDA-MB 231 cells stably expressing FRK-WT and FRK-YF displayed significantly diminished cell proliferation compared with parental cells after 4 days ($P < 0.005$) (**Figure 4.18A**). Similar results were obtained when cell viability assay was performed using 7AAD with transient transfection of FRK-WT and FRK-YF in MDA-MB 231 breast cancer cells (**Figure 4.18 B, C, and D**).

Next, we used the FRK-WT and FRK-YF stable cell lines to determine their rates of tumorigenesis *in vivo*. At least four mice were allocated to each treatment group and housed in the same cage. The fourth mammary fat pad of these mice was injected with one of the following cells; parental MDA-MB 231 cells, MDA-MB 231 stably expressing FRK-WT, FRK-YF, while the control group received Matrigel. The mice were monitored and their body weights measured after every 7 days over a period of 60 days. The mice were then sacrificed, and the tumor mass (gm) and volume (cm^3) was measured (**Figures 4.19A and B**). All mice developed tumors 10 days after injection, however, mice injected with FRK-WT and FRK-YF had slow tumor growth rate when compared to the parental group. There was no tumor growth in the mice injected with Matrigel. At the end of the experiments, the average tumor mass weight was 0.37 g for the parental group and 0.25 g for FRK-WT group and 0.25 g for FRK-YF group. There was no significant difference between the tumor weight of the FRK-WT group and the FRK-YF group. Our results, however, suggest that FRK can potentially suppress breast cancer tumorigenesis *in vivo.*

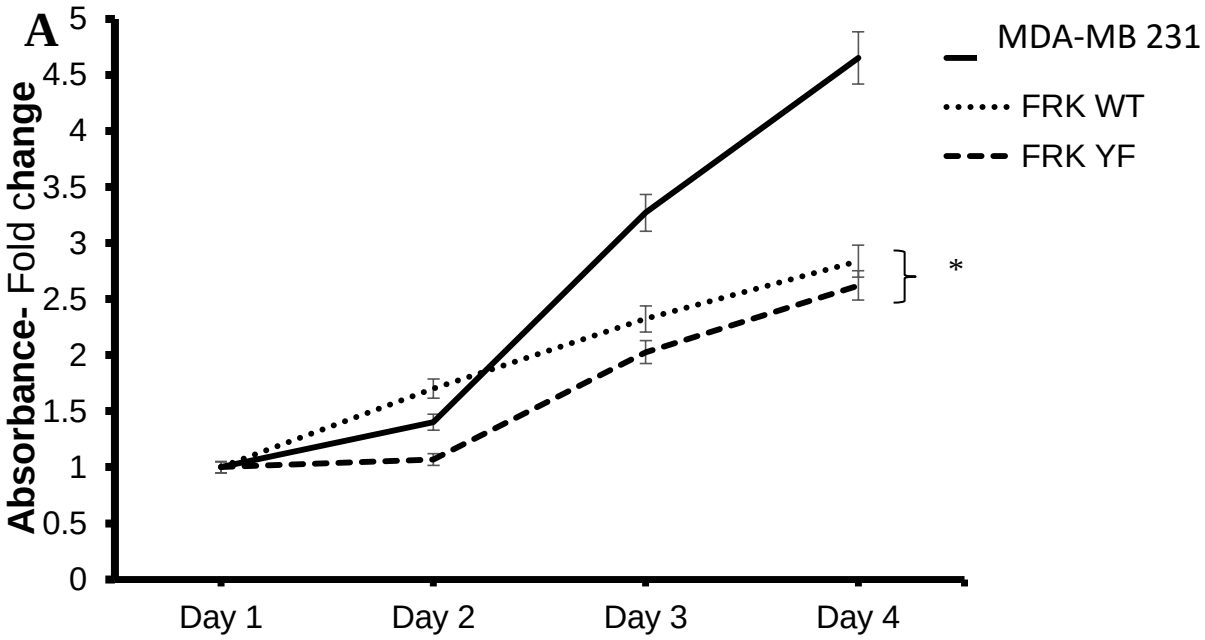
A
Absorbance- Fold change
5
4.5
4
3.5
3
2.5
2
1.5
1
0.5
0
Day 1
Day 2
Day 3
Day 4
MDA-MB 231
FRK WT
FRK YF
*

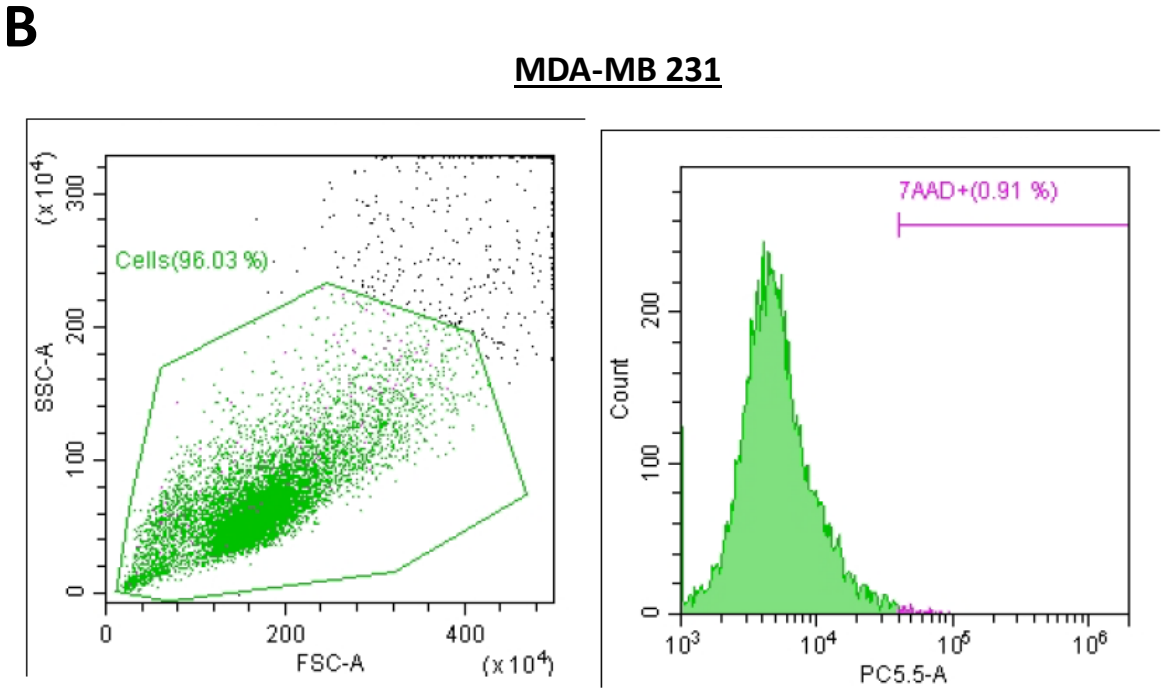
B
MDA-MB 231
Cells(96.03 %)
SSC-A
(x 10^4)
300
200
100
0
0
200
400
FSC-A
(x 10^4)
7AAD+(0.91 %)
Count
200
100
0
10^3
10^4
10^5
10^6
PC5.5-A

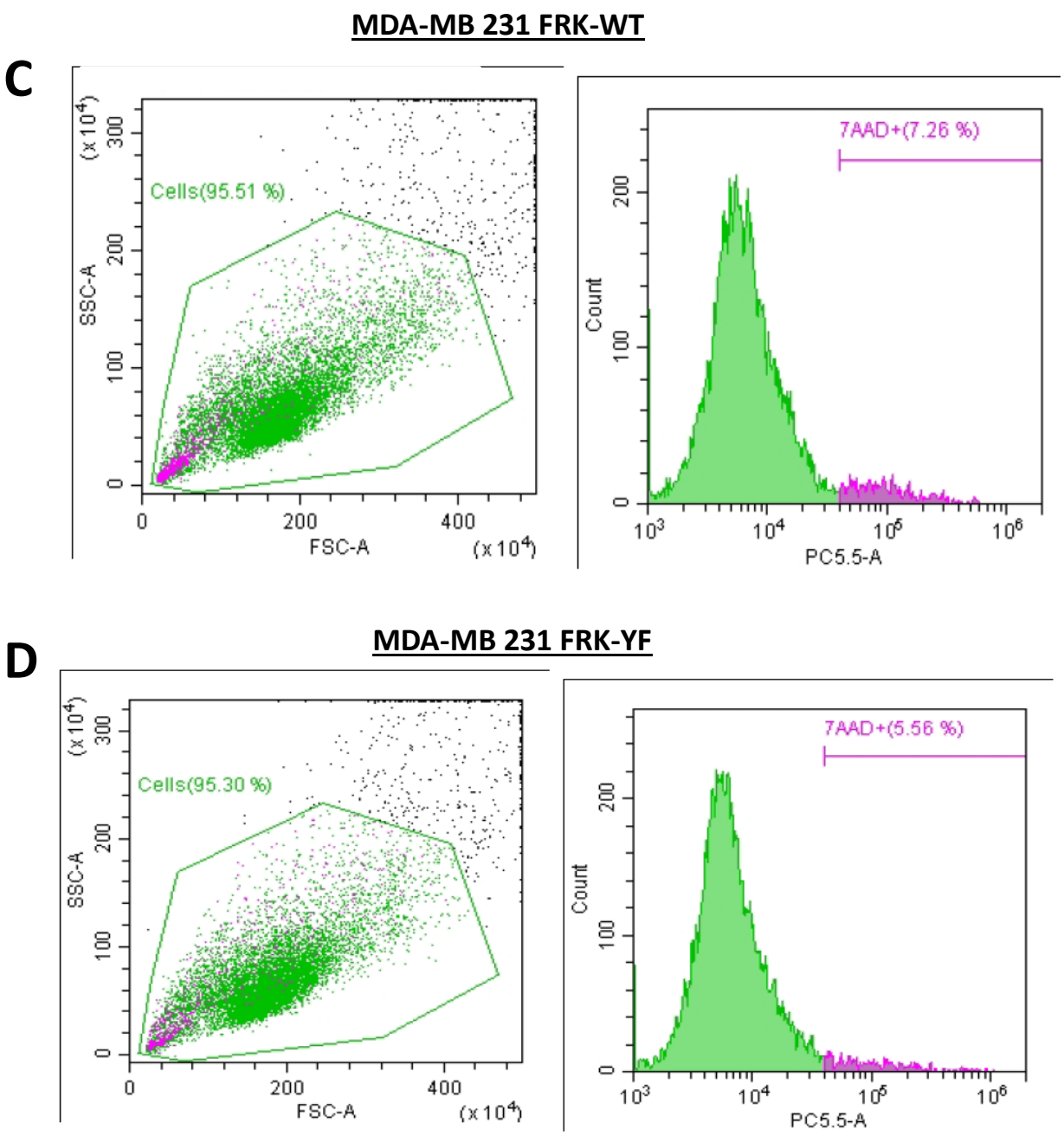

Figure 4.18: Effect of FRK overexpression on cell proliferation: Vectors encoding wild-type FRK (FRK-WT) or FRK Y497F (FRK-YF) were retrovirally introduced into MDA-MB 231 cells and polyclonal populations derived and designated as indicated. **A).** Cell proliferation rates of the indicated FRK transfected cell lines and the control cells were measured using the CCK8 assay. **B), C), and D).** The number of live and dead cells were quantified using 7AAD assay in the transiently transfected MDA-MB 231 cell lines. Overexpression of FRK suppresses cell proliferation and also increased the number of dead cells when compared to the parental cells. The data are presented as mean ± S.D. (p-value ≤ 0.05)

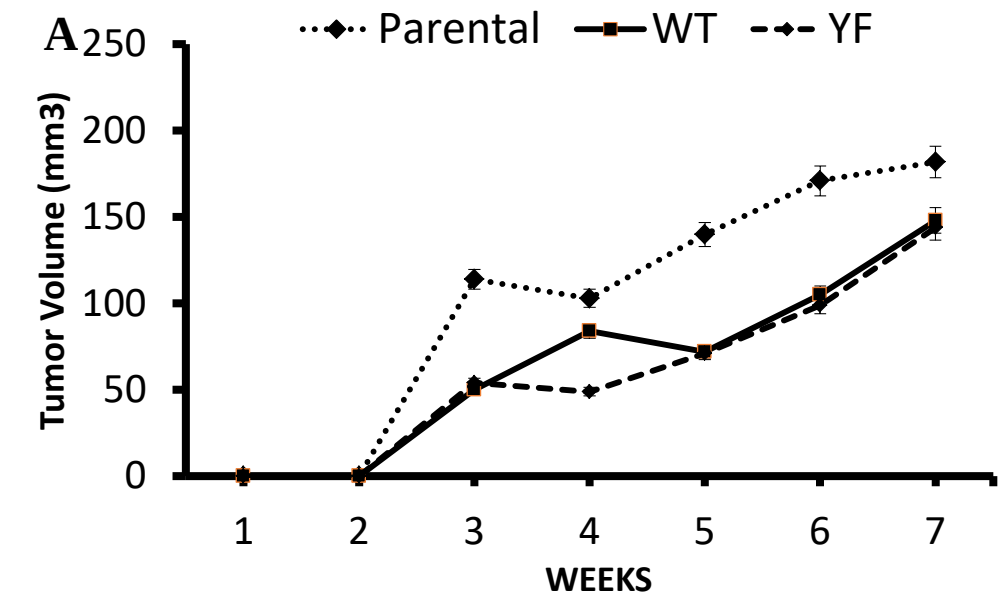
A
Parental
WT
YF
Tumor Volume (mm3)
250
200
150
100
50
0
1
2
3
4
5
6
7
WEEKS

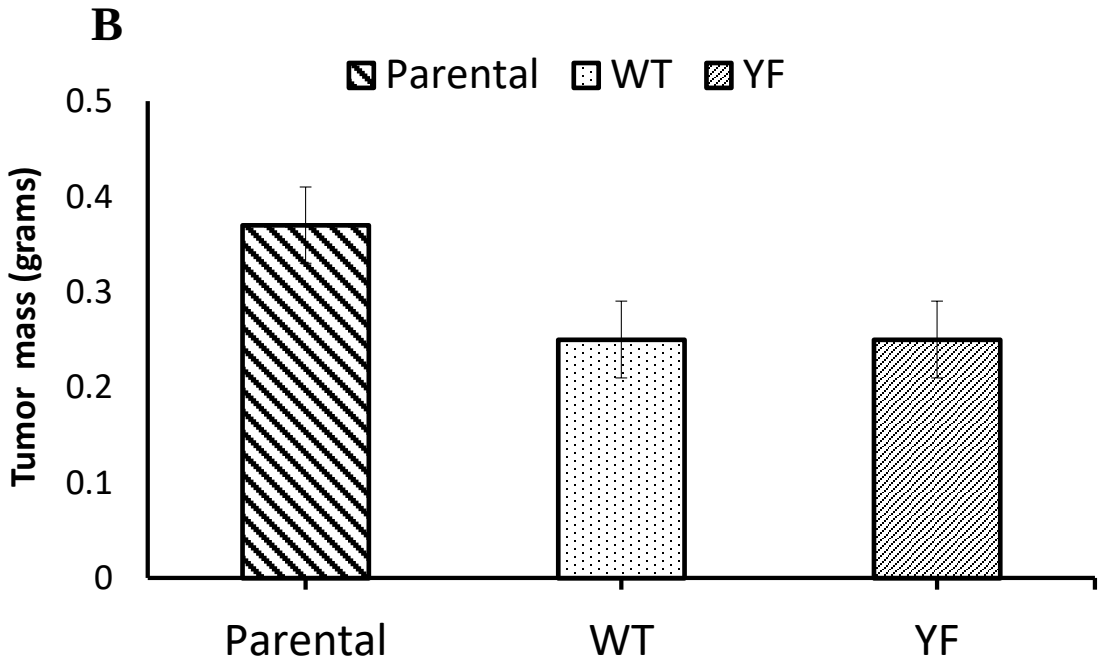
B
Parental
WT
YF
Tumor mass (grams)
0.5
0.4
0.3
0.2
0.1
0
Parental
WT
YF

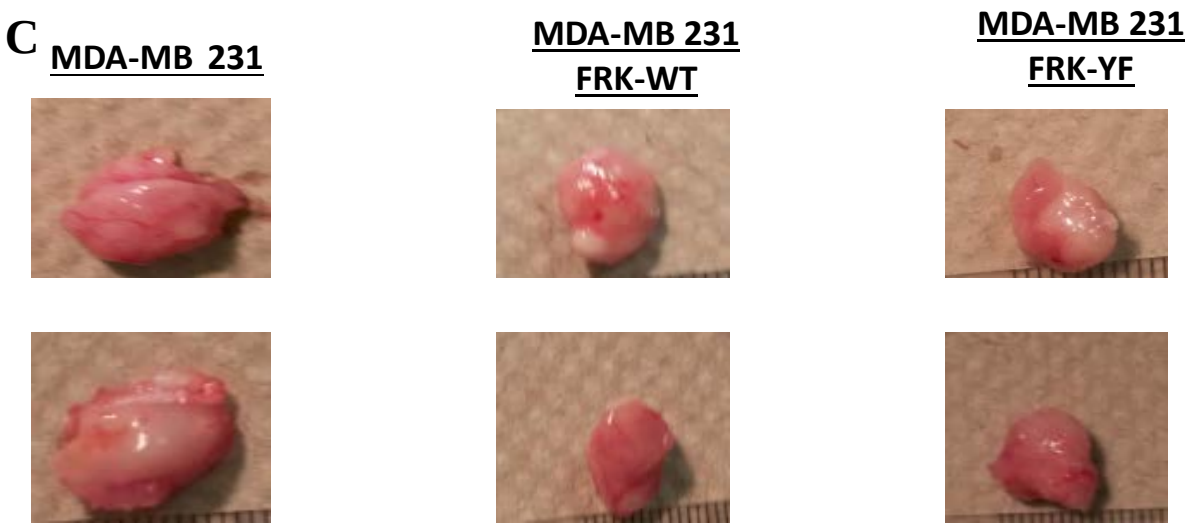

Figure 4.19: Effect of FRK overexpression in xenograft tumor growth 400,000 MDA-MB 231 stably overexpressing FRK-WT and FRK-YF cells were injected subcutaneously into mammary fat pads of four animals injected per cell line. The tumors were monitored and measured weekly for about 8 weeks. Tumor volume was calculated as follows 0.50 X length X width ^{2} . **A)** The tumor volume for a period of 8 weeks was measured and represented graphically **B)** The tumors of these mice at endpoint were isolated and weighed, the average weights were represented graphically. These figures representative are graph or image of mice tumor at endpoint showing the tumor mass, volume and size.

5.0 Discussion

Deregulation of some PTKs is known to modulate critical pathways that drive the hallmarks of cancers, these include cell growth, survival, and metastasis (Krause and Van Etten, 2005; Manning *et al*., 2002; Parsons and Parsons, 2004). However, others members of the tyrosine kinases are known to suppress cancer growth, progression and metastasis, for example, SYK (Coopman and Mueller, 2006) and FRK (Goel and Lukong, 2016; Yim *et al*., 2009b). FRK is a non-receptor tyrosine kinase that has been described as a candidate tumor suppressor in various cancers; this includes breast, glioma, cervical and non-small lung cancers (Brauer and Tyner, 2009; Goel and Lukong, 2016). The tumor suppressive role of FRK have been widely studied in breast cancers, and several studies have shown various mechanisms by which FRK suppresses breast cancer tumorigenesis. These include the arrest of the G1 phase of the cell cycle, (Craven *et al*., 1995b; Oberg-Welsh *et al*., 1998), AKT regulation (Yim *et al*., 2009a), stabilization of

BRCA1 (Kim *et al*., 2015), and internationalization of EGFR (Jin and Craven, 2014). Previous data from our lab also indicated that FRK could suppress breast tumorigenesis by regulating other signaling pathways (Bagu *et al*., 2017; Ogunbolude *et al.,* 2017). Previous data from our lab showed that constitutively active form of FRK (FRK-YF) induced the phosphorylation of numerous cellular signaling proteins targets, including intermediates of the PI3K/Akt, MAPK and STAT3 signaling pathways (Ogunbolude *et al.,* 2017). STAT3 was found to be one of the top targets of FRK, and overexpression of FRK in breast cancer cells was shown to downregulate the phosphorylation of STAT3 (Ogunbolude *et al.,* 2017). Therefore, validating STAT3 as a downstream target of FRK was the main focus of this Ph.D. project.

The STAT3 signaling pathway is one of the important signaling pathways that is activated in most cancers, including breast cancer (Yu *et al*., 2014). STAT3 is a transcription factor that regulates the expression of a wide range of genes that promotes cell proliferation and migration (Levy and Lee, 2002; Sansone *et al*., 2007; Siveen *et al*., 2014; Yu *et al*., 2014). To validate STAT3 as a target of FRK, first, we checked if there was any correlation between FRK and pSTAT3 expression in a panel of 24 breast cancer cell lines. We found an inverse correlation between FRK and pSTAT3 in the 24 breast cancer cell lines tested, since IL-6 (a cytokine) is known to activate the JAK\STAT pathway leading to constitutive activation of STAT3 (Hirano *et al*., 2000), we then investigated the effect of IL-6 stimulation on pSTAT3 in various breast cancer cell lines such as SKBR3, MCF-7 and MDA-MB 231. Stimulation of SKBR3 and MCF-7 with IL-6 stimulation increased STAT3 phosphorylation. However, we observed no respond to IL-6 or EGF stimulation with MDA-MB 231 breast cancer cells. We are not sure why no effect was seen, it is possible that the phosphorylation of STAT3 in this cell line was already saturated, hence no response to both IL-6 and EGF stimulation. However, we found a decrease in the phosphorylation of STAT3 in MDA-MB 231 transiently expressing FRK-WT as well as FRK-YF. This further supports our hypothesis that FRK is a negative regulator of STAT3 signaling. Transient knockdown of negative regulators of STAT3 for instance, N-myc downstream-regulated gene 2 (NDRG2) has been reported to promote constitutive activation of STAT3 (Kim *et al*., 2014). However, transient knockdown of FRK in SKBR3, as well as MCF-7, had no significant effect on STAT3 phosphorylation/activation. We expected to see an increase in STAT3 phosphorylation with the knockdown of FRK as was seen with NDRG2 gene (Kim *et al*., 2014). However, we obtained no significant effect. It is possible that the stable knockdown of

FRK would have had a significant effect on STAT3 activation/phosphorylation other than the transient knocked down we performed.

In order to determine the mechanisms by which FRK decreased the phosphorylation of STAT3, we co-immunoprecipitated FRK with STAT3. We had hoped to establish that STAT3 was a direct substrate of FRK but found no interaction between FRK and STAT3. Previous work from our lab showed that FRK regulates the MAPK signaling pathway by increasing ERK1/2 phosphorylation. Phosphorylation of ERK 1/2 has also been shown to negatively regulate the activation of STAT3 (Tyr705) in specific cells by activating STAT3 (Ser727) (Chung *et al*., 1997). Phosphorylation of STAT3 (Ser727) has been reported to negatively modulate STAT3 activation (phosphorylation of Tyr705) (Wakahara *et al*., 2012). Interestingly, we also saw an increase in pSTAT3 Ser727 in MDA-MB 231 overexpressing FRK when compared to the parental cells; it's possible that FRK inhibits STAT3 activation by activating ERK1/2, which activates STAT3 Ser727. The knockdown of FRK had no significant effect on the levels of STAT3 (Ser727), this could explain why we saw no effect with FRK knockdown on STAT3 phosphorylation in SKBR3 and MCF-7 breast cancer cells. It is worth mentioning that a previous study on murine FRK-transgenic mice has been shown to demonstrate higher phosphorylation level of ERK1/2 but lower levels of phosphorylated p38 in islet cells compared with control islets (Anneren and Welsh, 2000). Furthermore, Jin *et al.*, showed that overexpression FRK phosphorylates EGFR Y1173 (Jin and Craven, 2014) and phosphorylated EGFR Tyr1173 have been reported to activate ERK (Hsu *et al*., 2011). Therefore, it possible that FRK decreases STAT3 (Tyr705) phosphorylation through the EGFR signaling pathway and not the JAK/STAT signaling pathway. Future studies beyond the scope of this thesis will examine the role of FRK on ERK1/2 activation and identify the particular substrate/phosphatase activated by FRK which inactivate STAT3.

Several of STAT3 downstream target genes associated with tumorigenesis have been previously validated (Carpenter and Lo, 2014). Some of the well-characterized STAT3 target genes include Survivin, matrix metalloproteinase 1 (MMP-1), Cyclin D1, BCL2, MYC and MCL1 (Carpenter and Lo, 2014). Thus, we examined the effect of FRK on selected STAT3 target genes (Survivin, MMP-1, and Cyclin D1). Survivin (encoded by BIRC5 gene) is an inhibitor of caspases, while MMP-1 promotes invasiveness via the degradation of the basal membrane and Cyclin D1 is a cell cycle regulator (Carpenter and Lo, 2014). The presence of

FRK-WT or FRK-reduced the mRNA expression of Survivin, and MMP-1; however only FRK-WT had an effect on the mRNA expression of Cyclin D1. We are not sure why FRK-YF had no effect on Cyclin D1, it is possible that the constitutive form of FRK activates other genes that upregulate Cyclin D1. The levels of Survivin and MMP-1 were upregulated in FRK knocked down SKBR3 and MCF-7 breast cancer cells. The most dramatic effect of FRK was observed with Survivin. Survivin is a member of the inhibitor of apoptosis (IAP) family, and one of its functions is to inhibit caspase activation thereby negatively regulate apoptosis (Banerjee and Resat, 2016). Immunohistochemical analysis of several invasive breast tumor specimens showed a positive correlation between Survivin protein expression and high STAT3 activity chemotherapy (Gritsko *et al*., 2006). The elevated levels of Survivin in the specimens tested were presumed to be responsible for promoting breast cancer progression and resistance to chemotherapy (Gritsko *et al*., 2006). In our future studies, we will examine how the expression of FRK correlates with STAT3 phosphorylation and Survivin expression. Although, the knockdown of FRK had no significant effect on STAT3 phosphorylation we observed a significant effect on some STAT3 target genes in both MCF-7 and SKBR3. It is possible that the downregulation of cyclin D1, MMP-1, and Survivin by FRK was through other signaling pathways other than STAT3 signaling pathway.

In glioma cells, FRK has been reported to suppress glioma cell migration by suppressing several mesechenmyal markers (Shi *et al*., 2015). There is little information on the mechanisms by which FRK suppresses breast cancer migration and invasion. Interestingly, FRK has been reported to be expressed mainly in epithelial cells or tissues but not in mesenchymal cells (Cance *et al*., 1994; Berclaz *et al*., 2000). Based on this, we hypothesized that FRK probably regulates EMT in breast cancer cells. Breast cancer is a heterogeneous disease with multiple criteria for classification based on clinical, histopathological markers and gene expression profiling (Coady *et al*., 2001; Musgrove and Sutherland, 2009; Perou *et al*., 2000; Prat and Perou, 2011; Weigelt *et al*., 2005). Some of the breast cancer subtypes include luminal A, luminal B, basal-like and HER2-positive profiling (Coady *et al*., 2001; Musgrove and Sutherland, 2009; Perou *et al*., 2000; Prat and Perou, 2011; Weigelt *et al*., 2005). Basal breast cancer cell lines have been classified into 3 subtypes based on the morphology and invasive potential; the subtypes include Basal A, Basal B and Luminal (Neve *et al*., 2006) . Luminal cells are more differentiated with epithelial-like phenotype while the Basal B cells are less differentiated and possess a mesenchymal-like

appearance, Basal A cells have either luminal-like or basal-like morphology (Neve *et al*., 2006). Previous studies on the role of FRK expression in breast cancers were based on molecular subtypes of breast cancers (Yim *et al*., 2009a). We investigated the expression pattern of FRK in breast cancer cell lines classified based according to their morphology and invasiveness. We found that the expression of FRK was high in epithelial-like breast cancer cell lines and normal mammary tissue. The expression was low or lost in basal B breast cancer cell lines which display a mesenchymal phenotype. The expression patterns suggest that FRK might play a role in the maintenance of the normal epithelium.

Kenny *et al*. also classified breast cancer cell lines into four distinct morphological groups (Kenny *et al*., 2007). These groups were denoted as Round, Mass, Grape-like, and Stellate. The MDA-MB 231 breast cancer cell line was classified in the stellate group that also includes BT-549, MDA-MB-436, and Hs578T. Cells that were grouped in the Mass class display disorganized nuclei and include; BT-474, HCC70, MCF-7, and T-47D cell lines. While the Round cell class was comprised of HCC1500, MCF-12A, and MDA-MB-415 and the Grape-like class characterized by a reduced cell-cell interaction included AU565, MDA-MB-468, and SK-BR-3 cell lines. The Stellate class cells are distinctively more invasive than members of the other three groups, and their stellate projections tend to bridge multiple colonies of cells (Kenny *et al*., 2007). In the present study, we noted that all three stellate-shaped cell lines (MDA-MB 231, BT-549, and Hs578T) had very low or no detectable FRK protein expression. Interestingly, stable overexpression of FRK in MDA-MB 231 cells altered the morphology of the cells from stellate to a more rounded phenotype (**Figure 4.11**). Yim *et al*. described their MCF-7 cells as round and observed a dramatic morphological change to stellate-like in these cells upon the exogenous expression of FRK (Yim *et al*., 2009a). It is unclear why FRK would induce different morphological phenotypes in the MDA-MB 231 cell line, which we used in our study, and MCF-7 in the Yim *et al*. study (Yim *et al*., 2009a). Nonetheless, since stellate/FRK-negative MDA-MB 231 cell line is characterized as highly invasive (Kenny *et al*., 2007), and we observed that overexpression of FRK alters the morphology of rounded, we hypothesized that the tumor suppressor activity of FRK might play a significant role in suppressing EMT in breast cancers.

EMT is a mechanism that enhances metastasis of breast cancer by enabling epithelial cells to become more like mesenchymal cells with increased motility and invasiveness (Felipe Lima *et al*., 2016). Mesenchymal markers include Vimentin, Fibronectin, Slug, Snail, and N-

cadherin, whereas E-cadherin is a classic epithelial marker (Felipe Lima *et al*., 2016). First, we found an inverse correlation between FRK and the mesenchymal marker, Fibronectin in the Basal B breast cancer cell lines, MDA-MB 231, BT549, and Hs578T. Vimentin, Fibronectin, Slug, and N-cadherin were downregulated, while the expression of E-cadherin was upregulated with FRK overexpression in MDA-MB 231 cells (**Figure 4.11**).

E-cadherin is a cell-cell adhesion molecule that is essential for the formation and maintenance of the epithelium (Lecuit and Yap, 2015). Downregulation or loss E-cadherin expression or any other mechanisms that interfere with the integrity of the cell-cell interaction are phenomena in many cancers (Frixen *et al*., 1991). Cell-cell adhesion is altered by a switch from E-cadherin to N-cadherin expression (the so-called "cadherin switch") (Kotiyal and Bhattacharya, 2016). The role of E-cadherin has been defined as anti-invasive or tumor suppressive because the loss of E-cadherin correlates with the loss of the epithelial morphology and in most cases with the acquisition of metastatic potential by the cancer cell (Pecina-Slaus, 2003). In our study, we found that these properties are mirrored by FRK.

The trend of correlation of FRK with the epithelial marker, E-cadherin that we observed in our study was consistent with the mRNA expression dataset mined from the Affymetrix platform 133plus2. FRK transcript levels were positively correlated with the transcript levels of E-cadherin and Cytokeratin 18 as well as in the breast cancer tissues mined from TCGA database where FRK correlated positively with E-cadherin in both normal and breast tumor tissue samples. Although, as expected, a negative correlation was observed with the transcript levels of Vimentin, N-cadherin, Fibronectin, and TWIST in the breast cancer cells lines mined from GEO accession numbers GSE10021, GSE10843, GSE3156, GSE10890 and GSK's cell line project (https://array.nci.nih.gov/caarray/project/woost-00041/). We, however, did not see an inverse correlation between FRK and Fibronectin/Vimentin in the breast tumor samples. We believe that this may be due to the heterogeneous nature of the breast tumor sample cohort, represented by various breast cancer subtypes. The TNBC subtype, for instance, is sub-classified as, luminal androgen receptor positive, basal-like-1, basal-like-2, immunomodulatory, claudin-low-enriched mesenchymal, and mesenchymal stem-like (MSL) (Lehmann *et al*., 2011). We noted that FRK expression was low/lost in the mesenchymal-like basal B subset of TNBCs. Therefore, the availability of a stratified mesenchymal-like subset of breast cancer patient samples in the TCGA database or any other database will be a help to further validate the correlation between FRK and

the mesenchymal properties of breast tumor cells. Furthermore, the overexpression of FRK in both MDA-MB 231 and Hs578T lead to the decrease in menschenmyal markers such as Fibronectin. Based on these findings, it's possible that the suppression of EMT by FRK is not only limited to MDA-MB 231 cells but affect all basal B cells.

Our findings as a whole suggest that FRK either may play a role in the maintenance of the cell-cell interaction and the protection of the normal epithelium by upregulating E-cadherin and inhibiting EMT via the downregulation of Vimentin, Fibronectin, and N-cadherin. Therefore, the restraint of EMT might be one of the mechanisms underlying the anti-migration/invasion effect of FRK in breast cancer cells.

In addition to suppression of cell invasion and metastasis, FRK have been reported to suppress breast cancer cell proliferation through various mechanisms that include promoting PTEN stability and function (Yim *et al*., 2009a), EGFR internalization (Jin and Craven, 2014), and induction of the G1 arrest of the cell cycle (Meyer *et al*., 2003). The uncontrollable growth of cancer cells is as a result of defects in the cell cycle (Bendris *et al*., 2015). The roles of FRK in cell cycle have not been fully investigated. Apart from the arrest of the cell cycle, FRK has been shown to interact with pRb, a known tumor suppressor known to regulate the G1-S phase transition of the cell cycle, suggesting a possible mechanism by which FRK induces the G1 arrest of the cell cycle (Craven *et al*., 1995a). However, Meyer *et al*. found that the suppression of cell proliferation by FRK is independent of pRb. Interestingly, EMT has been reported to promote cell proliferation by regulating the cell cycle, TWIST a transcription factor that regulates EMT has been shown to inhibit oncogene-induced senescence by inhibiting the tumor suppressor proteins p16 and p21, alongside inducing EMT (Jiang *et al*., 2011; Karlsson *et al*., 2017). Since data from our findings show that FRK suppresses EMT and EMT have been reported to inhibit other cell cycle regulators such as p16 and p21 (Jiang *et al*., 2011; Karlsson *et al*., 2017), we investigated the role of FRK on other cell cycle regulators and determined other possible mechanisms by which FRK induces the G1 arrest of the cell cycle other than binding with pRb.

Previous studies in breast cancer cells on the role of FRK in cell cycle was done using Luminal/epithelial cells, for instance, FRK was reported to induce the G1 arrest in Luminal/ epithelial breast cancer cells such as MCF-7 and BT-474 (Meyer *et al*., 2003). We investigated the effect of FRK on the G1 arrest in mesenchymal breast cancer cell MDA-MB 231 and found

that FRK also induces G1 arrest in mesenchymal breast cancer cells. The arrest of the G1 phase of the cell cycle with FRK overexpression in MDA-MB 231 confirms that it is one of the primary mechanisms by which FRK suppress tumorigenesis, and this is irrespective of the molecular grade or subtype of breast cancer cells. Although, we hypothesized that the knockdown of FRK in MCF-7 cells would facilitate the transition of cells from the G1/S to the G2 phase as seen with the kinase-dead FRK when transfected in MCF-7 (Meyer *et al*., 2003). The little or no transition of cells from the G1/S to the G2 phase of the cell cycle shown in our data could be because partial knockdown in the MCF-7 cells.

Cells undergoing G1 arrest mostly undergo apoptosis or become senescent (Gire and Dulic, 2015; Terzi *et al*., 2016) Our data shows that stable overexpression of FRK in MDA-MB 231 breast cancer cells had no significant effect on apoptosis. Although, previous studies showed that transient overexpression of FRK in both breast and glioma cells induces apoptosis (Hua *et al*., 2014; Meyer *et al*., 2003). We are not sure why there was no induction of apoptosis with stable overexpression of FRK in MDA-MB 231. Based on our data, we believe that the induction of apoptosis is not one primary mechanism by which FRK suppresses cell proliferation. Furthermore, we investigated the effect of FRK overexpression and knockdown on cellular senescence. Cellular senescence can be defined as irreversible growth arrest or lack of proliferative potential characterized by distinct metabolic activity and dramatic changes in cell morphology (Gire and Dulic, 2015; Terzi *et al*., 2016). Our data shows that stable overexpression of FRK in MDA-MB 231 cells induce cellular senescence.

p21 is known to mediate senescence by blocking the inactivating phosphorylation of pRb by Cdk2 and Cdk4/6 (Gire and Dulic, 2015). Although FRK has been shown to interact with pRb (Giacinti and Giordano, 2006), there is little/no information on the role of FRK on the phosphorylation status of pRb. From our results, we found that overexpression of FRK resulted in a decrease in the phosphorylation levels of pRb and vice-versa with the knockdown of FRK. Hypophosphorylated pRb is known to bind with E2F1 thus preventing the progression of the cell cycle (Giacinti and Giordano, 2006; Hua *et al*., 2014). E2F1 is known to regulates the expressions of genes required for cell cycle progression; these genes include Cyclin E, Cyclin A (Giacinti and Giordano, 2006). Although, we obtained downregulation and upregulation of E2F1 at both protein and mRNA levels with overexpression and knockdown of FRK respectively and also found downregulation of Cyclin E mRNA levels with the overexpression of FRK in MDA-

MB 231. We, however, found no effect on cyclin E protein expression with FRK knocked down and overexpression. Cyclin E is known to be regulated by other transcription factors other than E2F1, including DEC1 (Bi *et al*., 2015). It is, therefore, possible that the effect of FRK could be compensated by these- factor.

Since, p21 promotes facilitates cellular senescence by dephosphorylation of pRb protein, subsequent inhibition of E2F transcription factor and triggering pivotal genes responsible for senescence (Abbas and Dutta, 2009; Chakraborty *et al*., 2016). We also investigated the effect of FRK on p21, we found that FRK overexpression leads to the upregulation of p21 protein, but downregulation of p21 transcript levels. The reason for this discrepancies is unknown. However, the upregulation of p21 and induction of cellular senescence seen with FRK overexpression has also been seen with other tumor suppressors, For example, overexpression of SYK in melanoma cells has been shown to induce senescence growth arrest via p21 upregulation (Bailet *et al*., 2009). Together, our findings show that FRK regulates cell cycle progression potentially by inducing cellular senescence via upregulation of p21.

From our result *in vitro,* we have been able to show that FRK significantly suppresses breast tumorigenesis. We were also interested in the tumor suppressive role of FRK *in vivo*. Although, *in vivo* studies by Yim *et al*. showed that the knockdown of FRK in MCF-10 A; a normal breast cell for xerograph studies promotes breast tumorigenesis (Yim *et al*., 2009a). There little/no information on the tumor suppressive role of FRK-WT and the constitutively active form of FRK, FRK-YF *in vivo* using breast cancer cell lines. Thus, we investigated the tumor suppressive role of FRK *in vivo* using MDA-MB 231 stably overexpressing FRK. Our result shows that FRK-WT and FRK-YF suppress the tumor growth when compared to the parental groups. Although we expected FRK-YF group to significantly suppress the tumor growth when compared to the FRK-WT group, we, however, obtained no significant effect between these groups. We are not exactly sure why, but we hope to find a reason for this in our future research. Taking together, our data suggest that FRK suppresses breast tumor growth *in vivo*.

5.1 Conclusion

FRK is a non-receptor tyrosine kinase with unpredicted tumor suppressor activity. We have shown that stable overexpression of FRK suppressed cell proliferation, migration, and invasion both *in vitro* and *in vivo*. Our data presented provide first evidence that:

1) **FRK is lost in breast cancer cells with mesenchymal phenotype:** From our data, we found that FRK is highly expressed in luminal breast cancer cell or breast cancer cells with epithelial-like phenotype, however, lost in basal or mesenchymal-like breast cancer cells. We also found the expression of FRK to be present in the epithelium of breast tissues. Luminal breast cancer cells are more differentiated with epithelial-like traits while basal B breast cancers are less differentiated with mesenchymal-like phenotype. Hence, our study suggests that FRK regulates Epithelial to Mesenchymal Transition in breast cancer.

2) **FRK expression correlates positively with epithelial markers:** We found that luminal breast cancer cells with high FRK expression had high protein and mRNA expression of the epithelial marker, E-cadherin, while basal B breast cancer cells with little or no FRK expression had low levels of both protein and mRNA expression of E-cadherin. However, these basal B breast cancer cells had high protein and mRNA expression of mesenchymal markers such as Fibronectin and N-cadherin. We also found FRK transcript levels to correlate positively with the transcript levels of E-cadherin and Cytokeratin 18 in the breast cancer tissues mined from TCGA database. Also, FRK correlated positively with E-cadherin in both normal and breast tumor tissue samples. Although we did not see an inverse correlation between FRK and Fibronectin/Vimentin in the breast tumor samples, we believe that this may be due to the heterogeneous nature of the breast tumor sample cohort, represented by various breast cancer subtypes.

3) FRK suppresses breast cancer cell migration by suppressing EMT: EMT is a mechanism that promotes breast cancer metastasis. From our data, we showed FRK to regulate EMT in breast cancer cells. Overexpression of FRK in basal B breast cancer cells such as MDA-MB 231 and Hs578T suppresses EMT by downregulating the protein and mRNA expression of mesenchymal markers such as Fibronectin enabling mesenchymal cells to become more like epithelial-like cells with decrease motility and invasiveness. We also found the overexpression of FRK in basal B breast cancer cells to induce a change in morphology of the breast cancers cells from stellate shape to a round shape. However, the knockdown of FRK in luminal breast cancer cells such as MCF-7 and SKBR3 increased the expression of mesenchymal markers such as fibronectin and decreased the expression of the epithelial marker, E-cadherin.

4) The overexpression of FRK suppresses STAT3 activation leading to reduced STAT3 phosphorylation: In addition to regulation of EMT by FRK, we also found that FRK possibly

suppresses breast cancer cell migration and proliferation by regulating several signaling pathways, such as the STAT3 signaling pathway. Overexpression of FRK in FRK-negative breast cancer cell MDA-MB 231 decreased STAT3 phosphorylation and also the expression of STAT3 downstream target genes such as Survivin, Cyclin D1, and MMP-1. Although the transient knockdown of FRK in FRK-positive cells such as MCF-7 and SKBR3 did not affect the STAT3 phosphorylation, we, however, obtained upregulation of STAT3 target genes with FRK knockdown, suggesting that FRK may regulate these genes through other signaling pathways.

5). FRK suppresses breast cancer proliferation by inducing cellular senescence via upregulation of p21: FRK has been known to suppress breast cancer cell proliferation by inducing the G1 arrest of the cell cycle (Meyer *et al.,* 2003). However, the mechanism by which FRK induces this growth arrest is unknown. We found that overexpression of FRK in breast cancer cell line (MDA-MB 231) induces G1 growth arrest by upregulating pRb, p21, and downregulating E2F1 expression. We also found that overexpression of FRK in MDA-MB 231 promotes cellular senescence and p21 expression. We conclude that upregulation of p21 expression with FRK overexpression is probably one of the mechanisms by which FRK induces cellular senescence in breast cancer, hence suppressing breast cancer cell proliferation.

Taken together, our findings indicate that FRK plays a tumor suppressor role in breast cancer by inhibiting breast cancer tumorigenesis both *in vitro* and *in vivo*. Hence, upregulation of FRK in breast cancers can be targeted as therapy for breast tumorigenesis.

5.2. Future direction

From our studies, we showed that FRK regulates several signaling pathways including the STAT3 signaling pathway. Overexpression of FRK in basal B breast cancer cells (MDA-MB 231) decreased the phosphorylation of STAT3; however, the knockdown of FRK in luminal breast cancer cells such as MCF-7 and SKBR3 had no effect on STAT3 signaling pathway. Why the effect of FRK on STAT3 phosphorylation is cell line/subtype-dependent is unclear. The identification and characterization of FRK-specific substrates and signaling pathways may provide better information on the context-specific effect of FRK.

Furthermore, our study shows that FRK-KM (i.e., kinase-dead FRK) decreased STAT3 phosphorylation (**Figure 4.4**). Also, recently published data from our lab also showed that FRK-VK, an FRK mutant with increased kinase activity, did not affect STAT3 phosphorylation

(Ogunbolude *et al.*, 2017). We had hypothesized that the tumor suppressive function of FRK would correlate with it enzymatic activity. However, the kinase-dead FRK (FRK-KM) (with no kinase activity) decreased pSTAT3, while the mutant with high kinase activity FRK-VK did not affect pSTAT3. Hence, it would be interesting to investigate if the tumor suppressive activity of FRK depends on its kinase activity. Is it possible that the FRK domains (SH2 and SH3) to play critical roles in the tumor suppressive function of FRK? It would be interesting to investigate the effect of FRK SH2, SH3 and kinase domains on several cellular processes such as migration and proliferation in breast cancer cells.

Lastly, we found out that overexpression of FRK in highly invasive/basal B breast cancer cells (i.e., breast cancer cells with little or no FRK expression) repressed breast cancer cell migration and invasion. Recent epigenetics studies from our lab found FRK to be hypermethylated in basal B breast cancer cells (Bagu *et al.*, 2017). Epigenetics drugs such as DAC, (demethylating agent) and HDI (Histone Deacetylase Inhibitors) have been reported to reactivate silenced genes (Bagu *et al.*, 2017; Ceccacci and Minucci, 2016). Interestingly, when basal B breast cancer cells such as Hs578T, BT549 were treated with both DAC and HDI such as Entinostat and Mocetinostat, it induced both mRNA and protein expression of FRK in these cell lines. However, there is no study on the use of these drugs on the re-expression of FRK in breast tissues. We hope to investigate the effect of FRK upregulation using epigenetics drugs such as HDIs in FRK-negative breast tissue samples using mouse models and determine its effect on Epithelial to Mesenchymal Transition. We hope this will highlight the clinical relevance of FRK in suppressing breast cancer tumorigenesis.

LIST OF REFERENCES

Abbas, T., and Dutta, A. (2009). p21 in cancer: intricate networks and multiple activities. Nat Rev Cancer *9*, 400-414.

Abukhdeir, A.M., and Park, B.H. (2008). P21 and p27: roles in carcinogenesis and drug resistance. Expert reviews in molecular medicine *10*, e19.

Akira, S. (2000). Roles of STAT3 defined by tissue-specific gene targeting. Oncogene *19*, 2607-2611.

Anneren, C., Reedquist, K.A., Bos, J.L., and Welsh, M. (2000). GTK, a Src-related tyrosine kinase, induces nerve growth factor-independent neurite outgrowth in PC12 cells through activation of the Rap1 pathway. Relationship to Shb tyrosine phosphorylation and elevated levels of focal adhesion kinase. J Biol Chem *275*, 29153-29161.

Anneren, C., and Welsh, M. (2000). Role of the Bsk/Iyk non-receptor tyrosine kinase for the control of growth and hormone production in RINm5F cells. Growth Factors *17*, 233-247.

Arancibia Hernández, P.L., Taub Estrada, T., López Pizarro, A., Díaz Cisternas, M.L., Sáez Tapia, C (2016). Breast calcifications: description and classification according to BIRADS 5th edition, Rev. Chil. Radiol. 22 80–91.

Arima, Y., Hayashi, H., Sasaki, M., Hosonaga, M., Goto, T.M., Chiyoda, T., Kuninaka, S., Shibata, T., Ohata, H., Nakagama, H., *et al.* (2012). Induction of ZEB proteins by inactivation of PRB protein is key determinant of mesenchymal phenotype of breast cancer. J Biol Chem *287*, 7896-7906.

Bagu, E.T., Miah, S., Dai, C., Spriggs, T., Ogunbolude, Y., Beaton, E., Sanders, M., Goel, R.K., Bonham, K., and Lukong, K.E. (2017). Repression of Fyn-related kinase in breast cancer cells is associated with promoter site-specific CpG methylation. Oncotarget *8*, 11442-11459.

Bailet, O., Fenouille, N., Abbe, P., Robert, G., Rocchi, S., Gonthier, N., Denoyelle, C., Ticchioni, M., Ortonne, J.P., Ballotti, R., *et al.* (2009). Spleen tyrosine kinase functions as a tumor suppressor in melanoma cells by inducing senescence-like growth arrest. Cancer Res *69*, 2748-2756.

Banerjee, K., and Resat, H. (2016). Constitutive activation of STAT3 in breast cancer cells: A review. Int J Cancer *138*, 2570-2578.

Bendris, N., Lemmers, B., and Blanchard, J.M. (2015). Cell cycle, cytoskeleton dynamics and beyond: the many functions of cyclins and CDK inhibitors. Cell Cycle *14*, 1786-1798.

Berclaz, G., Altermatt, H.J., RohpRbach, V., Dreher, E., Ziemiecki, A., and Andres, A.C. (2000). Hormone-dependent nuclear localization of the tyrosine kinase iyk in the normal human breast epithelium and loss of expression during carcinogenesis. Int J Cancer *85*, 889-894.

Bertoli, C., Skotheim, J.M., and de Bruin, R.A. (2013). Control of cell cycle transcription during G1 and S phases. Nat Rev Mol Cell Biol *14*, 518-528.

Bhargava S., Bhargava S.K. (2014). Differential diagnosis in radiology. Jaypee brothers,medical publishers Pvt. New Delhi: Limited.

Bi, H., Li, S., Qu, X., Wang, M., Bai, X., Xu, Z., Ao, X., Jia, Z., Jiang, X., Yang, Y., *et al.* (2015). DEC1 regulates breast cancer cell proliferation by stabilizing cyclin E protein and delays the progression of cell cycle S phase. Cell Death Dis *6*, e1891.

Blagosklonny, M.V. (2013). Hypoxia, MTOR and autophagy: converging on senescence or quiescence. Autophagy *9*, 260-262.

Blume-Jensen, P., and Hunter, T. (2001). Oncogenic kinase signalling. Nature *411*, 355-365.
Brauer, P.M., and Tyner, A.L. (2009). RAKing in AKT: a tumor suppressor function for the intracellular tyrosine kinase FRK. Cell Cycle *8*, 2728-2732.
Brauer, P.M., and Tyner, A.L. (2010). Building a better understanding of the intracellular tyrosine kinase PTK6 - BRK by BRK. Biochim Biophys Acta *1806*, 66-73.
Brenton, J.D., Carey, L.A., Ahmed, A.A., and Caldas, C. (2005). Molecular classification and molecular forecasting of breast cancer: ready for clinical application? J Clin Oncol *23*, 7350-7360.
Campisi, J., and d'Adda di Fagagna, F. (2007). Cellular senescence: when bad things happen to good cells. Nat Rev Mol Cell Biol *8*, 729-740.
Cance, W.G., Craven, R.J., Bergman, M., Xu, L., Alitalo, K., and Liu, E.T. (1994). Rak, a novel nuclear tyrosine kinase expressed in epithelial cells. Cell Growth Differ *5*, 1347-1355.
Carey, L., Winer, E., Viale, G., Cameron, D., and Gianni, L. (2010). Triple-negative breast cancer: disease entity or title of convenience? Nat Rev Clin Oncol *7*, 683-692.
Carpenter, R.L., and Lo, H.W. (2014). STAT3 Target Genes Relevant to Human Cancers. Cancers (Basel) *6*, 897-925.
Catlett-Falcone, R., Landowski, T.H., Oshiro, M.M., Turkson, J., Levitzki, A., Savino, R., Ciliberto, G., Moscinski, L., Fernandez-Luna, J.L., Nunez, G., *et al.* (1999). Constitutive activation of Stat3 signaling confers resistance to apoptosis in human U266 myeloma cells. Immunity *10*, 105-115.
Ceccacci, E., and Minucci, S. (2016). Inhibition of histone deacetylases in cancer therapy: lessons from leukaemia. Br J Cancer *114*, 605-611.
Chakraborty, S., Rasool, R.U., Kumar, S., Nayak, D., Rah, B., Katoch, A., Amin, H., Ali, A., and Goswami, A. (2016). Cristacarpin promotes ER stress-mediated ROS generation leading to premature senescence by activation of p21(waf-1). Age *38*.
Chandrasekharan, S., Qiu, T.H., Alkharouf, N., Brantley, K., Mitchell, J.B., and Liu, E.T. (2002). Characterization of mice deficient in the Src family nonreceptor tyrosine kinase FRK/rak. Mol Cell Biol *22*, 5235-5247.
Chen, J.S., Hung, W.S., Chan, H.H., Tsai, S.J., and Sun, H.S. (2013). In silico identification of oncogenic potential of fyn-related kinase in hepatocellular carcinoma. Bioinformatics *29*, 420-427.
Chen, Z., and Han, Z.C. (2008). STAT3: a critical transcription activator in angiogenesis. Med Res Rev *28*, 185-200.
Chlebowski, R.T., Manson, J.E., Anderson, G.L., Cauley, J.A., Aragaki, A.K., Stefanick, M.L., Lane, D.S., Johnson, K.C., Wactawski-Wende, J., Chen, C., *et al.* (2013). Estrogen plus progestin and breast cancer incidence and mortality in the Women's Health Initiative Observational Study. J Natl Cancer Inst *105*, 526-535.
Choi, H.J., and Han, J.S. (2012). Overexpression of phospholipase D enhances Bcl-2 expression by activating STAT3 through independent activation of ERK and p38MAPK in HeLa cells. Biochim Biophys Acta *1823*, 1082-1091.
Chung, J., Uchida, E., Grammer, T.C., and Blenis, J. (1997). STAT3 serine phosphorylation by ERK-dependent and -independent pathways negatively modulates its tyrosine phosphorylation. Mol Cell Biol *17*, 6508-6516.

Coady, S.A., Sorlie, P.D., Cooper, L.S., Folsom, A.R., Rosamond, W.D., and Conwill, D.E. (2001). Validation of death certificate diagnosis for coronary heart disease: the Atherosclerosis Risk in Communities (ARIC) Study. J Clin Epidemiol *54*, 40-50.

Coopman, P.J., and Mueller, S.C. (2006). The Syk tyrosine kinase: a new negative regulator in tumor growth and progression. Cancer Lett *241*, 159-173.

Craven, R.J., Cance, W.G., and Liu, E.T. (1995a). The Nuclear Tyrosine Kinase Rak Associates with the Retinoblastoma Protein PRb. Cancer Research *55*, 3969-3972.

Craven, R.J., Cance, W.G., and Liu, E.T. (1995b). The nuclear tyrosine kinase Rak associates with the retinoblastoma protein pRb. Cancer Res *55*, 3969-3972.

Denoix, P.F. (1952). [Note on the possible role of the International Union against Cancer in nomenclature, classification, analytical index, bibliography and documentation]. Acta Unio Int Contra Cancrum *8*, 92-96.

Derry, J.J., Richard, S., Valderrama Carvajal, H., Ye, X., Vasioukhin, V., Cochrane, A.W., Chen, T., and Tyner, A.L. (2000). Sik (BRK) phosphorylates Sam68 in the nucleus and negatively regulates its RNA binding ability. Mol Cell Biol *20*, 6114-6126.

Dick, F.A., and Rubin, S.M. (2013). Molecular mechanisms underlying PRB protein function. Nat Rev Mol Cell Biol *14*, 297-306.

Dikshith T.S.S. (2013). Hazardous chemicals: safety management and global regulations. CRC Press:Boca Raton; 2.

Eliyatkin, N., Yalcin, E., Zengel, B., Aktas, S., and Vardar, E. (2015). Molecular Classification of Breast Carcinoma: From Traditional, Old-Fashioned Way to A New Age, and A New Way. Journal of breast health (2013) *11*, 59-66.

Fedele, M., Cerchia, L., and Chiappetta, G. (2017). The Epithelial-to-Mesenchymal Transition in Breast Cancer: Focus on Basal-Like Carcinomas. Cancers (Basel) *9*.

Felipe Lima, J., Nofech-Mozes, S., Bayani, J., and Bartlett, J.M. (2016). EMT in Breast Carcinoma-A Review. Journal of clinical medicine *5*.

Ferlay, J., Soerjomataram, I., Dikshit, R., Eser, S., Mathers, C., Rebelo, M., Parkin, D.M., Forman, D., and Bray, F. (2015). Cancer incidence and mortality worldwide: sources, methods and major patterns in GLOBOCAN 2012. Int J Cancer *136*, E359-386.

Frame, M.C. (2002). Src in cancer: deregulation and consequences for cell behaviour. Biochim Biophys Acta *1602*, 114-130

Frappart L, Boudeulle M, Boumendil J, Lin HC, Martinon I, Palayer C, et al.(1984) Structure and composition of microcalcifications in benign and malignant lesions of the breast: study by light microscopy, transmission and scanning electron microscopy, microprobe analysis, and X-ray diffraction. Hum Pathol 15(9): 880–9.

Freund, A., Orjalo, A.V., Desprez, P.Y., and Campisi, J. (2010). Inflammatory networks during cellular senescence: causes and consequences. Trends Mol Med *16*, 238-246.

Frixen, U.H., Behrens, J., Sachs, M., Eberle, G., Voss, B., Warda, A., Lochner, D., and Birchmeier, W. (1991). E-cadherin-mediated cell-cell adhesion prevents invasiveness of human carcinoma cells. J Cell Biol *113*, 173-185.

Gao, T., Li, J.Z., Lu, Y., Zhang, C.Y., Li, Q., Mao, J., and Li, L.H. (2016). The mechanism between epithelial mesenchymal transition in breast cancer and hypoxia microenvironment. Biomed Pharmacother *80*, 393-405.

Georgakilas, A.G., Martin, O.A., and Bonner, W.M. (2017). p21: A Two-Faced Genome Guardian. Trends Mol Med *23*, 310-319.

Georgescu, M.M. (2010). PTEN Tumor Suppressor Network in PI3K-Akt Pathway Control. Genes Cancer *1*, 1170-1177.

Giacinti, C., and Giordano, A. (2006). PRB and cell cycle progression. Oncogene *25*, 5220-5227.

Gire, V., and Dulic, V. (2015). Senescence from G2 arrest, revisited. Cell Cycle *14*, 297-304.

Gocek, E., Moulas, A.N., and Studzinski, G.P. (2014). Non-receptor protein tyrosine kinases signaling pathways in normal and cancer cells. Crit Rev Clin Lab Sci *51*, 125-137.

Goel, R.K., and Lukong, K.E. (2015). Tracing the footprints of the breast cancer oncogene BRK - Past till present. Biochim Biophys Acta *1856*, 39-54.

Goel, R.K., and Lukong, K.E. (2016). Understanding the cellular roles of Fyn-related kinase (FRK): implications in cancer biology. Cancer Metastasis Rev *35*, 179-199.

Gritsko, T., Williams, A., Turkson, J., Kaneko, S., Bowman, T., Huang, M., Nam, S., Eweis, I., Diaz, N., Sullivan, D., *et al.* (2006). Persistent activation of stat3 signaling induces Survivin gene expression and confers resistance to apoptosis in human breast cancer cells. Clin Cancer Res *12*, 11-19.

Guo, L., Chen, C., Shi, M., Wang, F., Chen, X., Diao, D., Hu, M., Yu, M., Qian, L., and Guo, N. (2013). Stat3-coordinated Lin-28-let-7-HMGA2 and miR-200-ZEB1 circuits initiate and maintain oncostatin M-driven epithelial-mesenchymal transition. Oncogene *32*, 5272-5282.

Hirano, T., Ishihara, K., and Hibi, M. (2000). Roles of STAT3 in mediating the cell growth, differentiation and survival signals relayed through the IL-6 family of cytokine receptors. Oncogene *19*, 2548-2556.

Holmqvist, K., Cross, M.J., Rolny, C., Hagerkvist, R., Rahimi, N., Matsumoto, T., Claesson-Welsh, L., and Welsh, M. (2004). The adaptor protein shb binds to tyrosine 1175 in vascular endothelial growth factor (VEGF) receptor-2 and regulates VEGF-dependent cellular migration. J Biol Chem *279*, 22267-22275.

Hosoya, N., Qiao, Y., Hangaishi, A., Wang, L., Nannya, Y., Sanada, M., Kurokawa, M., Chiba, S., Hirai, H., and Ogawa, S. (2005). Identification of a SRC-like tyrosine kinase gene, FRK, fused with ETV6 in a patient with acute myelogenous leukemia carrying a t(6;12)(q21;p13) translocation. Genes Chromosomes Cancer *42*, 269-279.

Hsieh, F.C., Cheng, G., and Lin, J. (2005). Evaluation of potential Stat3-regulated genes in human breast cancer. Biochem Biophys Res Commun *335*, 292-299.

Hsu, J.M., Chen, C.T., Chou, C.K., Kuo, H.P., Li, L.Y., Lin, C.Y., Lee, H.J., Wang, Y.N., Liu, M., Liao, H.W., *et al.* (2011). Crosstalk between Arg 1175 methylation and Tyr 1173 phosphorylation negatively modulates EGFR-mediated ERK activation. Nat Cell Biol *13*, 174-181.

Hua, L., Zhu, M., Song, X., Wang, J., Fang, Z., Zhang, C., Shi, Q., Zhan, W., Wang, L., Meng, Q., *et al.* (2014). FRK suppresses the proliferation of human glioma cells by inhibiting cyclin D1 nuclear accumulation. J Neurooncol *119*, 49-58.

Hydbring, P., Malumbres, M., and Sicinski, P. (2016). Non-canonical functions of cell cycle cyclins and cyclin-dependent kinases. Nat Rev Mol Cell Biol *17*, 280-292.

Ingley, E. (2008). Src family kinases: regulation of their activities, levels and identification of new pathways. Biochim Biophys Acta *1784*, 56-65.

Irby, R.B., and Yeatman, T.J. (2000). Role of Src expression and activation in human cancer. Oncogene *19*, 5636-5642.

Ishizawar, R., and Parsons, S.J. (2004). c-Src and cooperating partners in human cancer. Cancer Cell *6*, 209-214.

Jarnicki, A., Putoczki, T., and Ernst, M. (2010). Stat3: linking inflammation to epithelial cancer - more than a "gut" feeling? Cell Div *5*, 14.

Je, D.W., O, Y.M., Ji, Y.G., Cho, Y., and Lee, D.H. (2014). The inhibition of SRC family kinase suppresses pancreatic cancer cell proliferation, migration, and invasion. Pancreas *43*, 768-776.

Jiang, Z., Jones, R., Liu, J.C., Deng, T., Robinson, T., Chung, P.E., Wang, S., Herschkowitz, J.I., Egan, S.E., Perou, C.M., *et al.* (2011). PRB and p53 at the crossroad of EMT and triple-negative breast cancer. Cell Cycle *10*, 1563-1570.

Jin, L., and Craven, R.J. (2014). The Rak/FRK tyrosine kinase associates with and internalizes the epidermal growth factor receptor. Oncogene *33*, 326-335.

Johnson, J., Thijssen, B., McDermott, U., Garnett, M., Wessels, L.F., and Bernards, R. (2016). Targeting the PRB-E2F pathway in breast cancer. Oncogene *35*, 4829-4835.

Kalluri, R. (2009). EMT: when epithelial cells decide to become mesenchymal-like cells. J Clin Invest *119*, 1417-1419.

Kalluri, R., and Weinberg, R.A. (2009). The basics of epithelial-mesenchymal transition. J Clin Invest *119*, 1420-1428.

Kaneko, T., Sidhu, S.S., and Li, S.S. (2011). Evolving specificity from variability for protein interaction domains. Trends Biochem Sci *36*, 183-190.

Kang, M.R., Park, K.H., Yang, J.O., Lee, C.W., Oh, S.J., Yun, J., Lee, M.Y., Han, S.B., and Kang, J.S. (2016). miR-6734 Up-Regulates p21 Gene Expression and Induces Cell Cycle Arrest and Apoptosis in Colon Cancer Cells. PLoS One *11*, e0160961.

Karlsson, M.C., Gonzalez, S.F., Welin, J., and Fuxe, J. (2017). Epithelial-mesenchymal transition in cancer metastasis through the lymphatic system. Mol Oncol *11*, 781-791.

Kenny, P.A., Lee, G.Y., Myers, C.A., Neve, R.M., Semeiks, J.R., Spellman, P.T., Lorenz, K., Lee, E.H., Barcellos-Hoff, M.H., Petersen, O.W., *et al.* (2007). The morphologies of breast cancer cell lines in three-dimensional assays correlate with their profiles of gene expression. Mol Oncol *1*, 84-96.

Kim, M.J., Lim, J., Yang, Y., Lee, M.S., and Lim, J.S. (2014). N-myc downstream-regulated gene 2 (NDRG2) suppresses the epithelial-mesenchymal transition (EMT) in breast cancer cells via STAT3/Snail signaling. Cancer Lett *354*, 33-42.

Koch, C.A., Anderson, D., Moran, M.F., Ellis, C., and Pawson, T. (1991). SH2 and SH3 domains: elements that control interactions of cytoplasmic signaling proteins. Science *252*, 668-674.

Kotiyal, S., and Bhattacharya, S. (2016). Events of Molecular Changes in Epithelial-Mesenchymal Transition. Crit Rev Eukaryot Gene Expr *26*, 163-171.

Kovatcheva, M., Liu, D.D., Dickson, M.A., Klein, M.E., O'Connor, R., Wilder, F.O., Socci, N.D., Tap, W.D., Schwartz, G.K., Singer, S., *et al.* (2015). MDM2 turnover and expression of ATRX determine the choice between quiescence and senescence in response to CDK4 inhibition. Oncotarget *6*, 8226-8243.

Krause, D.S., and Van Etten, R.A. (2005). Tyrosine kinases as targets for cancer therapy. N Engl J Med *353*, 172-187.

Lecuit, T., and Yap, A.S. (2015). E-cadherin junctions as active mechanical integrators in tissue dynamics. Nat Cell Biol *17*, 533-539.

Le Gal M, Chavanne G, Pellier D (1984). Diagnostic value of clustered microcalcifications discovered by mammography (apropos of 227cases with histological verification and without a palpable breast tumor). Bull Cancer.;71(1):57–64.

Lee, J., Wang, Z., Luoh, S.M., Wood, W.I., and Scadden, D.T. (1994). Cloning of FRK, a novel human intracellular SRC-like tyrosine kinase-encoding gene. Gene *138*, 247-251.

Lee, J.Y., and Kong, G. (2016). Roles and epigenetic regulation of epithelial-mesenchymal transition and its transcription factors in cancer initiation and progression. Cell Mol Life Sci *73*, 4643-4660.

Leemans, C.R., Braakhuis, B.J., and Brakenhoff, R.H. (2011). The molecular biology of head and neck cancer. Nat Rev Cancer *11*, 9-22.

Lehmann, B.D., Bauer, J.A., Chen, X., Sanders, M.E., Chakravarthy, A.B., Shyr, Y., and Pietenpol, J.A. (2011). Identification of human triple-negative breast cancer subtypes and preclinical models for selection of targeted therapies. J Clin Invest *121*, 2750-2767.

Lemmon, M.A., and Schlessinger, J. (2010). Cell signaling by receptor tyrosine kinases. Cell *141*, 1117-1134.

Leslie, K., Lang, C., Devgan, G., Azare, J., Berishaj, M., Gerald, W., Kim, Y.B., Paz, K., Darnell, J.E., Albanese, C., *et al.* (2006). Cyclin D1 is transcriptionally regulated by and required for transformation by activated signal transducer and activator of transcription 3. Cancer Res *66*, 2544-2552.

Levy, D.E., and Lee, C.K. (2002). What does Stat3 do? J Clin Invest *109*, 1143-1148.

Lukong, K.E. (2017). Understanding breast cancer - The long and winding road. BBA Clin *7*, 64-77.

Lukong, K.E., Ogunbolude, Y., and Kamdem, J.P. (2017). Breast cancer in Africa: prevalence, treatment options, hepRbal medicines, and socioeconomic determinants. Breast Cancer Res Treat.

Ma, X., Zhang, Y., Kang, Y., Li, L., and Zheng, W. (2016). A recombinant protein TmSm(T34A) can inhibit proliferation and proapoptosis to breast cancer stem cells(BCSCs) by down-regulating the expression of Cyclin D1. Biomed Pharmacother *84*, 373-381.

Malumbres, M., and BapRbacid, M. (2009). Cell cycle, CDKs and cancer: a changing paradigm. Nat Rev Cancer *9*, 153-166.

Manning, G., Whyte, D.B., Martinez, R., Hunter, T., and Sudarsanam, S. (2002). The protein kinase complement of the human genome. Science *298*, 1912-1934.

Masutomi, K., Yu, E.Y., Khurts, S., Ben-Porath, I., Currier, J.L., Metz, G.B., Brooks, M.W., Kaneko, S., Murakami, S., DeCaprio, J.A., *et al.* (2003). Telomerase maintains telomere structure in normal human cells. Cell *114*, 241-253.

Meyer, T., Xu, L., Chang, J., Liu, E.T., Craven, R.J., and Cance, W.G. (2003). Breast cancer cell line proliferation blocked by the Src-related Rak tyrosine kinase. Int J Cancer *104*, 139-146.

Miah, S., Goel, R.K., Dai, C., Kalra, N., Beaton-Brown, E., Bagu, E.T., Bonham, K., and Lukong, K.E. (2014). BRK targets Dok1 for ubiquitin-mediated proteasomal degradation to promote cell proliferation and migration. PLoS One *9*, e87684.

Miah, S., Martin, A., and Lukong, K.E. (2012). Constitutive activation of breast tumor kinase accelerates cell migration and tumor growth in vivo. Oncogenesis *1*, e11.

Morgan MP, Cooke MM, Christopherson PA, Westfall PR, McCarthy GM (2001). Calcium hydroxyapatite promotes mitogenesis and matrix metalloproteinase expression in human breast cancer cell lines. Mol Carcinog. 32(3):111–7.

Morgan M.P, Cooke M.M, McCarthy G.M. (2005) Microcalcifications associated with breast cancer: an epiphenomenon or biologically significant feature of selected tumors? J Mammary Gland Biol Neoplasia. 10(2):181–7.

Musgrove, E.A., and Sutherland, R.L. (2009). Biological determinants of endocrine resistance in breast cancer. Nat Rev Cancer *9*, 631-643.

Nantajit, D., Lin, D., and Li, J.J. (2015). The network of epithelial-mesenchymal transition: potential new targets for tumor resistance. J Cancer Res Clin Oncol *141*, 1697-1713.

Narod S.A., Iqbal, J. Miller, A.B. (2015). Why have breast cancer mortality rates declined? J. Cancer Policy 5 8–17.1

Neve, R.M., Chin, K., Fridlyand, J., Yeh, J., Baehner, F.L., Fevr, T., Clark, L., Bayani, N., Coppe, J.P., Tong, F., *et al.* (2006). A collection of breast cancer cell lines for the study of functionally distinct cancer subtypes. Cancer Cell *10*, 515-527.

Oberg-Welsh, C., Anneren, C., and Welsh, M. (1998). Mutation of C-terminal tyrosine residues Y497/Y504 of the Src-family member Bsk/Iyk decreases NIH3T3 cell proliferation. Growth Factors *16*, 111-124.

Ogunbolude, Y., Dai, C., Bagu, E.T., Goel, R.K., Miah, S., MacAusland-Berg, J., Ng, C.Y., Chibbar, R., Napper, S., Raptis, L., *et al.* (2017). FRK inhibits breast cancer cell migration and invasion by suppressing epithelial-mesenchymal transition. Oncotarget *8*, 113034-113065.

O'Grady, S., Morgan M.P. (2018). Microcalcifications in breast cancer: From pathophysiology to diagnosis and prognosis BBA - Reviews on Cancer 1869. 310–320 311

Otto, T., and Sicinski, P. (2017). Cell cycle proteins as promising targets in cancer therapy. Nat Rev Cancer *17*, 93-115.

Parsons, S.J., and Parsons, J.T. (2004). Src family kinases, key regulators of signal transduction. Oncogene *23*, 7906-7909.

Pasteris J, Chou I. (1998). Fluid-deposited graphitic inclusions in quartz: Comparison between KTB core samples and artifi- cally re-equilibrated natural inclusions. Geochim Cosmochim Acta;62:109–2

Pecina-Slaus, N. (2003). Tumor suppressor gene E-cadherin and its role in normal and malignant cells. Cancer Cell Int *3*, 17.

Pendergast, A.M. (1996). Nuclear tyrosine kinases: from Abl to WEE1. Curr Opin Cell Biol *8*, 174-181.

Pendergast, A.M. (2002). The Abl family kinases: mechanisms of regulation and signaling. Adv Cancer Res *85*, 51-100.

Perou, C.M., Sorlie, T., Eisen, M.B., van de Rijn, M., Jeffrey, S.S., Rees, C.A., Pollack, J.R., Ross, D.T., Johnsen, H., Akslen, L.A., *et al.* (2000). Molecular portraits of human breast tumours. Nature *406*, 747-752.

Pilati, C., Letouze, E., Nault, J.C., Imbeaud, S., Boulai, A., Calderaro, J., Poussin, K., Franconi, A., Couchy, G., Morcrette, G., *et al.* (2014). Genomic profiling of hepatocellular adenomas reveals recurrent FRK-activating mutations and the mechanisms of malignant transformation. Cancer Cell *25*, 428-441.

Prat, A., and Perou, C.M. (2011). Deconstructing the molecular portraits of breast cancer. Mol Oncol *5*, 5-23.

Prieto-Garcia, E., Diaz-Garcia, C.V., Garcia-Ruiz, I., and Agullo-Ortuno, M.T. (2017). Epithelial-to-mesenchymal transition in tumor progression. Med Oncol *34*, 122.

Rakha, E.A., Reis-Filho, J.S., Baehner, F., Dabbs, D.J., Decker, T., Eusebi, V., Fox, S.B., Ichihara, S., Jacquemier, J., Lakhani, S.R., *et al.* (2010). Breast cancer prognostic classification in the molecular era: the role of histological grade. Breast Cancer Res *12*, 207.

Rao, A.A., Feneis, J., Lalonde, C., Ojeda-Fournier, H (2016). A pictorial review of changes in the BI-RADS fifth edition, Radiographics 36 (3) 623–639.

Resh, M.D. (1999). Fatty acylation of proteins: new insights into membrane targeting of myristoylated and palmitoylated proteins. Biochim Biophys Acta *1451*, 1-16.

Roskoski, R., Jr. (2004). Src protein-tyrosine kinase structure and regulation. Biochem Biophys Res Commun *324*, 1155-1164.

Sansone, P., Storci, G., Tavolari, S., Guarnieri, T., Giovannini, C., Taffurelli, M., Ceccarelli, C., Santini, D., Paterini, P., Marcu, K.B., *et al.* (2007). IL-6 triggers malignant features in mammospheres from human ductal breast carcinoma and normal mammary gland. J Clin Invest *117*, 3988-4002.

Serfas, M.S., and Tyner, A.L. (2003). Brk, Srm, FRK, and Src42A form a distinct family of intracellular Src-like tyrosine kinases. Oncol Res *13*, 409-419.

Seshacharyulu, P., Ponnusamy, M.P., Haridas, D., Jain, M., Ganti, A.K., and Batra, S.K. (2012). Targeting the EGFR signaling pathway in cancer therapy. Expert Opin Ther Targets *16*, 15-31.

Sharma, T. Radosevich, J.A, Pachori G.,. Mandal. C.C (2016). A Molecular View of Pathological Microcalcification in Breast CancerJ Mammary Gland Biol Neoplasia 21:25–40

Shi, Q., Song, X., Wang, J., Gu, J., Zhang, W., Hu, J., Zhou, X., and Yu, R. (2015). FRK inhibits migration and invasion of human glioma cells by promoting N-cadherin/beta-catenin complex formation. J Mol Neurosci *55*, 32-41.

Siveen, K.S., Sikka, S., Surana, R., Dai, X., Zhang, J., Kumar, A.P., Tan, B.K., Sethi, G., and Bishayee, A. (2014). Targeting the STAT3 signaling pathway in cancer: role of synthetic and natural inhibitors. Biochim Biophys Acta *1845*, 136-154.

Skrypek, N., Goossens, S., De Smedt, E., Vandamme, N., and Berx, G. (2017). Epithelial-to-Mesenchymal Transition: Epigenetic Reprogramming Driving Cellular Plasticity. Trends Genet.

Sorlie, T., Perou, C.M., Tibshirani, R., Aas, T., Geisler, S., Johnsen, H., Hastie, T., Eisen, M.B., van de Rijn, M., Jeffrey, S.S., *et al.* (2001). Gene expression patterns of breast carcinomas distinguish tumor subclasses with clinical implications. Proc Natl Acad Sci U S A *98*, 10869-10874.

Suhail Z, Sarwar M, Murtaza K (2015). Automatic detection of abnormalities in mammograms. BMC Med Imaging.;15. doi:10.1186/s12880-015-0094-8.

Summy, J.M., and Gallick, G.E. (2003). Src family kinases in tumor progression and metastasis. Cancer Metastasis Rev *22*, 337-358.

Sun, B., Yang, N., Jiang, Y., Zhang, H., Hou, C., Ji, C., Liu, Y., and Zuo, P. (2015). Antagomir-1290 suppresses CD133(+) cells in non-small cell lung cancer by targeting fyn-related Src family tyrosine kinase. Tumour Biol *36*, 6223-6230.

Sunitha, I., and Avigan, M.I. (1996). The apical membranes of maturing gut columnar epithelial cells contain the enzymatically active form of a newly identified fyn-related tyrosine kinase. Oncogene *13*, 547-559.

Sunitha, I., Shen, R., McKillop, I.H., Lee, J.H., Resau, J., and Avigan, M. (1999). A src-related kinase in the brush border membranes of gastrointestinal cells is regulated by c-met. Exp Cell Res *250*, 86-98.

Tabar L., Yen M-F, Vitak B., Chen H-HT, Smith R.A, Duffy S.W (2003). Mammography service screening and mortality in breast cancer patients: 20-year follow-up before and after introduction of screening. The Lancet.361(9367):1405–10.

Terzi, M.Y., Izmirli, M., and Gogebakan, B. (2016). The cell fate: senescence or quiescence. Mol Biol Rep *43*, 1213-1220.

Tomas, A., Futter, C.E., and Eden, E.R. (2014). EGF receptor trafficking: consequences for signaling and cancer. Trends Cell Biol *24*, 26-34.

Torre, L.A., Bray, F., Siegel, R.L., Ferlay, J., Lortet-Tieulent, J., and Jemal, A. (2015). Global cancer statistics, 2012. CA Cancer J Clin *65*, 87-108.

Torre, L.A., Siegel, R.L., Ward, E.M., and Jemal, A. (2016). Global Cancer Incidence and Mortality Rates and Trends--An Update. Cancer Epidemiol Biomarkers Prev *25*, 16-27.

Tye, H., Kennedy, C.L., Najdovska, M., McLeod, L., McCormack, W., Hughes, N., Dev, A., Sievert, W., Ooi, C.H., Ishikawa, T.O., *et al.* (2012). STAT3-driven upregulation of TLR2 promotes gastric tumorigenesis independent of tumor inflammation. Cancer Cell *22*, 466-478.

Vazquez, F., Ramaswamy, S., Nakamura, N., and Sellers, W.R. (2000). Phosphorylation of the PTEN tail regulates protein stability and function. Mol Cell Biol *20*, 5010-5018.

Wakahara, R., Kunimoto, H., Tanino, K., Kojima, H., Inoue, A., Shintaku, H., and Nakajima, K. (2012). Phospho-Ser727 of STAT3 regulates STAT3 activity by enhancing dephosphorylation of phospho-Tyr705 largely through TC45. Genes Cells *17*, 132-145.

Wang, H., Lafdil, F., Kong, X., and Gao, B. (2011). Signal transducer and activator of transcription 3 in liver diseases: a novel therapeutic target. Int J Biol Sci *7*, 536-550.

Weerasinghe, P., Li, Y., Guan, Y., Zhang, R., Tweardy, D.J., and Jing, N. (2008). T40214/PEI complex: a potent therapeutics for prostate cancer that targets STAT3 signaling. Prostate *68*, 1430-1442.

Weigelt, B., Peterse, J.L., and van 't Veer, L.J. (2005). Breast cancer metastasis: markers and models. Nat Rev Cancer *5*, 591-602.

Weinberg, R.A. (1995). The retinoblastoma protein and cell cycle control. Cell *81*, 323-330.

Wen, F.C., Chang, T.W., Tseng, Y.L., Lee, J.C., and Chang, M.C. (2014). hRAD9 functions as a tumor suppressor by inducing p21-dependent senescence and suppressing epithelial-mesenchymal transition through inhibition of Slug transcription. Carcinogenesis *35*, 1481-1490.

Wendt, M.K., Balanis, N., Carlin, C.R., and Schiemann, W.P. (2014). STAT3 and epithelial-mesenchymal transitions in carcinomas. JAKSTAT *3*, e28975.

Witkiewicz, A.K., Cox, D.W., Rivadeneira, D., Ertel, A.E., Fortina, P., Schwartz, G.F., and Knudsen, E.S. (2014). The retinoblastoma tumor suppressor pathway modulates the invasiveness of EpRbB2-positive breast cancer. Oncogene *33*, 3980-3991.

Wu, J., Patmore, D.M., Jousma, E., Eaves, D.W., Breving, K., Patel, A.V., Schwartz, E.B., Fuchs, J.R., Cripe, T.P., Stemmer-Rachamimov, A.O., *et al.* (2014). EGFR-STAT3 signaling promotes formation of malignant peripheral nerve sheath tumors. Oncogene *33*, 173-180.

Xin, H., Lu, R., Lee, H., Zhang, W., Zhang, C., Deng, J., Liu, Y., Shen, S., Wagner, K.U., Forman, S., *et al.* (2013). G-protein-coupled receptor agonist BV8/prokineticin-2 and STAT3 protein form a feed-forward loop in both normal and malignant myeloid cells. J Biol Chem *288*, 13842-13849.

Xu, Y., Li, N., Xiang, R., and Sun, P. (2014). Emerging roles of the p38 MAPK and PI3K/AKT/mTOR pathways in oncogene-induced senescence. Trends Biochem Sci *39*, 268-276.

Yim, E.K., Peng, G., Dai, H., Hu, R., Li, K., Lu, Y., Mills, G.B., Meric-Bernstam, F., Hennessy, B.T., Craven, R.J., *et al.* (2009a). Rak functions as a tumor suppressor by regulating PTEN protein stability and function. Cancer Cell *15*, 304-314.

Yim, E.K., Siwko, S., and Lin, S.Y. (2009b). Exploring Rak tyrosine kinase function in breast cancer. Cell Cycle *8*, 2360-2364.

Yoon, S.O., Shin, S., and Mercurio, A.M. (2006). Ras stimulation of E2F activity and a consequent E2F regulation of integrin alpha6beta4 promote the invasion of breast carcinoma cells. Cancer Res *66*, 6288-6295.

Youlden, D.R., Cramb, S.M., Yip, C.H., and Baade, P.D. (2014). Incidence and mortality of female breast cancer in the Asia-Pacific region. Cancer Biol Med *11*, 101-115.

Yu, H., Lee, H., Herrmann, A., Buettner, R., and Jove, R. (2014). Revisiting STAT3 signalling in cancer: new and unexpected biological functions. Nat Rev Cancer *14*, 736-746.

Zagouri, F., Kotoula, V., Kouvatseas, G., Sotiropoulou, M., Koletsa, T., Gavressea, T., Valavanis, C., Trihia, H., Bobos, M., Lazaridis, G., *et al.* (2017). Protein expression patterns of cell cycle regulators in operable breast cancer. PLoS One *12*, e0180489.

Zhang, X., Li, F., and Zhu, P.L. (2016). Fyn-related kinase expression predicts favorable prognosis in patients with cervical cancer and suppresses malignant progression by regulating migration and invasion. Biomed Pharmacother *84*, 270-276.

Zhou, X., Hua, L., Zhang, W., Zhu, M., Shi, Q., Li, F., Zhang, L., Song, C., and Yu, R. (2012). FRK controls migration and invasion of human glioma cells by regulating JNK/c-Jun signaling. J Neurooncol *110*, 9-19.

Zhu, X.W., and Gong, J.P. (2013). Expression and role of icam-1 in the occurrence and development of hepatocellular carcinoma. Asian Pac J Cancer Prev *14*, 1579-1583.

Zugowski, C., Lieder, F., Muller, A., Gasch, J., Corvinus, F.M., Moriggl, R., and Friedrich, K. (2011). STAT3 controls matrix metalloproteinase-1 expression in colon carcinoma cells by both direct and AP-1-mediated interaction with the MMP-1 promoter. Biol Chem *392*, 449-459.

LIST OF APPENDICES

1. **License/permission to reproduce Table 2. 1**

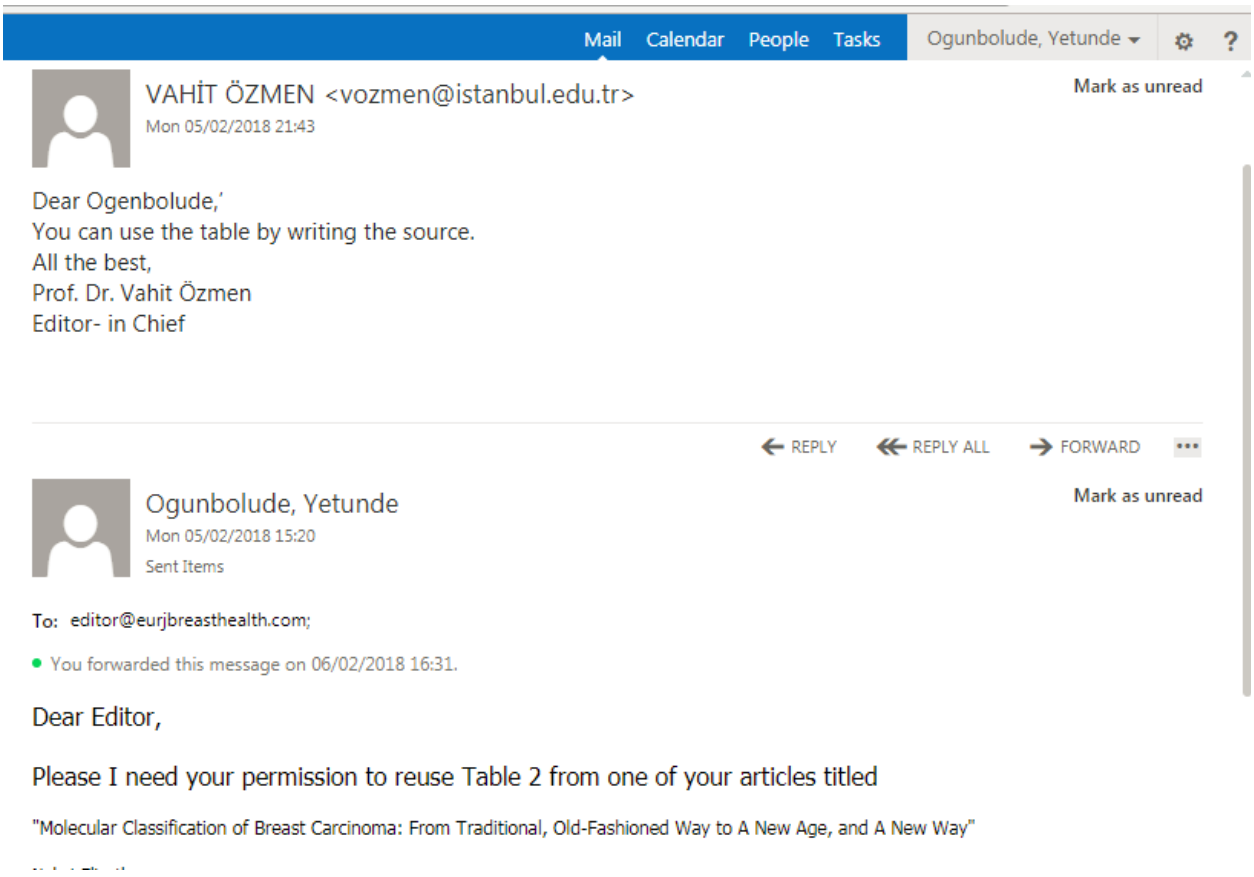

Mail Calendar People Tasks Ogunbolude, Yetunde

VAHİT ÖZMEN <vozmen@istanbul.edu.tr>
Mon 05/02/2018 21:43

Mark as unread

Dear Ogenbolude,'
You can use the table by writing the source.
All the best,
Prof. Dr. Vahit Özmen
Editor- in Chief

REPLY REPLY ALL FORWARD

Ogunbolude, Yetunde
Mon 05/02/2018 15:20
Sent Items

Mark as unread

To: editor@eurjbreasthealth.com;

You forwarded this message on 06/02/2018 16:31.

Dear Editor,

Please I need your permission to reuse Table 2 from one of your articles titled

"Molecular Classification of Breast Carcinoma: From Traditional, Old-Fashioned Way to A New Age, and A New Way"

2. License/permission to reproduce Figure 2. 1

3. License/permission to reproduce Figure 2. 2

SPRINGER NATURE LICENSE TERMS AND CONDITIONS

Feb 05, 2018

This Agreement between Mrs. Yetunde ogunbolude ("You") and Springer Nature ("Springer Nature") consists of your license details and the terms and conditions provided by Springer Nature and Copyright Clearance Center.

License Number	4282690228526
License date	Feb 05, 2018
Licensed Content Publisher	Springer Nature
Licensed Content Publication	Oncogene
Licensed Content Title	Src family kinases, key regulators of signal transduction
Licensed Content Author	Sarah J Parsons, J Thomas Parsons
Licensed Content Date	Oct 18, 2004
Licensed Content Volume	23
Licensed Content Issue	48
Type of Use	Thesis/Dissertation
Requestor type	academic/university or research institute
Format	print and electronic
Portion	figures/tables/illustrations
Number of figures/tables/illustrations	1
High-res required	no
Will you be translating?	no
Circulation/distribution	501 to 1000
Author of this Springer Nature content	no
Title	Characterizing the signaling and tumor suppressor role of FRK in breast cancer
Instructor name	Yetunde ogunbolude
Institution name	university of Saskatchewan
Expected presentation date	Mar 2018
Portions	figure 1
Requestor Location	Mrs. Yetunde ogunbolude University of Saskatchewan Health science building 107 Wiggins Road saskatoon, SK S7N5E5 Canada Attn: Mrs. Yetunde ogunbolude
Billing Type	Invoice
Billing Address	Mrs. Yetunde ogunbolude University of Saskatchewan Health science building 107 Wiggins Road

4. License/permission to reproduce Figure 2. 3

ELSEVIER LICENSE
TERMS AND CONDITIONS

Feb 15, 2018

This Agreement between Mrs. Yetunde ogunbolude ("You") and Elsevier ("Elsevier") consists of your license details and the terms and conditions provided by Elsevier and Copyright Clearance Center.

License Number	4290361182818
License date	Feb 15, 2018
Licensed Content Publisher	Elsevier
Licensed Content Publication	Biochimica et Biophysica Acta (BBA) - Proteins and Proteomics
Licensed Content Title	Src family kinases: Regulation of their activities, levels and identification of new pathways
Licensed Content Author	Evan Ingley
Licensed Content Date	Jan 1, 2008
Licensed Content Volume	1784
Licensed Content Issue	1
Licensed Content Pages	10
Start Page	56
End Page	65
Type of Use	reuse in a thesis/dissertation
Intended publisher of new work	other
Portion	figures/tables/illustrations
Number of figures/tables/illustrations	1
Format	both print and electronic
Are you the author of this Elsevier article?	No
Will you be translating?	No
Original figure numbers	Figure 1
Title of your thesis/dissertation	Characterizing the signaling and tumor suppressor role of FRK in breast cancer
Publisher of new work	university of Saskatchewan
Author of new work	Yetunde ogunbolude
Expected completion date	Mar 2018
Estimated size (number of pages)	1
Requestor Location	Mrs. Yetunde ogunbolude University of Saskatchewan Health science building 107 Wiggins Road saskatoon, SK S7N5E5 Canada Attn: Mrs. Yetunde ogunbolude

5. License/permission to reproduce Figure 2. 4 A and B

ELSEVIER LICENSE
TERMS AND CONDITIONS

Feb 06, 2018

This Agreement between Mrs. Yetunde ogunbolude ("You") and Elsevier ("Elsevier") consists of your license details and the terms and conditions provided by Elsevier and Copyright Clearance Center.

License Number	4283180333747
License date	Feb 06, 2018
Licensed Content Publisher	Elsevier
Licensed Content Publication	Biochimica et Biophysica Acta (BBA) - Reviews on Cancer
Licensed Content Title	Tracing the footprints of the breast cancer oncogene BRK — Past till present
Licensed Content Author	Raghuveera Kumar Goel,Kiven Erique Lukong
Licensed Content Date	Aug 1, 2015
Licensed Content Volume	1856
Licensed Content Issue	1
Licensed Content Pages	16
Start Page	39
End Page	54
Type of Use	reuse in a thesis/dissertation
Portion	figures/tables/illustrations
Number of figures/tables/illustrations	2
Format	both print and electronic
Are you the author of this Elsevier article?	No
Will you be translating?	No
Original figure numbers	figure 1 and Figure 2
Title of your thesis/dissertation	Characterizing the signaling and tumor suppressor role of FRK in breast cancer
Publisher of new work	university of Saskatchewan
Author of new work	Yetunde ogunbolude
Expected completion date	Mar 2018
Estimated size (number of pages)	1
Requestor Location	Mrs. Yetunde ogunbolude University of Saskatchewan Health science building 107 Wiggins Road saskatoon, SK S7N5E5 Canada Attn: Mrs. Yetunde ogunbolude
Publisher Tax ID	GB 494 6272 12

6. License/permission to reproduce Figure 2. 5

SPRINGER NATURE LICENSE TERMS AND CONDITIONS

Feb 06, 2018

This Agreement between Mrs. Yetunde ogunbolude ("You") and Springer Nature ("Springer Nature") consists of your license details and the terms and conditions provided by Springer Nature and Copyright Clearance Center.

License Number	4283180796737
License date	Feb 06, 2018
Licensed Content Publisher	Springer Nature
Licensed Content Publication	Cancer and Metastasis Reviews
Licensed Content Title	Understanding the cellular roles of Fyn-related kinase (FRK): implications in cancer biology
Licensed Content Author	Raghuveera Kumar Goel, Kiven Erique Lukong
Licensed Content Date	Jan 1, 2016
Licensed Content Volume	35
Licensed Content Issue	2
Type of Use	Thesis/Dissertation
Requestor type	academic/university or research institute
Format	print and electronic
Portion	figures/tables/illustrations
Number of figures/tables/illustrations	1
Will you be translating?	no
Circulation/distribution	>50,000
Author of this Springer Nature content	no
Title	Characterizing the signaling and tumor suppressor role of FRK in breast cancer
Instructor name	Yetunde ogunbolude
Institution name	university of Saskatchewan
Expected presentation date	Mar 2018
Portions	Figure 2
Requestor Location	Mrs. Yetunde ogunbolude University of Saskatchewan Health science building 107 Wiggins Road saskatoon, SK S7N5E5 Canada Attn: Mrs. Yetunde ogunbolude
Billing Type	Invoice
Billing Address	Mrs. Yetunde ogunbolude University of Saskatchewan Health science building 107 Wiggins Road

7. License/permission to reproduce Figure 2. 6

SPRINGER NATURE LICENSE
TERMS AND CONDITIONS

Feb 06, 2018

This Agreement between Mrs. Yetunde ogunbolude ("You") and Springer Nature ("Springer Nature") consists of your license details and the terms and conditions provided by Springer Nature and Copyright Clearance Center.

License Number	4283181338191
License date	Feb 06, 2018
Licensed Content Publisher	Springer Nature
Licensed Content Publication	Nature Reviews Cancer
Licensed Content Title	Revisiting STAT3 signalling in cancer: new and unexpected biological functions
Licensed Content Author	Hua Yu, Heehyoung Lee, Andreas Herrmann, Ralf Buettner, Richard Jove
Licensed Content Date	Oct 24, 2014
Licensed Content Volume	14
Licensed Content Issue	11
Type of Use	Thesis/Dissertation
Requestor type	academic/university or research institute
Format	print and electronic
Portion	figures/tables/illustrations
Number of figures/tables/illustrations	1
High-res required	no
Will you be translating?	no
Circulation/distribution	>50,000
Author of this Springer Nature content	no
Title	Characterizing the signaling and tumor suppressor role of FRK in breast cancer
Instructor name	Yetunde ogunbolude
Institution name	university of Saskatchewan
Expected presentation date	Mar 2018
Portions	Figure 1
Requestor Location	Mrs. Yetunde ogunbolude University of Saskatchewan Health science building 107 Wiggins Road saskatoon, SK S7N5E5 Canada Attn: Mrs. Yetunde ogunbolude
Billing Type	Invoice
Billing Address	Mrs. Yetunde ogunbolude University of Saskatchewan

8. License/permission to reproduce Figure 2. 7

ELSEVIER LICENSE
TERMS AND CONDITIONS

Feb 06, 2018

This Agreement between Mrs. Yetunde ogunbolude ("You") and Elsevier ("Elsevier") consists of your license details and the terms and conditions provided by Elsevier and Copyright Clearance Center.

License Number	4283190236519
License date	Feb 06, 2018
Licensed Content Publisher	Elsevier
Licensed Content Publication	Biochimica et Biophysica Acta (BBA) - Reviews on Cancer
Licensed Content Title	Targeting the STAT3 signaling pathway in cancer: Role of synthetic and natural inhibitors
Licensed Content Author	Kodappully Sivaraman Siveen,Sakshi Sikka,Rohit Surana,Xiaoyun Dai,Jingwen Zhang,Alan Prem Kumar,Benny K.H. Tan,Gautam Sethi,Anupam Bishayee
Licensed Content Date	Apr 1, 2014
Licensed Content Volume	1845
Licensed Content Issue	2
Licensed Content Pages	19
Start Page	136
End Page	154
Type of Use	reuse in a thesis/dissertation
Intended publisher of new work	other
Portion	figures/tables/illustrations
Number of figures/tables/illustrations	1
Format	both print and electronic
Are you the author of this Elsevier article?	No
Will you be translating?	No
Original figure numbers	Figure 2
Title of your thesis/dissertation	Characterizing the signaling and tumor suppressor role of FRK in breast cancer
Publisher of new work	university of Saskatchewan
Author of new work	Yetunde ogunbolude
Expected completion date	Mar 2018
Estimated size (number of pages)	1
Requestor Location	Mrs. Yetunde ogunbolude University of Saskatchewan Health science building 107 Wiggins Road saskatoon, SK S7N5E5

9. License/permission to reproduce Figure 2. 8

Public Domain Mark 1.0

No Copyright

This work has been **identified** as being free of known restrictions under copyright law, including all related and neighboring rights.

You can copy, modify, distribute and perform the work, even for commercial purposes, all without asking permission. See **Other Information** below.

Other Information

- The work may not be free of known copyright restrictions in all **jurisdictions**.
- Persons may have other rights in or related to the work, such as patent or trademark rights, and others may have rights in how the work is used, such as **publicity or privacy** rights.
- In some jurisdictions **moral rights** of the author may persist beyond the term of copyright. These rights may include the right to be identified as the author and the right to object to derogatory treatments.
- Unless expressly stated otherwise, the person who identified the work makes no warranties about the work, and disclaims liability for all uses of the work, to the fullest extent permitted by applicable law.
- When using or citing the work, you should not imply **endorsement** by the author or the person who identified the work.

10. License/permission to reproduce Figure 2. 9

Creative Commons License Deed

Attribution 4.0 International (CC BY 4.0)

This is a human-readable summary of (and not a substitute for) the license.

You are free to:

Share — copy and redistribute the material in any medium or format

Adapt — remix, transform, and build upon the material

for any purpose, even commercially.

The licensor cannot revoke these freedoms as long as you follow the license terms.

Under the following terms:

Attribution — You must give appropriate credit, provide a link to the license, and indicate if changes were made. You may do so in any reasonable manner, but not in any way that suggests the licensor endorses you or your use.

No additional restrictions — You may not apply legal terms or technological measures that legally restrict others from doing anything the license permits.

Notices:

You do not have to comply with the license for elements of the material in the public domain or where your use is permitted by an applicable exception or limitation.

No warranties are given. The license may not give you all of the permissions necessary for your intended use. For example, other rights such as publicity, privacy, or moral rights may limit how you use the material.

11. License/permission to reproduce Figure 2. 9

SPRINGER NATURE LICENSE TERMS AND CONDITIONS

Feb 06, 2018

This Agreement between Mrs. Yetunde ogunbolude ("You") and Springer Nature ("Springer Nature") consists of your license details and the terms and conditions provided by Springer Nature and Copyright Clearance Center.

License Number	4283190870584
License date	Feb 06, 2018
Licensed Content Publisher	Springer Nature
Licensed Content Publication	Nature Reviews Cancer
Licensed Content Title	The molecular biology of head and neck cancer
Licensed Content Author	C. René Leemans, Boudewijn J. M. Braakhuis, Ruud H. Brakenhoff
Licensed Content Date	Dec 16, 2010
Licensed Content Volume	11
Licensed Content Issue	1
Type of Use	Thesis/Dissertation
Requestor type	academic/university or research institute
Format	print and electronic
Portion	figures/tables/illustrations
Number of figures/tables/illustrations	1
High-res required	no
Will you be translating?	no
Circulation/distribution	>50,000
Author of this Springer Nature content	no
Title	Characterizing the signaling and tumor suppressor role of FRK in breast cancer
Instructor name	Yetunde ogunbolude
Institution name	university of Saskatchewan
Expected presentation date	Mar 2018
Portions	Figure 1
Requestor Location	Mrs. Yetunde ogunbolude University of Saskatchewan Health science building 107 Wiggins Road saskatoon, SK S7N5E5 Canada Attn: Mrs. Yetunde ogunbolude
Billing Type	Invoice
Billing Address	Mrs. Yetunde ogunbolude University of Saskatchewan Health science building 107 Wiggins Road